**NTNU – Trondheim**
Norwegian University of
Science and Technology

# Cytotoxicity and Genotoxicity of Functionalised Multi Walled Carbon Nanotubes in the PLHC-1 Cell Line

Marita Ballestad

Environmental Toxicology and Chemistry
Submission date: July 2015
Supervisor: Åse Krøkje, IBI
Co-supervisor: Andy Booth, SINTEF

Norwegian University of Science and Technology
Department of Biology

## Acknowledgements

This master's project in Environmental Toxicology was conducted at the Department of Biology, Norwegian University of Science and Technology (NTNU). My supervisor was Associate professor Åse Krøkje and my co-supervisor was Senior researcher Andy Booth (SINTEF).

I would like to thank all those who have kindly helped me during this master's project. I would like to thank my supervisor, Åse Krøkje, for the time spent giving me feedback on my thesis, even during her holiday. Your support and patient supervision during my project have been highly valued. I would further like to thank my co-supervisor Andy Booth for keeping me motivated and positive during my project, and always finding solutions to my problems. A very special thanks is also extended to Lisbet Støen at SINTEF for her kind support and interest in my project. Your practical knowledge and generosity in time and assistance has been greatly appreciated, and has helped me considerably during my project. I would also like to thank Chris Bingham for training and helping me with my practical work at NTNU. Your knowledge and assistance was highly valued. Further I would like to thank Ingvild F. Størdal for valuable advice on my thesis and Vu To for sharing her knowledge about cell culture. Recognition should also be given to Randi Røsbak for her help with my lab work. I would also like to thank Synnøve Lofthus for her good company and support during my lab work at SINTEF; and I would like to thank Kristin, Inger, Marianne and many more at SINTEF for their help and positive spirit.

Finally, I would like to thank my family, friends, boyfriend and classmates for their company, encouragement and help during my master thesis! Your help was invaluable.

Trondheim 15th July, 2015

Marita Ballestad

The financial support for this project was received from SINTEF and NTNU.

## Abstract

The field of nanotechnology is rapidly expanding in all sectors of society due to its increasingly large number of applications. This field deals with materials at the nanoscale, defined as having at least one dimension below 100 nm. The rapid increase in production of nanomaterials is a cause of concern, as their exposure to the environment may increase rapidly, in combination with lacking knowledge of exposure effects. Carbon nanotubes (CNTs) are one type of nanomaterial that have a wide range of properties, which make them very useful in a variety of products. Their applications range from transporters of drugs to superconductors. There exist single-walled, double-walled and multi-walled CNTs (MWCNT) which are often functionalised by adding functional groups on the CNT surface. This enhances the CNT's solubility and applicability in many circumstances, but may also alter its toxicity. Due to the continuously increasing production of CNTs it is inevitable that these compounds will be released to the environment, and the aquatic environment is often a sink for such pollutants.

In the current study, the aim was to investigate if differently functionalised MWCNTs with identical size had the potential to induce cytotoxic and genotoxic damage *in vitro* in liver cells of the fish *Poeciliopsis lucida* (PLHC-1); and if this potential damage differed with the type of functionalisation. Four MWCNTs were assessed, with different functionalisations as follows: COOH, OH, $NH_2$ and one pristine (MWCNT-P). Cytotoxicity was assessed by the MTT-assay after 48 hours exposure to each MWCNT in the range 0.5-2048 µg/mL. Genotoxicity was assessed after 48 hours exposure to 4 and 64 µg/mL of each MWCNT with the DNA double strand break (DSB) assay.

The results demonstrated that each of the four MWCNTs tested induced some cytotoxicity, but at relatively high concentrations. MWCNT-COOH appeared to be slightly more cytotoxic than the other CNTs, whereas MWCNT-$NH_2$ appeared to be the least cytotoxic. MWCNT-$NH_2$ was not particularly cytotoxic until a concentration of ~100 µg/mL was reached. The difference in cytotoxicity was hypothesised to be due to degree of dispersability and therefore bioavailability of the CNT, which was related to surface functionalisation of the CNT. However, CNT adsorption of formazan could have influenced the results, causing false positive results for cytotoxicity.

Results obtained in the genotoxicity assay were inconsistent, mostly due to problems with cell lysis. The initial assessment of the fraction of DNA that migrated into the gel (DNA-FTM) relative to the amount loaded, did not indicate any apparent differences between MWCNT groups or within each group. However, investigation of median molecular lengths (MMLs) of the damaged DNA indicated that MWCNT-OH and MWCNT-$NH_2$ was genotoxic at the low (4 µg/mL) and high (64 µg/mL) exposures respectively. Due to

inconsistencies in genotoxic data it was difficult to draw any conclusions on the genotoxic potential of any of the MWCNTs.

The results from this study indicate that the risk of cytotoxic effects to PLHC-1 cells is relatively small even at high concentrations (mg/L). Since current environmental concentrations are much lower (ng-µg/L), cytotoxic effects in liver of adult fish in the environment is relatively unlikely. However, the current study was conducted *in vitro*, therefore it was not possible to study toxicokinetics in relation to CNTs. Moreover, it could not be determined with accuracy at what concentrations genotoxic effects may occur. It is also important to consider that CNTs may interact with other toxic substances (such as pesticides) and enhance their toxic effects. Future evaluations of CNT toxicity would benefit from keeping a higher level of standardisation, as well as determining CNT interactions with assay/serum components.

## Sammendrag

Nanoteknologi er en voksende teknologi i alle sektorer i samfunnet på grunn av stadig flere bruksområder. Dette feltet omhandler materialer i nanoskala, definert som å ha minst én dimensjon under 100 nm. Den raske økningen i produksjon av nanomaterialer er bekymringsverdig ettersom det kan gi betydelig økte utslipp i naturmiljøet; i kombinasjon med manglende kunnskap om effektene av slik eksponering. Karbonnanorør (CNT) er en type nanomateriale som har et bredt spekter av egenskaper, som gjør dem svært nyttige i en rekke produkter. Bruksområdene spenner fra transport av legemidler, til bruk som superledere. Det eksisterer enkeltveggede, dobbeltveggede og flerveggede (MWCNT) CNTer, som ofte funksjonaliseres ved å feste funksjonelle grupper på overflaten til røret. Dette gjør CNTet mer vannløselig og anvendbart i mange tilfeller, men dette kan også forandre CNTets potensielle toksisitet. På grunn av den stadig økende produksjonen av CNT er det høy sannsynlighet for utslipp til omgivelsene, og det akvatiske miljøet er ofte et samlepunkt for slike forurensninger.

I denne studien var målet å undersøke om MWCNT med ulike funksjonelle grupper og identisk størrelse, har potensial til å indusere cytotoksiske og gentoksiske skader *in vitro* i leverceller fra fisken *Poeciliopsis lucida* (PLHC-1); og om eventuelle skader er forskjellige ved ulik type funksjonalisering. Fire MWCNT ble vurdert, med forskjellige funksjonaliseringer: COOH, OH, $NH_2$ og en ikke-funksjonalisert (MWCNT-P). Cytotoksisitet ble undersøkt med MTT-assayet etter 48 timers eksponering for hvert MWCNT, med konsentrasjoner fra 0,5 til 2048 µg/mL. Gentoksistet ble vurdert med DNA dobbeltrådbrudd (DSB) analyse etter 48 timers eksponering for 4 og 64 µg/mL av hvert MWCNT.

Resultatene viste at hver av de fire MWCNTene induserte cytotoksisitet, men kun ved relativt høye konsentrasjoner. MWCNT-COOH syntes å være litt mer cytotoksisk enn de andre CNTene, mens MWCNT-$NH_2$ viste seg å være minst cytotoksisk. MWCNT-$NH_2$ var først cytotoksisk ved en konsentrasjon på ~ 100 µg/mL. Forskjellen i cytotoksisitet ble antatt å være knyttet til vannløselighet og biotilgjengelighet av hver CNT, som har sammenheng med CNT funksjonaliseringen. Imidlertid kan CNT adsorpsjon av formazan ha hatt innflytelse på resultatene, som kan ha forårsaket falske positive resultater for cytotoksisitet.

Resultater av gentoksisitetsanalysen var inkonsekvent, hovedsaklig på grunn av problemer med cellelysering. Vurderingen av fraksjon av DNA som migrerte (DNA-FTM), i forhold til den totale mengden DNA, indikerte ingen tilsynelatende forskjell mellom MWCNT-grupper eller innen hver gruppe. Undersøkelse av median molekylærlengde (MMLs) av migrert DNA

indikerte at MWCNT-OH og MWCNT-$NH_2$ var genotoksiske ved respektivt lav (4 µg/mL) og høy (64 µg/mL) eksponering. På grunn av inkonsekvente data var det vanskelig å trekke noen konklusjoner vedrørende det gentoksiske potensialet til de ulike MWCNTene.

Resultatene fra denne studien indikerer at risikoen for cytotoksiske effekter av MWCNT i PLHC-1-celler er forholdsvis liten, selv ved høye konsentrasjoner (mg/L). Foreløpige rapporterte miljøkonsentrasjoner er mye lavere (ng - µg/L), og det er derfor forholdsvis lite sannsynlig at slike effekter vil oppstå i fisk i naturmiljøet. Siden dette var en *in vitro* studie, var det ikke mulig å studere hvordan toksikokinetikken virker på CNT. Dessuten kan det ikke fastslås med sikkerhet ved hvilke konsentrasjoner gentoksiske effekter kan forekomme. Det er også viktig å ta i betraktning at CNT kan virke synergistisk sammen med andre giftige stoffer (for eksempel plantevernmidler). Fremtidige evalueringer av CNT toksisitet ville dra nytte av å holde et høyere nivå av standardisering, og å undersøke interaksjoner mellom CNT og analyse/serumskomponenter.

## List of abbreviations

| | |
|---|---|
| BSA | Bovine serum albumin |
| CNT | Carbon nanotube |
| CVD | Chemical vapour deposition |
| DCM | Dichloromethane |
| DMSO | Dimethylsulphoxide |
| DNA-FTM | Fraction of total DNA that migrated |
| DSB | Double strand break |
| DWCNT | Double-walled carbon nanotube |
| EDTA | Ethylenediaminetetraacetic acid |
| ENM | Engineered nanomaterial |
| FBS | Fetal bovine serum |
| FCS | Fetal calf serum |
| FE | Field emission |
| LMPA | Low melting point agarose |
| MEM | Eagle's minimal essential medium |
| MML | Median molecular length |
| MN | Micronuclei |
| MQ | MilliQ |
| MRI | Magnetic resonance imaging |
| MTS | (3-(4,5-dimethylthiazol-2-yl)-5-(3-carboxymethoxyphenyl)-2-(4-sulfophenyl)-2H-tetrazolium) assay |
| MTT | (3-(4,5-dimethylthiazol-2-yl)-2,5-diphenyltetrazolium bromide) |
| MWCNT | Multi-walled carbon nanotube |
| MWCNT-P | Multi-walled carbon nanotube pristine |
| NM | Nanomaterial |
| NP | Nanoparticle |
| PBS | Phosphate buffered saline |
| PC | Protein corona |
| PEI | Polyethyleneimine |
| PLHC-1 | Poecillopsis lucida hepatocellular carcinoma |
| RF | Radio frequency |
| ROS | Reactive oxygen species |

| | |
|---|---|
| RPM | Rounds per minute |
| SWCNT | Single-walled carbon nanotube |
| TBE buffer | Tris-borate-EDTA buffer |
| TCF | Transparent conductive film |
| TE buffer | Tris-EDTA buffer |
| UV | Ultraviolet |
| UV-vis | Ultraviolet-visible |
| UVR | Ultraviolet radiation |

## Contents

# 1 Introduction

Nanotechnology can be defined as the study, manipulation and/or building of materials, devices and objects that are normally at nanoscale (1 nm = $10^{-9}$ m) (Durán et al., 2014). The size-scale of this technology is illustrated in Figure 1.1, and is related to structures that are on the molecular level. Thus, the possibilities opened up by this technology may seem indefinite as new knowledge is discovered. In fact, the field of nanomaterial (NM) sciences is very rapidly evolving in all sectors of society due to its increasingly large number of applications. It has been estimated that the use and production of engineered nanomaterials (ENM) will increase rapidly over the next years, due to lowering costs, improved performance and availability, and end user adaptability. For example, the global production capacity of carbon nanotubes (CNTs) at the end of 2010 reached an estimated 2,500 metric tonnes, and is expected to exceed 12,800 metric tonnes in 2016 (Figure 1.2) (Patel, 2011). Although exact numbers are difficult to estimate there seems to be an increasing trend in regards to production volumes and use of nanomaterials. This is a cause of concern, as nanomaterial exposure to plants, animals and humans may increase rapidly, in combination with lacking knowledge of the exposure effects. Moreover, nanomaterials are very small particles, which enables them to move with ease into cells where they can cause damage (Maynard, 2006, Durán et al., 2014).

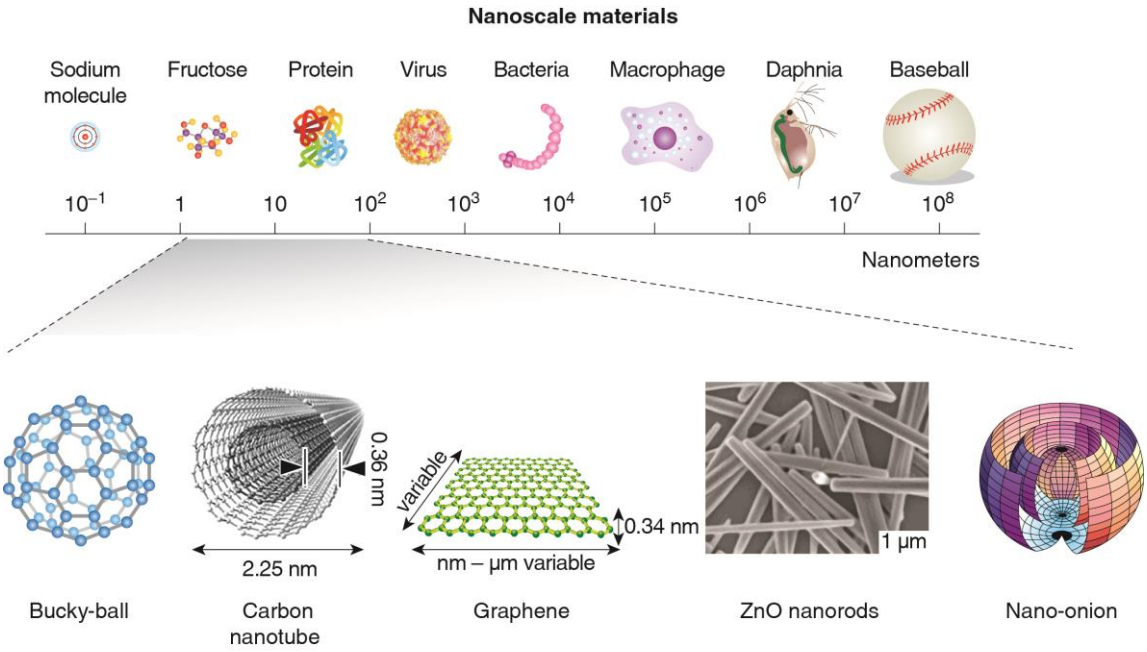


**Figure 1.1**: Size scale comparison between various nanomaterials and natural and synthetic structures (adapted from Oberdörster et al. (2013)).

Nanoparticles (NPs) (defined as having at least two dimensions between 1-100 nm (Klaine et al., 2008)) have always been present in the environment. They exist in forms such as colloids in water and soil, or as ultrafine particles in air; produced either naturally or by anthropogenic sources (Lead and Wilkinson, 2006). Intentionally produced NPs are usually referred to as ENMs, and can have a wide range of different applications. They may address global environmental and societal challenges within fields as diverse as structural engineering, electronics, optics, consumer products, soil and water remediation and medicine (Oberdörster et al., 2007). This diverse range of products not only enables economic and societal benefits, but also requires the use of several different nanomaterials, all of which can pose potential risks to humans and the environment. Both metallic and carbonaceous nanomaterials are frequently used, but in this study the focus will be on carbon nanotubes, and then specifically multi-walled carbon nanotubes (MWCNTs) (see next section).

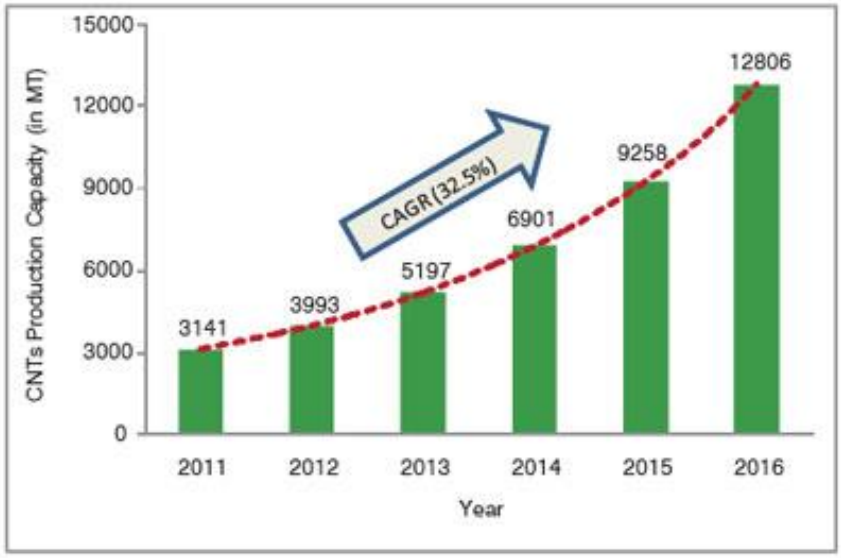


**Figure 1.2**: Estimated annual global production volumes of CNTs in metric tonnes (based on volumes from 2010) (Patel, 2011).CAGR= Compound annual growth rate.

## 1.1 Carbon nanotubes: Properties and structure

Carbon nanotubes have been subject to increasing interest since their discovery in 1991, due to their large range of useful properties (Iijima, 1991). These include high surface area to volume ratio, ultralight composition, unique electronic and thermal properties, and high mechanical strength (Sgobba and Guldia, 2009, Green and Hersam, 2011). The structural organisation of CNTs give them these unique properties, as they are composed of $sp^2$ hybridised carbon atoms which are arranged into fused hexagonal rings (Petersen and Henry, 2012). Carbon nanotubes have therefore attracted increasing attention in recent years for their applications in both electronic and biomedical fields. They have been found useful as electrical conductors and amplifiers (transistors) (Park et al., 2013), transporters of drugs and other biomolecules (Liu et al., 2007, Wu et al., 2008, Zucker et al., 2012), as well as scaffolds for cell growth (Fabbro et al., 2012) and as imaging reagents (Wu et al., 2011).

A CNT is often described as a graphene sheet rolled into a cylinder of only a few nanometers in diameter, and capped with a spherical fullerene. These cylinders are referred to as single-walled carbon nanotubes (SWCNT), but several concentric cylinders can also form CNTs and are then termed double-walled- (DWCNT) or multi-walled carbon nanotubes (Figure 1.3) (Mauter and Elimelech, 2008). Multi-walled carbon nanotubes were the first product of CNT synthesis, whereas SWCNTs were discovered later by the use of a cobalt-nickel catalyst (Klaine et al., 2008). Multi walled CNTs can be composed of up to 30 concentric cylinders, with outer diameters usually between 30-50 nm (Petersen and Henry, 2012). The way the graphene sheets are wrapped varies and is thus represented by two unit vectors (*n*, *m*), which relate the structure of the CNT to its diameter and chirality. The vectors also determine whether the CNT has conductive or semi-conductive character (Tans et al., 1997, Sgobba and Guldia, 2009). For good quality metallic SWCNTs, the transport of electrons do not suffer from scattering events over a length of several micrometers, and equally for semiconducting SWCNT over a few hundred nanometers. This conducting electron density is about 1000 times better than in copper wires, and shows the tremendous potential of these nanostructures (Robertson, 2004, Sgobba and Guldia, 2009). Furthermore, the $sp^2$-hybridised carbons contribute to the high mechanical strength observed for CNTs, which are stronger than the $sp^3$ hybridised carbons in diamond. This composition also promotes good chemical stability. Additionally, a SWCNT with a surface area up to 1500 $m^2 g^{-1}$ is lighter than aluminium, thermally stable at temperatures exceeding 1000 °C, and has a thermal conductivity that is twice that of diamond (Pop et al., 2006).

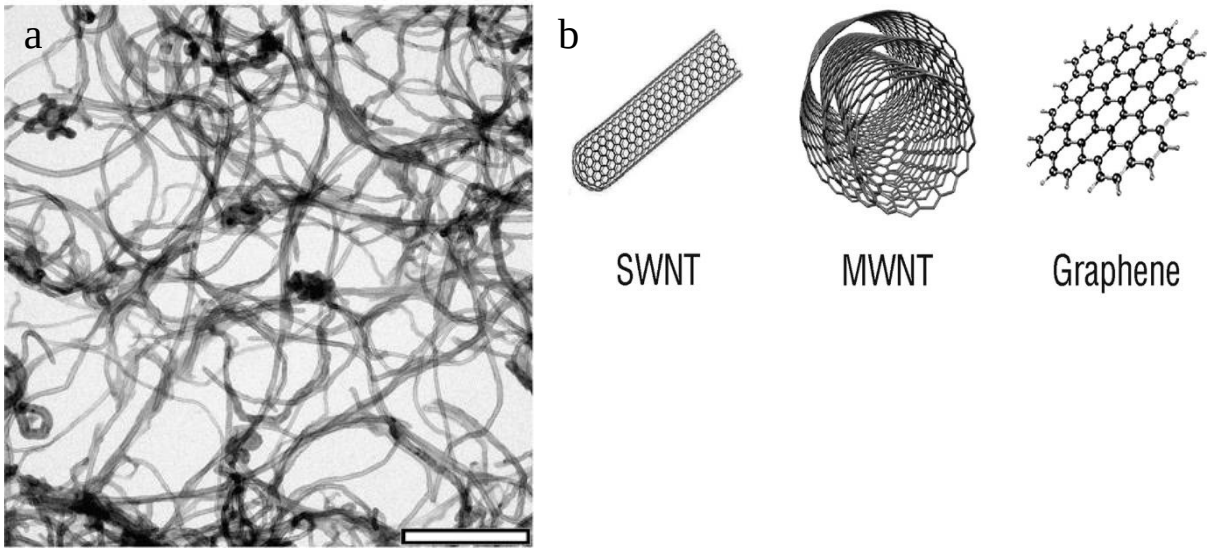


**Figure 1.3**: Carbon nanotubes **a**) Transmission electron microscopy of multiwalled carbon nanotubes (adapted from Stéfani et al. (2011)), and **b**) SWCNT, MWCNT and graphene sheet (adapted from Mauter and Elimelech (2008)). Bar = 200 nm.

Structural differences between SWCNTs and MWCNTs also result in some differences in their properties. The various layers of a MWCNT usually have different chiralities and may alternate randomly between metallic and semi-conducting properties (Saito et al., 1993,

Collins et al., 2001). Larger diameter tubes usually have greater defect densities, such as gaps (Bandaru, 2007). In relation to conductivity, the current flow only seems to occur through the outermost nanotube cylinder of MWCNTs (Bachtold et al., 1999), with only slight interaction between concentric cylinders (Saito et al., 1993). However, due to the many variations arising from several concentric nanotubes within MWCNTs, a more complex situation will usually be the case. Thus, conductivity will depend on several factors such as conducting ability of each concentric nanotube, the diameter of the MWCNT and the number of nanotubes within the MWCNT (Bandaru, 2007). Due to the higher number of nanotubes in MWCNTs than SWCNT, their mechanical stiffness is better than for SWCNTs. Thus they are often preferred in applications which requires more robustness such as field emission (FE) technologies (see next section) (Robertson, 2004).

There are several ways to produce CNTs, and the arc discharge method is the most commonly used. This method was initially used to produce $C_{60}$ fullerenes and is perhaps the easiest way to produce CNTs. However, a complex mixture of components are produced from this method, and purification is necessary to separate the CNTs from soot and residual catalytic metals. Other methods that are often used to produce CNTs are laser vaporisation, which produces CNTs in highly tangled forms mixed with various by-products; and catalytic chemical vapour deposition (CVD) of acetylene over cobalt and iron catalysts. All methods require further purification of the CNTs to remove by-products (Wilson et al., 2002).

### 1.1.1 Applications

Carbon nanotubes can have several useful applications, especially within sectors such as electronics, textile technology and nanomedicine. In a study by Kunhikrishnan et al. (2014), CNT production volumes per annum were reported to be among the top four on a worldwide scale (Table 1.1) Moreover, current annual demands of CNTs were estimated to increase from 3700-4100 tons to 5300-5720 in 2015 and finally 10500-12000 tons in 2020 (Jackson et al., 2013). Due to commercial confidentiality around the actual numbers, the estimates are not exact. Yet, these estimates give an indication of production volumes, and also suggest that it is important to assess CNT toxicity as these volumes are predicted to increase.

**Table 1.1**: Estimated global production volumes of engineered nanomaterials per annum. (Adapted from Kunhikrishnan et al. (2014)).

| Engineered nanomaterial (ENM) | ENM Production (tons year$^{-1}$) | | | | | | | | |
|---|---|---|---|---|---|---|---|---|---|
| | Worldwide | United States | Europe | Switzerland | Germany | Australia | China | Japan | Korea |
| $TiO_2$ | >60,000 | 7800–38,000 | 55–3000 | 435 | 400 | ~40,000 | 2000 | 1250 | >1600 |
| ZnO | >1,400,000 | >1000 | 5.5–28,000 | 70 | >500 | >15 | >1000 | 480 | — |
| $CeO_2$ | 0.55–2800 | 35–700 | >55 | — | — | — | — | — | — |
| $SiO_2$ | 55–55,000 | — | 55–55,000 | 75 | — | — | — | 13,500 | — |
| Fullerenes | 0.15–80 | 2–80 | 0.6–5.5 | — | — | — | — | 2 | — |
| CNT | >4065 | 55–1101 | 180–550 | 1 | >260 | >3 | >560 | >500 | 7–90 |
| Quantum dots | 0.6–5.5 | — | 0.6–5.5 | — | — | — | — | — | — |
| Nano Ag | >550 | 2.8–20 | 0.6–55 | 3.1 | >8 | — | >200 | — | ~390 |
| Major Sources | Cosmetics, textiles, paints and inks, sporting goods, battery electrodes, air and space vehicles, wind turbine blades, sensors, panel displays, membrane filters, catheters, surfactants, photonic devices, medical devices, solar cells, composites and ceramics, plastic additives, and glass materials. | | | | | | | | |
| References | Nanomaterials report (2008), Schmid and Reidiker (2008), Park et al. (2009), Wijnhoven et al. (2009), Batley and McLaughlin (2010), Carbon Nanotubes Report (2011), Hendren et al. (2011), Park et al. (2011), Zhang et al. (2011), Fries and Simkó (2012), Piccinno et al. (2012), Research and Markets (2012), Korea IT new (2013). | | | | | | | | |

#### *1.1.1.2 Electronics*

One of the major areas of application of CNTs is in the electronics sector, where they have been found very useful due to their conducting, thermal and mechanical properties. The CNTs are typically combined with other materials, or on nanostructured films deposited on various substrates such as glass, polymers and metals (Durán et al., 2014). For example, SWCNTs have been used to make flexible transparent conductive films (TCF) that can be used to amplify and conduct electricity. These films can thus be used in touch screen technology, flexible radio frequency (RF) devices, as chemical and biological sensors and to make stretchable and flexible electrodes (Park et al., 2013). Multi-walled carbon nanotubes are often preferred in TCFs to reduce the cost of the product, as SWCNT are more costly and difficult to produce (purify and disperse). Nevertheless, there are difficulties with using MWCNTs as well, particularly due to their tendency to self-aggregate in aqueous solution and form large bundles or ropes. MWCNTs were also found to be quite efficient as thermal conductors in carbon blocks for blast furnaces, although few MWCNTs remained in the specimen (Marulanda, 2011). Some additional applications include use of CNTs as superconductors, in field emission technology and as mirror actuators for space laser communication (Robertson, 2004, Marulanda, 2011). Field emission technology involves the emission of electrons from a solid under an intense electric field, which is very advantageous in CNTs due to their high surface area and low volume. This allows for use in scanning and transmission electron microscopes (de Jonge et al., 2002, Milne et al., 2004, Robertson, 2004). CNTs involved in mirror actuators for space laser communication on the other hand, are used to improve inter-satellite communications and communication between satellites and the ground; by being implemented in the motors that rotate mirrors involved in the communication (Bandaru, 2007, Marulanda, 2011).

#### *1.1.1.3 Nanomedicine*

Carbon nanotubes have also emerged in biomedical fields due to their many useful properties. In a recent review by Fabbro et al. (2013), CNTs were reported as effective substrates for neuronal growth (Cho and Borgens, 2010, Fabbro et al., 2012), effective in improving nerve cell performance (Cellot et al., 2009, Cellot et al., 2011, Fabbro et al., 2012) and able to spatially direct nerve cells (Jang et al., 2010, Jin et al., 2011a, Jin et al., 2011b) in *in vitro* regeneration studies. Moreover, CNTs have also been applied in delivery systems to transport vaccines (Singh et al., 2010), drugs (Liu et al., 2009, Zucker et al., 2012) and DNA/RNA (Liu et al., 2007, Wu et al., 2008) for potential use in gene therapy. As CNTs can be functionalised they can also be made biocompatible which is thought to enhance the process and reduce potential toxicity (Bianco et al., 2005). In addition, MWCNTs were found useful as magnetic resonance imaging (MRI) contrast agents in mice, when labelled with a MRI contrast agent (Wu et al., 2011). Others have also reported their effective use in photothermal cancer therapy studies (Marches et al., 2011), as fluorescent biological labels (Cherukuri et al., 2004) and biosensors (Park et al., 2013).

#### *1.1.1.4 Textiles*

Carbon nanotubes have also found use in textiles as a means to improve electronic textiles (e-textiles) for use in areas such as sportswear, healthcare, military and work ware (Panhuis et al., 2007). The incorporation of CNTs instead of traditional wires or conducting threads may enhance conductivity and reduce stiffness or breakage of the material/fibres (Holcombe, 2001, Service, 2003).

## 1.2 Release to the environment

Although the above mentioned structural and chemical characteristics of CNTs have proven very useful in a range of products, it is their incorporation into various materials which will eventually lead to their release in the environment. Environmental contamination by CNTs may occur through several routes (Figure 1.4), which may affect them differently (e.g. aggregation, functionalisation) (Petersen and Henry, 2012). One of the main routes of expected CNT disposal and ultimate release to the environment is suggested to be via wastewater treatment plants, although the modelling of release from contaminant sources is still limited (Mueller and Nowack, 2008, Gottschalk et al., 2009, Gottschalk et al., 2010). The expected environmental concentrations and associated risks are also currently uncertain, as much information is lacking and production volumes of CNTs may change in the future (Gottschalk et al., 2010). Yet, it is likely that much of the produced CNTs will be released into environments where they can have negative impacts on aqueous, soil and sedimentary organisms (Petersen and Henry, 2012). Current predicted environmental concentrations of CNTs in aquatic environments are in the ng/L (Gottschalk et al., 2009) and low µg/L range (Mueller and Nowack, 2008, Gottschalk et al., 2013). Aquatic systems are of particular concern as the small size, high surface reactivity and composition of CNT can cause excessive harm to aquatic organisms (Sayes et al., 2005, Kang et al., 2009, Gao et al., 2012).

However, the released CNTs present in the environment are not necessarily taken up by organisms. Uptake by the organism depends on several factors such as environmental concentration and bioavailability. Holbrook et al. (2010) found that coagulation treatment with certain factors in wastewater facilities can improve removal of MWCNTs from the liquid phase; and also that their coagulation behaviour follows the same pattern as colloids. Thus, MWCNT concentration in aquatic environments depends on other factors present in the water, which is important to consider when constructing ecotoxicity tests.

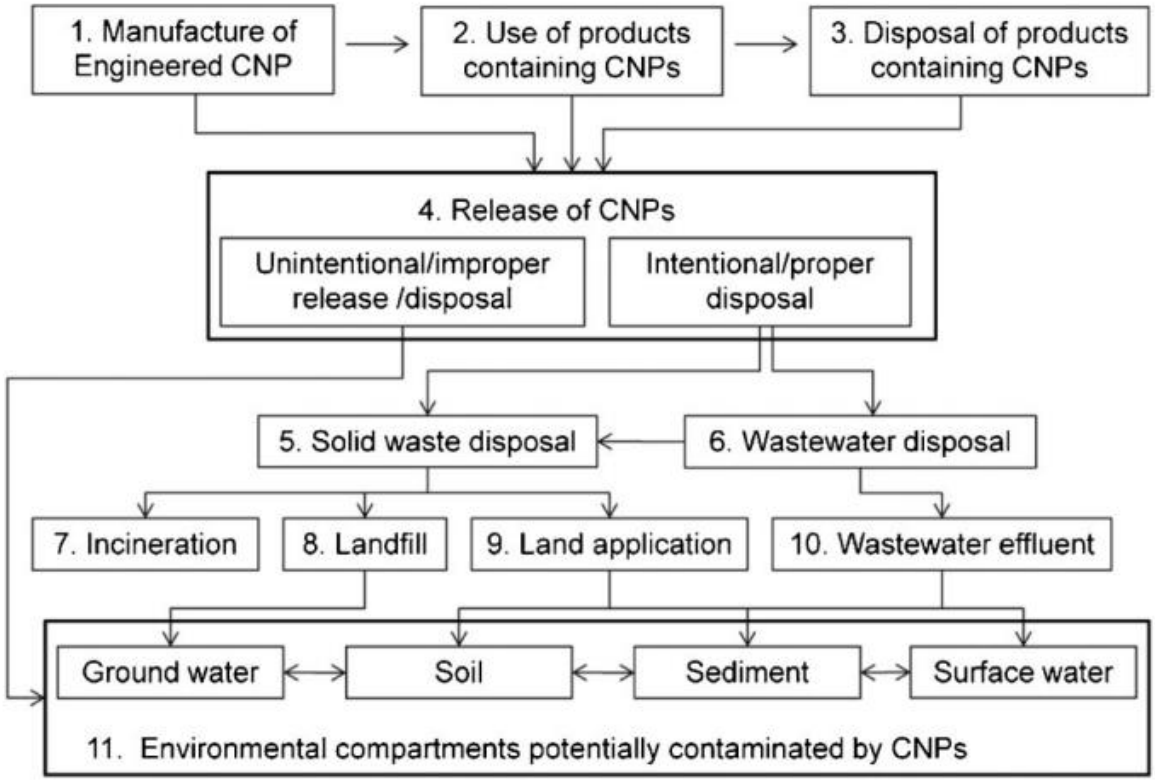


**Figure 1.4:** Contaminant sources that lead to the release and distribution of carbon nanoparticles in the environment, and their subsequent exposure to various organisms. CNP= carbon nanoparticles. Adapted from Petersen and Henry (2012).

### 1.2.1 CNT behaviour in the environment and bioavailability

Carbon nanoparticles do not naturally disperse in aqueous environments due to their inherent hydrophobic character, and will instead aggregate and form agglomerates. This is most often considered a problem, because it can be more difficult to study the effects of CNTs when agglomerated, and since this state may be harmful when for example using them in nanomedicine. Therefore CNTs are often functionalised, i.e. attaching "chemical functionalities" on the nanotube (e.g. hydrophilic groups), which will prevent this behaviour (Hirsch and Vostrowsky, 2005). However, this may also change bioavailability and effects of the CNTs.

Bioavailability of nanomaterials to fish has been reviewed by Handy et al. (2008b). This review reports that nanoparticles will usually interact with fish as emulsions or suspensions at very small sizes, and is therefore readily available to the gills of fish. Ingested NPs also presents a risk for example through stress induced drinking, and NPs in the liquid phase can therefore present either a respiratory or dietary exposure risk. Uptake of NPs across the gill and gut surfaces is more likely to occur through vesicular processes, than by membrane transport or diffusion. However, lipophilic NPs (such as CNTs) may be able to directly diffuse across the cell membrane. Uptake through the skin is less likely, especially in healthy

individuals. Although certain conditions may favour the formation of larger NP aggregates (e.g. saline or hard waters), possible bioavailability should not be excluded on this basis alone. Several interactions and mechanisms may still allow such aggregates to be bioavailable (for example through dietary uptake).

In relation to carbon-based nanomaterials, their inherent hydrophobicity may decrease bioavailability. However, NM functionalisation either during manufacture or in the water column will usually increase NM dispersability and potential bioavailability. The potential for functionalisation to occur in the environment is unknown (Handy et al., 2008b). However, carbon NMs will interact with dissolved organic matter in the water column, which will affect their presence in the aquatic environment (Lee et al., 2007). Such physicochemical properties will probably allow uptake via the water column, contact with sediments or via the diet. Following potential uptake it may also be possible for both individual and aggregated NPs to be endocytosed by cells. However, it is unknown how CNTs may behave in the blood, and this probably depends on the physico-chemical characteristics of the CNTs. Hydrophobic carbon NMs may accumulate in lipids and fatty tissues, whereas more hydrophilic NMs may accumulate in tissues with higher blood flow (Handy et al., 2008b).

Based on the most probable routes of uptake, carbon NMs are most likely to access the blood stream via the gills or the gut. It is unclear whether carbon NMs will be taken up in these compartments to allow transport to other organs, such as the liver. However, carbon NM uptake via the gut, unless damaged, seems less likely. In fact, these NMs may be more prone to be trapped in the gut mucus layer than other substances, as demonstrated with SWCNTs (Smith et al., 2007), but more data is required to determine potential NM uptake mechanisms (Handy et al., 2008b).

#### 1.2.1.1 Nanomaterial behaviour in cell media

In terms of *in vitro* toxicology studies, NM interactions with growth medium constituents is important for bioavailability. It has been demonstrated in several studies that serum proteins have a tendency to adsorb onto the nanomaterials present, to form a protein corona (PC) (Blunk et al., 1993, Lynch et al., 2007, Ehrenberg et al., 2009). This PC changes the size and surface composition of the NM, and gives it a distinct biological identity from its original synthetic profile. This can in turn alter the NM activity, biological distribution, clearance and toxicity. The PC appears to be unique for each NM depending on its physico-chemical characteristics such as surface charge and shape (Nel et al., 2009, Walkey and Chan, 2012). Such unique NM PCs can cause differential impacts on cellular uptake and cytotoxic responses as demonstrated in *in vitro* studies (Clift et al., 2010, Tedja et al., 2012).

### 1.2.2 Functionalisation

Functionalisation of CNTs are important for various applications of these NMs due to their inherent hydrophobic character. However, it is important to distinguish between covalent and non-covalent functionalisation, between SWCNTs and MWCNTs, and between individual

tubes as opposed to tube bundles. A covalent functionalisation refers to the covalent bonding of the chemical moiety to the nanotube, either at the termini or at the sidewalls. This will disrupt the $sp^2$ hybridisation between the carbon atoms, instead forming $sp^3$ hybridised atoms that have lost their conjugation. This effect can be used advantageously in defect functionalisation where defect sites already present are used for functionalisation. Defect sites may be open holes or ends in the structure or irregularities in the graphene framework. Non-covalent functionalisation on the other hand is based on adsorption forces such as van der Waals'. Most functionalisations are on the outside of the nanotube, but it is also possible to functionalise the inside of the tube (Hirsch and Vostrowsky, 2005).

Another consideration when working with functionalised CNTs is how this functionalisation may impact on CNT toxicity (Chen and Elimelech, 2007). Gao et al. (2012) showed that functionalised carbon NPs in suspension induced different effects in two aquatic species, where some suspensions did in fact reduce toxicity. Functionalisation of MWCNTs with polyethyleneimine (PEI) on the other hand, increased the toxicity of MWCNTs in *Daphnia magna* compared to the pristine form (Petersen et al., 2011). Thus, to be able to assess environmental risks, it is essential to account for the possible effects induced by CNT surface coatings.

#### *1.2.2.1 Attachment of oxidic groups*

One of the most common forms of covalent functionalisations is the oxidation of CNTs by liquid phase or gas phase, which introduces carboxylic groups and other oxygen containing moieties such as hydroxyl, carbonyl, ester, and nitro groups into the tubes (Hirsch and Vostrowsky, 2005). The oxidative treatment can be achieved by using boiling nitric acid (Dujardin et al., 1998, Rinzler et al., 1998, Holzinger et al., 2000), sulphuric acid (Sumanasekera et al., 1999) or mixtures of both (Rinzler et al., 1998); or oxygen containing gases (Ajayan and lijima, 1993, Tohji et al., 1996, Mawhinney et al., 2000) at elevated temperatures (Figure 1.5). This oxidative method of functionalisation also allows for the removal of metallic catalyst particles used during the nanotube synthesis, as well as removal of the by-product amorphous carbon (Liu et al., 1998). At the end of the process carboxylic acid or other oxygen containing groups are bound to the nanotube, which will also be useful sites for further modifications (Durán et al., 2014).

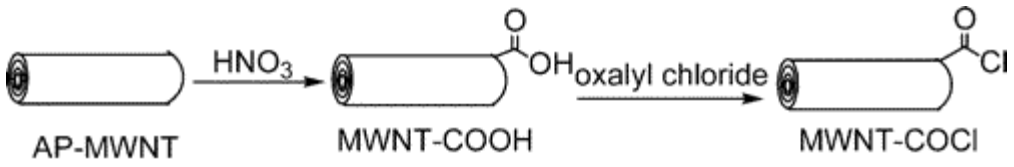


**Figure 1.5**: Chemical functionalisation of MWCNTs adapated from Hu et al. (2004).

#### *1.2.2.2 Amidation*

After the introduction of carboxylic groups to nanotubes by oxidative procedures there is a large spectrum of further modifications that can be achieved. For example, several

carboxamides can be formed via carboxylic acid chlorides and promote functionalisation with aliphatic amines, aryl amines, amino acid derivatives, peptides etc. There are several methods to prepare carboxamide, but one example could be to activate the carboxylic acid by conversion into acyl chloride groups with thionyl chloride (Chen et al., 1998, Liu et al., 1998), and then the acyl chlorides formed can be transformed to carboxamides by amidation (Figure 1.6).

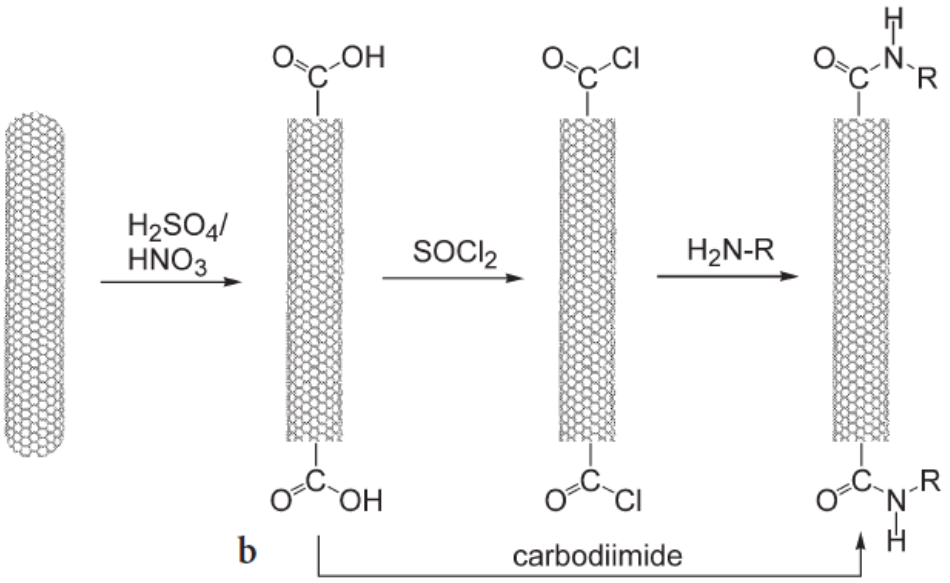


**Figure 1.6**: Illustration of oxidative etching of SWCNT followed by thionyl chloride treatment and subsequent amidation (adapted from Hirsch and Vostrowsky (2005)).

## 1.3 Toxicity of carbon nanotubes

### 1.3.1 Toxicity studies in aquatic organisms

In terms of possible adverse effects to aquatic ecosystems, there are still large knowledge gaps, especially in relation to the toxicity of MWCNTs in fish. Thus, more research is needed to evaluate exposure conditions and possible hazards related to MWCNT presence in the aquatic environment (Handy et al., 2011). Some studies have been conducted thus far to assess eco- and cytotoxicity of MWCNTs. Cheng et al. (2009) reported that purified MWCNTs induced an immune response *in vivo* in zebrafish, and also negatively affected reproduction. They concluded that this might indicate that purified MWCNTs have long-term toxicity effects when delivered into the body. A later study by Cheng and Cheng (2012) found malformations in zebrafish embryos exposed to functionalised MWCNTs of different length, and abnormal cell-organisation that lead to developmental arrest. It was suggested also that CNT length plays an important role in *in vivo* toxicity.

Other studies, with SWCNTs, have also reported potential toxic effects on aquatic organisms. Smith et al. (2007) reported that SWCNTs are a respiratory toxicant in trout, and caused

some oxidative stress and cellular pathologies. Another study, by Rocha et al. (2013), found a dual effect of SWCNT in *in vitro* assays with zebrafish. Oxidant behaviour was observed at low concentrations (0.1 and 1.0 mg/L) while an antioxidant effect was observed at the highest concentration (10.0 mg/L), indicative of oxidative stress at low doses. Thus, results are not clear in this area of research, and more studies with higher levels of standardisation are necessary to get a broader understanding of this research area (Petersen and Henry, 2012).

### 1.3.2 Genotoxic effects

A chemical or physical agent is considered genotoxic if it can cause an adverse effect on the structure and/or function of DNA. Examples of genotoxins are ultraviolet radiation (UVR) and heat, which can alter the DNA structure and cause repair related strand breaks or other DNA damages (Theodorakis et al., 1994). Thus, genotoxic effects may also be expected upon exposure to MWCNT in aquatic organisms, as it has been demonstrated that CNTs can interact with proteins and DNA and alter their native structures (Karajanagi et al., 2004, Patlolla et al., 2010, Wu et al., 2012). Such effects have for example been reported in human dermal fibroblast cells, where functionalised MWCNTs caused a loss of cell viability through DNA damage and programmed cell death (Patlolla et al., 2010). Another study also reported DNA damage in a human cell line, after SWCNTs exposure, which disrupted normal cell division by interfering with normal spindle function. In fact, it was suggested that the resemblance between SWCNTs and microtubules may be the reason for this interference (Sargent et al., 2012). Few such studies have been conducted in fish cell lines, which is the topic of investigation in the current study.

There are several ways in which CNTs have been proposed to be toxic, and it has been suggested by Durán et al. (2014) that genotoxicity is their main mechanism of toxicity. However, their mechanism of action seems to be different from classical genotoxicants, by presenting several DNA damage pathways (Singh et al., 2009, van Berlo et al., 2012) (Figure 1.7). This was illustrated in a study by Zhu et al. (2007), where the authors observed that MWCNTs increased the expression of a base excision repair protein, induced a double-strand break (DSB) repair protein and increased the mutation frequency, in mouse embryonic stem cells.

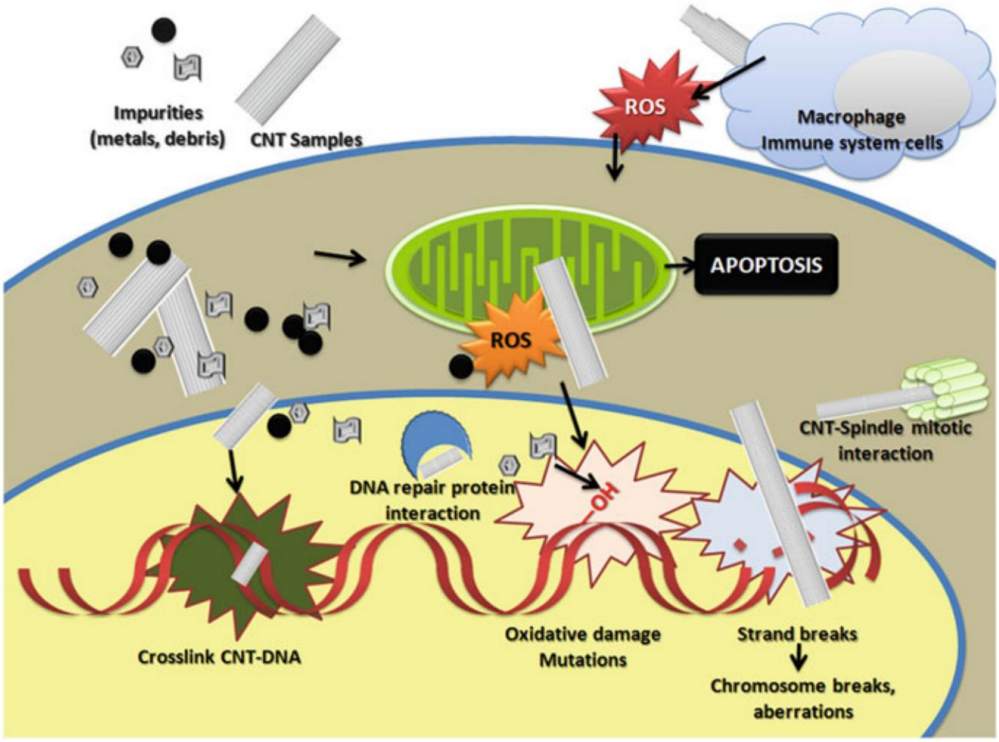


**Figure1.7:** Proposed mechanisms of CNT genotoxicity. CNTs can induce DNA damage directly and indirectly, and as a secondary event by induction of inflammation. Adapted from Durán et al. (2014).

The main pathway proposed to be associated with CNT toxicity is oxidative stress (Shvedova et al., 2008). Oxidative stress is the mechanisms in which the cell's redox conditions are imbalanced, usually due to increased levels of reactive oxygen species (ROS) within the cell and decreased antioxidant capacity. ROS molecules are highly reactive and can disrupt the cell homeostasis by interacting with for example lipids, proteins and DNA; but their generation depends largely on the presence of a metal catalyst that can take part in the Fenton reaction involved in ROS production (Durán et al., 2014). Such metal catalysts are used in the synthesis of CNTs and may include Fe, Co, Mn, Ni and Mo, which may be present even after purification of the nanotubes. Other impurities such as amorphous carbon, oxidation debris, and carbon nanostructures may also contribute to the genotoxicity (Silva et al., 2009, Campos-Delgado et al., 2010). However, it is also possible that the CNT subcellular presence in itself can cause genotoxicity. For example, Wang et al. (2012) found the presence of CNTs in mitochondria which caused an induction of ROS; this in turn generated DNA damage and cell death by apoptosis in mice alveolar macrophages.

Induction of DNA strand breaks is also a proposed mechanism responsible for CNT genotoxicity, which is often assessed by the comet assay. Several studies have detected DNA breaks by the comet assay in *in vitro* systems exposed to both MWCNTs and SWCNTs (Durán et al., 2014). In some cases, DNA breaks were detected independent of oxidative damage, possibly suggesting that high purity CNTs with few metal impurities may not cause oxidative DNA damage. Several studies support this mechanism which suggests that

oxidative stress is not a unique pathway of DNA damage induction by CNTs (Karlsson et al., 2008, Kisin et al., 2011, Cavallo et al., 2012, Ursini et al., 2012a, Pelka et al., 2013). Moreover, Ghosh et al. (2011) found that CNTs were able to interact directly with DNA via crosslinking, in combination with inhibition of DNA migration.

## 1.4 Cytotoxicity assay

To assess cytotoxic effects of CNTs there are various assays that can be apllied, but the MTT (3-(4,5-dimethylthiazol-2-yl)-2,5-diphenyltetrazolium bromide) assay was used in the present study. This assay detects living and metabolically active cells by the production of a dark blue product (formazan) from the pale yellow substrate MTT (a tetrazolium salt). Only live cells with functioning mitochondrial enzymes (dehydrogenases) will be able to metabolise MTT, by cleaving the tetrazolium ring of the salt. The resulting colour intensity is then measured by a scanning multiwell spectrophotometer (ELISA reader) to produce a quantitative cytotoxicity measure. The advantage of using this assay is its ability to quantitatively measure large numbers of samples, rapidly and with high precision. Furthermore, the assay is able to detect very small numbers of living cells (e.g., 200), and absorption is not significantly influenced by high cells concentrations ($1x10^6$ cell/mL) (Mosmann, 1983).

Despite being a widely used assay to assess cytotoxicity, cell viability, and proliferation of living cells, it may also have some weaknesses, especially in relation to carbonaceous nanomaterials (Berridge and Tan, 1993, Liu et al., 1997). Geys et al. (2010) investigated various assay conditions that can influence the outcome of cytotoxicity tests with nanomaterials. For MWCNTs, cell density of human lung cells (A549) were not found to have a large impact on cell viability, which was suggested to be due to the low toxicity of the nanotubes. Similar results were detected when MWCNT adsorption of assay components, such as MTT or formazan, were examined. Adsorption of formazan crystals to graphene nanoparticles were also found to be negligible in a recent study by Khim Chng et al. (2014).

However, another study have found opposing results, where formazan crystals adsorbed onto SWCNTs, creating false negative results for cell viability, by reducing the soluble formazan fraction (Wörle-Knirsch et al., 2006). Similarly, MTT has also been reported to be adsorbed by carbon black (a nanoscale particulate), which reduced the absorbance reading and gave false positive signals for cytotoxicity (Monteiro-Riviere and Inman, 2006). Nanotubes may also disturb the assay by absorbing or dispersing light during the measurement, and are found to stick to the cells (Geys et al., 2010). In addition, CNT interference with serum constituents should also be considered in the MTT assay. Again, Geys et al. (2010) reported only very slight impacts on cell viability between serum free and 10% fetal calf serum (FCS) assays, although the serum containing assay showed slightly higher cytotoxicity. This was suggested to be due to a better dispersion of the nanotubes, thus giving an increased effective dose. Conclusively, there are certain considerations that should be controlled for when conducting *in vitro* assays with carbonaceous nanoparticles in order to avoid biased results.

## 1.5 DNA double strand break analysis

DNA strand breaks are not uncommon in a cell, and breaks are continuously repaired. Heat energy can for example produce thousands of abasic sites per cell per day, which during repair cause transient strand breaks. This can in turn lead to permanent damage of the DNA if the repair is not successful (Elliott and Elliott, 1997, Shugart, 2000). Direct strand breaks may also occur, upon exposure to for example ionising radiation or radiomimetic compounds (Shugart, 2000, Helleday et al., 2007). DNA double-strand breaks (DSBs) are among the most severe types of DNA lesions, because it can disrupt the further replication and transcription of the DNA template. This in turn can result in loss of chromosomes and/or cell death, mutations, chromosomal rearrangements (Thacker, 1986, Jackson, 1999) and carcinogenesis (Jeggo, 1998, Kanaar et al., 1998, Pfeiffer, 1998). Moreover, such damages represent a major concern at an ecological level, because they can lead to impaired reproduction, accelerated ageing processes and tumour induction in individuals (Wurgler and Kramers, 1992).

To be able to detect such damages within a cell, several techniques can be used, including the comet assay, the alkaline unwinding assay and agarose gel electrophoresis (Shugart, 2000). Agarose gel electrophoresis have previously been used on blood from glaucous gulls (*Laurus hyperboreus*) (Krøkje et al., 2006), common eider (*Somateria mollisima*) (Fenstad et al., 2014) and on fish blood cells (Theodorakis et al., 1994) to assess DSBs after genotoxic exposure. By conducting the electrophoresis under neutral pH conditions, relative DSB frequency can be detected, as the DNA duplex structure remains intact. This will only allow DSB fragments to migrate in the gel as opposed to single stranded fragments which are detected at alkaline conditions. The fraction of DNA that migrates out of the sample well relative to the DNA loaded (DNA fraction of total DNA that migrated, DNA-FTM) can then give a measure of the DSB frequency (Wlodek et al., 1991, Theodorakis et al., 1994). A further application of this method is the measurement of median molecular length (MML) of the DNA that migrated, where a lower MML generally indicates more damaged DNA (Theodorakis et al., 1994).

The agarose gel electrophoresis method described above is advantageous because it embeds the cells containing the DNA in agarose plugs before electrophoresis. This reduces the number of steps used to isolate the DNA from the tissue, while simultaneously protecting the DNA from external damage. When DNA is prepared in this manner it will not undergo the usual shearing forces of a conventional isolation procedure (homogenisation, pipetting etc.). This may be especially important when working with fish liver cells, which have been found susceptible to rapid DNA degradation presumably by endonucleases within the cells. Thus, the above preparation will minimise external damage to DNA, while addition of Proteinase K in the procedure will digest cell components that may damage the DNA internally in the cell, such as endonucleases. Furthermore, this procedure minimises the number of pipetting stages, which improves its reproducibility over the alkaline unwinding assay; as well as enabling detection of both single- and double-strand breaks if relevant (Theodorakis et al., 1994).

## 1.6 Aims and objectives

The aim of this study was to investigate if different surface coatings of constant sized MWCNTs have the potential to induce cytotoxic and genotoxic effects *in vitro* in fish liver cells; and if these potential effects differ with the type of surface coating.

To accomplish this aim, the fish cell line PLHC-1 was exposed to four MWCNTs with different surface chemistries (from TimesNano). The four MWCNTs selected had the same outside diameter (8-15 nm) and length (~ 50 µm), but were functionalised with either -OH, -COOH, $-NH_2$, or remained uncoated (Table 1). Thus, it was possible to measure lethal and sublethal effects of various functionalised MWCNTs in the fish cell line. Results from the current study may therefore provide further insight into the ecotoxicology of functionalised MWCNTs, and more knowledge on how to perform risk assessment within this field.

# 2 Materials and methods

## 2.1 The PLHC-1 cell line

The hepatoma fish cell line from *Poeciliopsis lucida* (desert topminnow, PLHC-1) will be used to assess cyto- and genotoxicity of MWCNTs. The PLHC-1 cell line was initiated from a hepatocellular carcinoma and has been through over 200 passages *in vitro* (Hightower and Renfro, 1988). The original tumour was chemically induced in the desert topminnow *P. lucida* by the chemical 7, 12-dimethylbenz[*a*]anthracene and then carried *in vivo* as a serially transplantable dorsal muscle implant for several years before cultivation *in vitro* (Schultz and Schultz, 1985). The PLHC-1 cell line is often used in toxicological studies because the cells are epithelial-like and have maintained some of their original liver functions such as glycogen production and cytochrome P450 1A activity (Ryan and Hightower, 1994, Escher et al., 1997, Fernández-Cruz et al., 2013).

Several recent studies have also used this cell line to assess toxicity of various nanoparticles (Naha and Byrne, 2013, Lammel and Navas, 2014, Song et al., 2014). In the study by Lammel and Navas (2014), a preliminary sensitivity screening showed that the PLHC-1 cell line was more sensitive to the graphene nanoplatelets of interest than the rainbow trout hepatoma cell line RTH-149. The differing sensitivity of this cell line has also been documented in other studies, which points to important species specific differences (especially between mammalian and piscine cell lines) (Fernández-Cruz et al., 2013, Song et al., 2014). Moreover, the liver is known to play an important role in detoxification processes, and is considered one of the major target organs for nanoparticles (NPs) in fish, which makes PLHC-1 a suitable cell line (Kashiwada, 2006, Handy et al., 2008a, Hou et al., 2013). Additional benefits include its ability to be cultured at conditions (30°C, 5% $CO_2$ atmosphere) which are closer to most of mammalian hepatoma cell lines used up until now in cytotoxicity studies (Fernández-Cruz et al., 2013). The cell line was available from the genotoxicity lab at NTNU, Trondheim (Norway).

### 2.1.1 Cell culture

#### *2.1.1.1 Materials and chemicals*

Materials, chemicals and solutions used in cell culture are presented below. Compositions of the solutions are reported in Appendix I.

| Material | Catalogue number | Manufacturer |
|---|---|---|
| Autoclave | SX-700E | TOMY |
| Automated pipette, battery operated | 4-00-031 | Drummond scientific |
| Balance | AE 260 | Mettler |
| Cell cultivating flasks, 75 $cm^3$ | 83.1813 | Sarstedt |
| Centrifuge, 3-10 | 37622 | Sigma |
| Centrifuge tubes | 347856118559 | Thermo Scientific |
| Cryo tubes 2 mL | 87003-406 | VWR International |
| Incubator cabinet ($CO_2$, steri-cycle) | Model 371 | Thermo Fisher Scientific |
| Microscope | TS100 | Nikon eclipse |
| Nitrogen container | HCB00B137 | Thermolyne |
| Pipettes | | |
| 200 µL | X64031H | Gilson |
| 1000 µL | X63642H | Gilson |
| Pipette tips | | |
| 200 µL | 70.760.502 | Sarstedt |
| 1000 µL | 70.762.100 | Sarstedt |
| Sterile hood | S-2010 1.2 | Heto Holten AS |
| Sterile serological pipette tips 10 mL | P8100 | Biosorfa |

| Chemical | Catalogue number | Manufacturer |
|---|---|---|
| Dimethylsulfoxide (DMSO, spectrophotometric grade) | 1.02950 | Merck |
| Eagle's Minimal Essential Medium (MEM) | M4655 | Sigma |
| Ethanol, 96% | 24106 | Merck |
| Ethylenediaminetetraacetic acid disodium salt dihydrate (EDTA, 99+%) | E-5134 | Sigma |
| Foetal bovine serum (FBS) | F9665 | Sigma |
| Penicillin-streptomycin | 15070-063 | Gibco |
| Phosphate buffered saline (PBS) tablets | 18912-014 | Gibco |
| Trypsin 2.5% | 15090-046 | Gibco |

| Solutions |
|---|
| MEM – Growth medium |
| Phosphate buffered saline (PBS) |
| Trypsin, 2.5% with 1% EDTA |
| EDTA |

#### *2.1.1.2 Procedure for cultivating cells*

Original PLHC-1 cells were obtained from the American Type Culture Centre in the autumn of 2006 and stored in liquid nitrogen. Cells from passage 8 (2006) were retrieved from liquid nitrogen on the 15.01.15, thawed and subsequently transferred to a 75 $cm^2$ cell cultivating flask, containing 20 mL preheated Eagle's Minimum Essential Medium (MEM) with 5% FBS and 1% Pen/Strep. The growth medium was changed after 24 hours. Cells were grown in a humidified atmosphere (30°C, 5% $CO_2$), growth medium was changed 2-3 times a week and cells split 1-2 times per week, depending on experimental setup.

Sub culturing was performed when the cells were confluent. Growth medium was then removed from the culture flask and rinsed with 20 mL phosphate buffered saline (PBS), or expired growth medium (without additives). The PBS was then removed and replaced with 25 µL trypsin (2.5% Trypsin with 1% EDTA) in 5 mL PBS, and incubated for 2-3 minutes at 30°C. If required, the cells were suspended by firmly tapping the culture flask on a hard surface. Then, 5 mL of PBS or expired medium was quickly added to the cell suspension and the flask rinsed a few times with the mixture. Suspended cells were then transferred to a centrifuge tube, followed by centrifugation for 5 minutes at 1088 rounds per minute (rpm). The supernatant was removed by pouring and the cell pellet was resuspended by hitting the tube. The pellet was rinsed by adding 10 mL PBS to the tube, inverting it and centrifuging it again at the same parameters. Finally, the supernatant was removed and the pellet was resuspended in growth medium (1 mL). The desired dilution of cells was transferred to a culture flask(s) with 20 mL preheated growth medium. The cells were never diluted below 1:8.

The same sub culture procedure was used to prepare cells for storage in liquid nitrogen, but an additional washing step was added to remove trypsin remains. The cells were then suspended in 0.5 mL growth medium and added to a cryotube containing 0.5 mL freeze medium (comprising 20% DMSO, 20% FBS and 60% growth medium) to a final concentration of 1mL. Alternately, 0.5 mL of cell suspension was preserved in 0.5 mL of 20% DMSO and 80% FBS. The cryotube was then put in the freezer at -80 °C for one hour, and subsequently transferred to liquid nitrogen (-196 °C) for storage.

## 2.2 The carbon nanotubes

The carbon nanotubes were provided by SINTEF Materials and Chemistry (Trondheim, Norway), and were obtained from TimesNano (China). Below is a table describing the physical properties of the MWCNTs.

**Table 2.1**: Physical and chemical characteristics provided by TimesNano (www.timesnano.com) and determined by SINTEF staff, of four selected MWCNTs.

| | MWCNT-P | MWCNT-OH | MWCNT-COOH | MWCNT-$NH_2$ |
|---|---|---|---|---|
| **SINTEF-ID** | 2015-003 | 2015-005 | 2015-006 | 2015-007 |
| **TimesNano-ID** | TNM2 | TNMH2 | TNMC2 | TNMN2 |
| **Average diameter[a] [nm]** | 14,8 | 14,3 | 20,3 | 16,7 |
| **Length[b] [µm]** | ~50 | ~50 | ~50 | ~50 |
| **Oxygen surface content[h] (%)** | 1,48 | 3,89 | 5,7 | - |
| **Particle radius[fg] [nm]** | 185 | 180 | 143 | 251 |
| **Purity[b] (%)** | >95 | >95 | >95 | >95 |
| **Surface area[c] [$m^2$/g]** | 147,7 | 142,7 | 137,7 | 161,8 |
| **Surface moiety content[b] (wt%)** | - | 5.58 | 2.56 | 0.45 |
| **Volume mesopore[e] [cm3/g]** | 0,54796 | 0,601327 | 0,580744 | 0,663413 |
| **Volume micropore[d] [cm3/g]** | 0,012809 | 0,01072 | 0,013037 | 0,006008 |
| **Zeta potential[f]** | -17,6 | -18,5 | -18,9 | -15,7 |

[a] Measured from TEM images [b]Given by manufacturer [c]Calculated by the BET method [d]From t-plot [e]From BJH method [f]Measured on CNTs dispersed in NOM (natural organic matter) solution [g]Obtained from DLS [h]Obtained from XPS

According to TimesNano, MWCNT-Pristine (MWCNT-P) is produced by acetylene catalytic decomposition over a Ni-based catalyst and often exists in bundles. MWCNT-OH (hydroxyl) and MWCNT-COOH (carboxyl) are MWCNT-P hydroxyl and carboxyl derivates respectively. They are produced by $KMnO_4$ oxidation in $H_2SO_4$ solution at different temperature and $KMnO_4$ concentration. MWCNT-$NH_2$ (amino) was produced by chemical vapour deposition (CVD). Purity is reported as >95% (wt%) for all four MWCNTs (Sciences, 2014).

### 2.2.1 Preparation and quantification of carbon nanotube exposure solutions

The preparation of the MWCNT exposure solutions was conducted at SINTEF Sealab using the generic Nanogenotox dispersion protocol by Jensen et al. (2011). The quantification of the exposure solutions was also conducted at SINTEF Sealab according to the NANoREG CNT aqueous dispersion protocol (Booth and Sørensen, 2013).

### 2.2.2 Procedure for making 0.05% sterile filtered BSA water

According to the generic Nanogenotox dispersion protocol, bovine serum albumin (BSA) water (0.05%) was used to disperse the MWCNTs.

#### *2.2.2.1 Materials and chemicals*

Materials and chemicals used in preparation of sterile filtered BSA water 0.05% are presented below.

| Material | Catalogue number | Manufacturer |
|---|---|---|
| Automated pipette, battery operated | 4-00-031 | Drummond scientific |
| Balance | AE 260 | Mettler |
| Erlenmeyer flask (250 ml) | | |
| Sterile centrifuge tube (50 mL) | 430829 | Corning |
| Sterile disposable filterware with collection flask 200 mL (0.2 µm) | 431096 | Corning |
| Sterile serological pipette tips 10 mL | P8100 | Biosorfa |
| Volumetric flask (100 mL) | | |
| Weighing boat (plastic) | | Sigma Aldrich |

| Chemical | Catalogue number | Manufacturer |
|---|---|---|
| Bovine serum albumin | A-9418 | Sigma Aldrich |

#### *2.2.2.2 Procedure*

The production of 0.05% w/v BSA water was performed in two steps where step one involved the production of sterile filtered 1% w/v BSA stock solution. In Step 2 the stock solution was diluted to reach a concentration of 0.05% w/v, to be used as a dispersion medium.

***Step 1***

BSA (1 g) was weighed into a weighing boat. Then, 50 mL of MilliQ (MQ) water was pipetted into a 250 mL Erlenmeyer flask followed by addition of BSA. The weighing boat was then rinsed with MQ water into the Erlenmeyer flask, attempting to let the water flow down the sides of the flask to avoid foaming of the BSA. The flask contents were mixed in a slow eight figure motion to avoid foaming, until most of the BSA was dissolved. Then, the BSA water was transferred to a 100 mL volumetric flask followed by careful rinsing of the Erlenmeyer flask (adding MQ water along the sides of the flask) into the volumetric flask. Finally, MQ water was added along the sides of the volumetric flask until 100 mL was reached, to get a 1% w/v BSA water solution. The solution was then gently mixed by swirling for a few minutes (avoiding foam) and was then left in the fridge overnight for complete dissolution of the BSA. The next day, the 1% BSA-water solution was sterile filtered (by connecting the sterile filter to a vacuum) into a new flask through a 0.2 µm filter. The sterile stock solution was then diluted with MQ water to obtain a 0.05% w/w BSA-water solution (conducted in the sterile hood). The stock solution was kept in the fridge, and new stock solution was made every two weeks.

***Step 2***
The 1% w/v BSA water was diluted according to the Nanogenotox protocol (Jensen et al., 2011), by adding 2 mL of 1% BSA water to 38 mL MQ water in a sterile centrifugation tube.

### 2.2.3 Weighing out carbon nanotubes

#### *2.2.3.1 Materials and chemicals*
Materials and chemicals used to weigh out nanomaterials are shown below.

| Material | Catalogue number | Manufacturer |
|---|---|---|
| Asbestos mask | 9332 | 3M |
| Balance | AE240, MKLS-061 (sintef-ID) | Mettler |
| Dry wipes, Spec-Wipe | 21913-211 | VWR |
| Hairnet | D115 | Portwest |
| Laminated A4 sheets | | |
| KleenGuard A45, XL coverall | 99680 | Kimberly-Clark Professional |
| Nitrile gloves (1.5 AQL) long | 92-600 | AnsellPro |
| Nitril gloves (1.5 AQL) normal | 92-616 | AnsellPro |
| Pyrex glass with blue cap (150 mL) | | |
| Shoe protection | 113-0749 | VWR |
| Steel spatulas | | |
| Vials: Scint-Burk glass pp-lock+Alu-foil (20 mL) | WHEA986581 | Wheaton Industries Inc. |
| Vials with nanomaterials | | |
| Weighing boats (glass) | | |

| Chemical | Catalogue number | Manufacturer |
|---|---|---|
| Dichloromethane | 433195 | SigmaAldrich |
| Ethanol 70% | | |
| MWCNT-P | TNM2, (Sintef-ID: 2015-0003) | Chengdu Organic Chemicals Co |
| MWCNT-OH | TNMH2, (Sintef-ID: 2015-0005) | Chengdu Organic Chemicals Co |
| MWCNT-COOH | TNMC2, (Sintef-ID: 2015-0006) | Chengdu Organic Chemicals Co |
| MWCNT-$NH_2$ | TNMN2, (Sintef-ID: 2015-0007) | Chengdu Organic Chemicals Co |

#### *2.2.3.2 Procedure*

***Preparations***
First, the spatulas to be used were rinsed with dichloromethane (DCM) in a fume cupboard and left to dry. Next, the balance was assessed with reference weights of 20 and 100 mg and the data logged. Then, the bench in the working area was cleaned with 70% ethanol and dry tissues in straight lines away from the balance. The necessary equipment was placed on the bench (nanomaterials in pyrex glasses, laminated A4 sheets, 20 mL vials, glass beakers filled with water, marker pens, tray for storage of vials, dry wipes, gloves, spatulas and weighing boats). Then protection equipment was put on, which included asbestos suit, mask, hairnet,

shoe covers, safety goggles and two pairs of gloves (long gloves first and normal gloves on top).

***Weighing out nanomaterials***

Nanomaterials to be used for exposure solutions were carefully weighed out in 20 mL vials to 15.36 mg (± 0.06 mg), according to the generic Nanogenotox dispersion protocol. The weights were recorded on laminated paper sheets. Used spatulas were put on a dry wipe to avoid spills, or put in a glass beaker with water when finished. If a spill occurred, a wipe was gently dipped in water or 70% ethanol and blotted over the spill, avoiding wiping, which causes smudging of the nanomaterial. All waste was disposed of in an appropriate hazardous waste box. Outer gloves were changed if required, i.e. if they had significant amounts of black powder on them. The nanomaterials to be used in the calibration curves were weighed out in weighing boats of glass. 40 mg of each nanomaterial was added to the weighing boat, and then transferred to a 150 mL pyrex glass with lid. Used weighing boats were put in the glass beaker with water.

After weighing, the outside of all flasks/vials containing nanomaterials were wiped with moist wipes, followed by wiping with 70% ethanol. The laminated paper was also wiped with water. Then the working area and balance was wiped clean, first with water, then with 70% ethanol. Finally, the protection equipment was removed and disposed of in the hazardous waste box. The weighing room was then ventilated overnight.

### 2.2.4 Making MWCNT calibration curves

To be able to detect accurate concentrations of MWCNT in the exposure solutions, calibration curves were produced for each of the four MWCNTs. The calibration curve data can be found in Appendix II.

#### *2.2.4.1 Materials and chemicals*

Materials, chemicals and solutions used in the preparation of CNT calibration curves are presented below. Compositions of the solutions are reported in Appendix I.

| Material | Catalogue number | Manufacturer |
|---|---|---|
| Asbestos mask | 9332 | 3M |
| Arm protectors, PS32LA | 1431 | VWR |
| Dry wipes, Spec-Wipe | 21913-211 | VWR |
| Lens cleaning tissues | 111-5003 | VWR |
| Nitrile gloves (1.5 AQL) long | 92-600 | AnsellPro |
| Nitril gloves (1.5 AQL) normal | 92-616 | AnsellPro |
| Pipette 1000 uL | MKLS-671 (Sintef-ID), FA-1000R | Thermo Fisher |
| Pipette tips (1000 µL) | | Axygen |
| Pipetus | MKLS-675 (Sintef ID), 81208013 | Hirschmann |
| Precision cells (cuvettes, quartz SUPRASIL) | 100-QS | Hellma Analytics |
| Probe sonicator: | | Branson Ultrasonics Corp. |
| Branson sonifier (400 watts) | S-450D | |
| Disruptor horn (13 mm) | 101-147-037 | |
| Ultraviolet-visible spectrophotometer (U2000) | 121-0003 | Hitachi |
| Vials: Scint-Burk glass pp-lock+Alu-foil (20 mL) | WHEA986581 | Wheaton Industries Inc. |
| Wipers | TX2069 | Texwipe |

| Chemical | Catalogue number | Manufacturer |
|---|---|---|
| Bovine serum albumin | A-9418 | Sigma Aldrich |
| Ethanol 70% | | |
| Ethanol 96% | | |

| Solutions |
|---|
| Bovine serum albumin (BSA) water 0.05% |

#### *2.2.4.2 Procedure*

***Making stock solutions for calibration curves***

The stock solutions were made according to the NANoREG CNT aqueous dispersion protocol (Booth and Sørensen, 2013), with some adjustments. First, armprotectors, asbestos mask and long and short gloves were put on. Then the nanomaterial and 0.05% BSA water was placed in the fume hood. 25 mL BSA water (0.05%) was added along the sides of the flask containing MWCNT powder (40 mg), to wash down the particles. This mixture was then transferred to a 250 mL beaker, by rapid, but controlled pouring.

The beaker was then placed in a box containing ice (~80%) and water (~20%) to avoid heating during sonication. The probe was adjusted to be slightly above the bottom of the beaker, but still submerged in the solution. Then the solution was sonicated for 5 minutes at amplitude 15%. After sonication, the probe was rinsed with 1-2 mL BSA water (0.05%) into

the beaker. The mixture was then carefully swirled. The original flask with nanomaterial was then rinsed with 25 mL BSA water (minus the volume used in rinsing the probe) and the contents transferred into the 250 mL beaker (volume subtotal: 50 mL). The above steps were repeated until a final volume of 100 mL had been sonicated, adjusting the probe along with the volume so that only the tip of the probe was submerged in the solution.

After the last sonication the beaker was rapidly carried to the UV-visible spectrophotometer (UV-vis) to reduce aggregation/agglomeration of the nanomaterial. (The UV-vis had been previously calibrated with BSA water (0.05%) at 800 nm). The sample cuvette was rinsed with the MWCNT dispersion, and 3 mL of the dispersion was added to the cuvette to obtain an absorbance reading at 800 nm. This process was repeated to obtain three readings, before thoroughly rinsing the cuvette with distilled water and ethanol. (Note: the minimum volume required to obtain an accurate reading with the UV-vis was tested in order to reduce the volume needed. 2 mL was found to be the lowest volume to give an accurate reading, see Appendix III. Ethanol (used to prepare exposure solutions), and BSA water (0.05%) absorbance at 800 nm was also tested, and no absorbance was detected, see Appendix III).

***Preparing calibration curve dilutions***

Previously prepared vials with BSA water had been set up at appropriate volumes and the MWCNT stock solution was added to each vial to a total volume of 10 mL/vial. The concentrations used in the calibration curves were 0.5, 2, 8, 15, 25, 50, 100, 150, 170, 200, 250, 300 and 400 µg/mL. All samples were put on ice after preparation to cool them down before sonication. The probe was then cleaned with 50% ethanol and 50% MQ, total 60 mL, at the same settings as above (amp.:15%, min.:5). Then the probe was rinsed with 96% ethanol and wiped dry with a cloth.

***Constructing calibration curves***

Prepared dilutions of each MWCNT were sonicated from lowest to highest concentration to reduce potential contamination. Each dilution was sonicated for 3 minutes at amplitude 15% and then the sample absorbance was quickly measured in the UV-vis spectrophotometer (800 nm). Three absorbance measurements were taken, the first with 3 mL sample, and the remaining measurements with 2 mL sample. The probe was cleaned with 96% ethanol between each sample, and washed with 50:50 ethanol/d$H_2O$ at amplitude 15% for 3 minutes after every third sample.

### 2.2.5 Making CNT exposure solutions for *in vitro* assays

#### *2.2.5.1 Materials and chemicals*

Materials, chemicals and solutions used in preparation of CNT exposure dispersions are presented below. Compositions of the solutions are reported in Appendix I.

| Material | Catalogue number | Manufacturer |
|---|---|---|
| Arm protectors, PS32LA | 1431 | VWR |
| Pipetus | MKLS-675 (Sintef ID), 81208013 | Hirschmann |
| Pipette 5 mL | MKLS-684 (Sintef ID), Q19800D | Eppendorf |
| 1 mL | MKLS-670 (Sinted ID) | Eppendorf |
| 1 mL | MKLS-671 (Sintef-ID), FA-1000R | ThermoFisher |
| Pipette tips | | |
| 5mL | 82018-840/613-0339 | VWR |
| 1 mL | | Axygen |
| Dry wipes, Spec-Wipe | 21913-211 | VWR |
| Nitrile gloves (1.5 AQL) long | 92-600 | AnsellPro |
| Nitrile gloves (1.5 AQL) normal | 92-616 | AnsellPro |
| Precision cells (cuvettes, quartz SUPRASIL) | 100-QS | Hellma Analytics |
| Vortex, MS2 Minishaker IKA | 12819435 | Fisher Scientific |
| Sterile serological pipette tip (10 mL) | 612-1248 | VWR |
| Syringe (50 uL) | 80985 | Hamilton |
| Ultraviolet-visible spectrophotometer (U2000) | 121-0003 | Hitachi |
| Vials: Scint-Burk glass pp-lock+Alu-foil (20 mL) | WHEA986581 | Wheaton Industries Inc. |
| Wipers | TX2069 | Texwipe |

| Chemical | Catalogue number | Manufacturer |
|---|---|---|
| Bovine serum albumin | A-9418 | Sigma Aldrich |
| Eagle's Minimal Essential Medium (MEM) | M4655 | Sigma |
| Ethanol, 96% | 24106 | Merck |

| Solutions |
|---|
| MEM – Growth medium |
| BSA water (0.05%) |

#### 2.2.5.2 Procedure

Exposure solutions were made according to the generic Nanogenotox dispersion protocol, with some modifications. MWCNTs were dispersed in BSA water (0.05%) or Eagle's Minimum Essential Medium (5% FBS, 1% PenStrep) at amplitude 15% for 13 minutes and 15 seconds. The length of sonication was altered to 13 minutes and 45 seconds after changing the probe tip (May 2015). (After changing the probe tip, two sonications with the washing solution (50:50 ethanol/$dH_2O$) was always conducted before sonicating the samples). After sonication the dispersions were left to settle overnight (~16 hours) to enable settling of unstable particles from suspension. Then, 3 mL of the dispersion supernatant was transferred to a new vial and vortexed at 2000 for 5 minutes to resuspend the particles. Some of this dispersion was then diluted in BSA water or growth medium to enable measurement of the

absorbance by UV-vis (800 nm). The concentration of a sample was calculated from the corresponding calibration curve. The diluted sample and/or the supernatant was then used to expose the PLHC-1 cells. (The supernatant concentration was back calculated from the diluted sample).

## 2.3 The cytotoxicity assay: MTT assay

### 2.3.1 Materials and chemicals

Materials, chemicals and solutions used in the MTT assay are presented below. Compositions of the solutions are reported in Appendix I.

| Material | Catalogue number | Manufacturer |
|---|---|---|
| Costar sterile 96-well plate | 3599 | Corning Inc. |
| Cover slip for haemocytometer | 004710680 | Thermo Scientific |
| Filter paper circles 589 | 10300008 | Schleicher & Schuell |
| FLUOstar Omega plate reader | 415-0737 | BMG Labtech |
| Haemocytometer | Depth 0.1 mm | Bürker |
| Miscroscope (phase-contrast) | E400 | Nikon Eclipse |
| Multichannel pipette 100 µL | EP-8-100R | Eppendorf |
| 300 µL | E2-8-300R | |
| Reagent reservoirs, 25 mL | 82031-546 | VWR |
| Sterile tubes 15mL | 62.554.502 | Sarstedt |
| 50 mL | 430829 | Corning Inc |

| Chemical | Catalogue number | Manufacturer |
|---|---|---|
| Thiazolyl Blue Tetrazolium Bromide (MTT, ~98%) | M2128 | Sigma |
| Dimethyl sulfoxide (DMSO, spectrophotometric grade) | 1.02950.0500 | Merck |
| **Solutions** | | |
| MTT solution | | |
| MTT/growth medium solution | | |

### 2.3.2 Linear area of formazan formation

To enable detection of viable cells at concentrations that are not saturated, the linear area of formazan formation had to be determined. Cells were passaged as previously described (section 2.1.1) and a 1/10 dilution was prepared. Approximately 15 µL of this dilution was placed on each grid of a hemocytometer with an attached cover slip. Cells on three individual squares (3x1 $mm^2$) were counted on each grid and averaged, and the concentration of cells per mL was calculated (see appendix IV). Nine dilutions were then made from the 1/10 dilution and a total of ten dilutions were seeded into wells in a 96 well plate. Each dilution was seeded at 200 µL per well with six replicates per dilution. Edge wells were filled with expired or fresh growth medium to prevent excess evaporation and edge effects. Growth medium was changed after 24 hours incubation (30°C, 5% $CO_2$) to mimic exposure

conditions, followed by 48 hours incubation. Then, growth medium was replaced with 5 mg/mL MTT solution dissolved in growth medium to a final concentration of 0.5 mg/mL and incubated for 4 hours. The MTT solution was then replaced with 200 µL DMSO to dissolve the insoluble formazan crystals, and the plate was read in a spectrophotometric plate reader.

### 2.3.3 Exposure of the cells

When exposing the cells, the procedure in section 2.3.2 was followed until the cell concentrations of the harvested cells were known. A cell concentration within the linear area of formazan formation was prepared (~$1.74*10^5$ cells/mL) and 200 µL of this cell suspension was added to each well. The cells were incubated for 24 hours and then the growth medium was replaced with exposure solutions. Six to eight exposure concentrations were included in each 96-well plate at 6 replicates per condition, in the range 0.5 – 2048 µg/mL. Controls that were included were: a no cell control, DMSO (3%, cell death), no treatment, MWCNT control, and a BSA control where applicable. The exposed cells were incubated for 48 hours, the growth medium removed and the cells carefully washed 1-3 times (depending on CNT concentration) with PBS. MTT solution was diluted in growth medium (0.5 mg/mL) in the wells and incubated for 4 hours. The MTT solution was then replaced with 200 µL DMSO to dissolve the insoluble formazan crystals, and the plate was read in a spectrophotometric plate reader.

## 2.4 Genotoxicity assay: DNA double strand break assay

### 2.4.1 Materials and chemicals

Materials, chemicals and solutions used in the DNA double strand break assay are presented below. Compositions of the solutions are reported in Appendix I.

| **Material** | **Catalogue number** | **Manufacturer** |
|---|---|---|
| Cast for gels | | BioRad |
| Centrifuge | 5417R | Eppendorf |
| Comb, 15 wells | | BioRad |
| Electrophoreses power supply – EPS 200, GN003036 | 19-0200-00 | Pharmacia-Biotech |
| Eppendorf tubes 1.5 mL | 72.690.001 | Sarstedt |
| GelDoc 2000 | 755/00715 | BioRad |
| Heat block (Dri Block DB-2D, FDB02DD) | 117995-21 | Techne |
| Plug moulds | | BioRad |
| Sterile 24 well plates, Costar | CLS3524 | Corning Incorporated |
| Wide Mini sub cell GT | 63S-28031 | BioRad |

| **Chemical** | **Catalogue number** | **Manufacturer** |
|---|---|---|
| Activated charcoal | C3014-2 | SigmaAldrich |
| Agarose for routine use | A9539 | SigmaAldrich |
| Boric acid (for electrophoresis, $H_3BO_3$) | B7901 | SigmaAldrich |

| | | |
|---|---|---|
| Dimethylsulfoxide (DMSO, spectrophotometric grade) | 1.02950 | Merck |
| Ethidium bromide ($C_{21}H_{12}BrN_3$) | 161-0433 | BioRad |
| Lambda/Hind III marker 2 | SM0101 | Fermentas |
| Lambda DNA | SD0011 | Fermentas |
| Loading Dye × 6 | R0611 | Fermentas |
| Low Melting Point Agarose | 162-0019 | BioRad |
| Methyl methanesulfonate, MMS | M4016 | Sigma |
| Proteinase K (from *Tritirachium albumin*, 39 units/mg protein) | 108K8610 | SigmaAldrich |
| SDS (sodiumdodecylsulphate, $C_{12}H_{25}SO_4Na$) | L-3771 | SigmaAldrich |
| Trizma base | T6066 | SigmaAldrich |

| **Solutions** |
|---|
| Digestion buffer |
| Lambda-DNA marker |
| TBE-buffer |
| TE-buffer |

### 2.4.2 DNA double strand break analysis

Cells were passaged as described in section 2.1.1, and 1 mL of prepared cell suspension was seeded per well in a 24 well plate. See sample calculation for cell seeding suspension in appendix V. The cells were incubated for 24 hours and then exposed for 48 hours to the test solution. The cells were then washed in 1 mL of PBS (per well) and harvested in 0.5 mL of PBS with 0.0125% trypsin for 2-3 minutes. The cells were transferred to 1.5 mL eppendorf tubes and centrifuged at 4000 rpm for 2 minutes (4 °C). They were then resuspended in 1 mL of PBS and centrifuged again at the same parameters. The cell pellet was then resuspended in 0.3 mL of TE buffer, and 0.3 mL low melting point agarose (LMPA, 1% in TE-buffer) at 30 °C was added. From this mixture ~10 plugs (55 µL cell suspension/plug) were cast from each cell culture and subsequently cooled at 4°C. The cooled plugs were then transferred to 1.5 mL eppendorf tubes (5 plugs per tube) with 0.5 mL digestion buffer added fresh Proteinase K (1 mg/mL), and incubated overnight at 55°C. Plugs were cooled to room temperature and added to wells of a 0.6% agarose gel (10 cm) and sealed with LMPA (1% in TE-buffer). Samples were run at 23 V (2.3 V/cm) for 14 hours together with a marker (1 µL λDNA-mixture, 4 µL 6x loading dye and 15 µL distilled water). The marker was heated to 65°C for five minutes and then instantly put on ice for 3 minutes, and transferred to the gel (with samples already loaded). The next day, the gel was stained 1.5 hours in ethidium bromide (1 drop in 400 mL electrophoresis buffer) and destained in water for 30 minutes. Gel image data was acquired with a BioRad Geldoc 2000 system. Calculation of median molecular length (MML) of DNA fragments in the gel and DNA-FTM was conducted using densitometric data obtained from the gel image analysis.

### 2.4.3. Calculations

Median molecular length can be used as a measure of the frequency of DNA DSBs in cells (Theodorakis et al., 1994). The MML can be found from the curve obtained after analysis of

DNA staining intensities, showing DNA staining intensity as a function of relative front (Rf) for each lane/sample (Appendix VII). The Rf is representative of the migratory distance of bands in the gel, with a number between zero and one. Since the DNA staining intensity depends on the amount of DNA present, it is possible to find the MML by dividing the approximate area under the curve by two ($A_{1/2}$). The Rf value which corresponds to this number ($Rf_{1/2}$) is representative of the MML. The MML of the fragment can then be determined by the construction of a standard curve, relating Rf values to Lambda size markers (with known numbers of basepairs) separated on the same gel. A standard curve was constructed for each gel. The equation obtained for this relationship was used to calculate the number of base pairs of each sample, by inserting $Rf_{1/2}$ into the equation. MML is reported as kilobase pairs (kbp). The method for finding $Rf_{1/2}$ can be represented by the following formula:

$$A_{1/2} \approx \frac{1}{2}\sum_{i=1}^{n} y_i \, \Delta x \qquad (2.1)$$

The amount of DNA that had migrated into the gel after electrophoresis, relative to the total amount loaded in the well (DNA-FTM), was determined by the area under the respective DNA staining intensity curves. The fraction of DNA released into the gel by electrophoresis as a measure of DNA DSB frequency was determined by the following formula:

$$DNA - FTM = \frac{DNA\ in\ the\ gel}{DNA\ in\ well + DNA\ in\ gel} \times 100 \qquad (2.2)$$

MWCNTs were tested for interference with the detection of the DNA staining intensity (fluorescence), but no interference was detected (see Appendix VII). There were problems with streaking in the gels, but this could mostly be avoided during the analysis. If enough gel replicates were produced, the worst streaking was avoided by excluding the most affected gels.

## 2.5 Statistics

Results from the DNA DSB assays were tested for statistical significance by One-Way ANOVA and Tukey's or Games-Howell post hoc test for normal data. Non-normal data was tested with Kruskal-Wallis and Dunn's with a Bonferroni adjustment for multiple comparisons. Significance level was set to $p<0.05$. The analyses were performed in IBM SPSS statistics 21. Data normality was monitored using Shapiro-Wilk.

# 3 Results

## 3.1 MTT assay optimisation

### 3.1.1 Linear area of formazan formation

The linear area of formazan formation was determined as illustrated in Figure 3.1. The curve is a measure of absorbance (550 nm) as a function of increasing cell concentration. The linear area is indicated to be between 0 and 300 000 cells/mL.

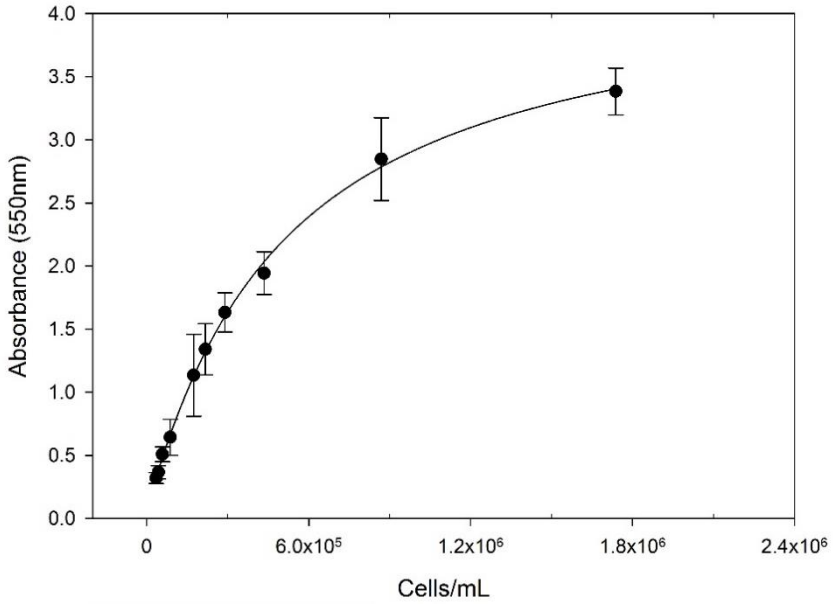


**Figure 3.1: Absorbance (550 nm) as a function of cell concentration (cells/mL). Each symbol represents the mean absorbance ± standard deviation, n=6.** The curve fit is based on a sigmoidal four parametric logistic curve $R^2 = 0.999$.

## 3.2 Quantification of MWCNTs

Quantification of the amount of MWCNTs were conducted with a UV-vis spectrophotometer based on calibration curves (see Appendix II). The quantification was used to determine the concentration of MWCNTs in each exposure solution after an overnight settling period. This allowed for accurate calculation of exposure concentrations to be used in the *in vitro* assays.

### 3.2.1 Detection of MWCNT absorbance at 550 nm

It was necessary to test if the MWCNTs absorbed at 550 nm to prevent interferences with the MTT assay. A pilot test was first conducted in a 96-well plate with MWCNT-OH and –COOH at concentrations from 1 – 32 µg/mL, where MWCNTs were added to wells with growth medium only (Figure 3.2). A second experiment was performed on all the MWCNTs at concentrations of CNTs estimated to remain in the wells after the washing step (Figure 3.3). (In the second experiment, MWCNTs were dispersed in growth medium and diluted in MQ water to simulate measurements in DMSO). Absorbance was tested at the highest (2048 µg/mL) and second lowest (1 µg/mL) concentrations of MWCNTs used in the MTT assay; by

assuming that 95% and 99% of MWCNTs were washed away at the highest concentration, whereas 95% was assumed washed away at the second lowest concentration.

The first test (Figure 3.2) revealed relatively low absorbance (mostly within the range of the blank control) of MWCNT-COOH and –OH at all the concentrations tested (1 – 32 µg/mL). MWCNT-OH seemed to show a more even absorbance (around 0.01) over the concentration range than MWCNT-COOH. MWCNT-COOH showed higher absorbance at the lowest and highest concentrations, which was higher than the blank, and any MWCNT-OH observations.

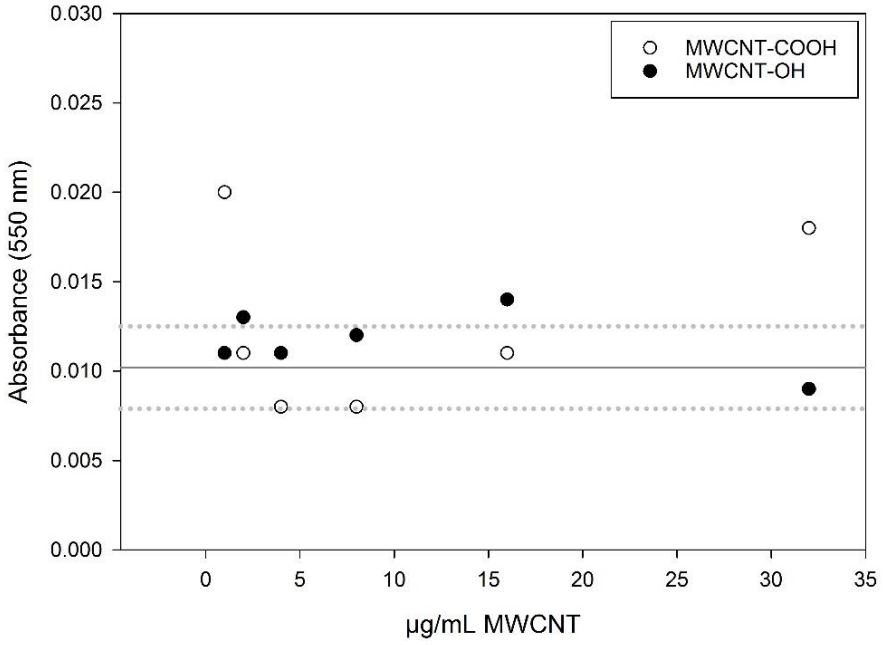


**Figure 3.2: Absorbance of MWCNT-OH and MWCNT-COOH at 550 nm in the concentrations range 1 -32 µg/mL.** Each symbol represents one sample (n=1), where filled circles denotes MWCNT-OH, and white circles represent MWCNT-COOH. The grey solid line represents the blank control (no cell) mean ± standard deviation (grey dotted lines), n=6.

In the second experiment (Figure 3.3), no absorbance was detected for any MWCNTs at the lowest concentration (95% assumed washed away of original 1 µg/mL). However, absorbance (550 nm) was very high at the highest concentration (95% assumed washed away of original 2048 µg/mL) for all CNTs, except MWCNT-$NH_2$. At this concentration (102.4 µg/mL) absorbance was higher in the order MWCNT-COOH> -P > -OH > $NH_2$. At the middle concentration (99% assumed washed away from original 2048 µg/mL) MWCNT-OH demonstrated a lower absorbance than MWCNT-P and –COOH, but no obvious difference was observed between MWCNT-P and –COOH. Absorbance was substantially lower at the middle concentration (20.48 µg/mL) compared to the high concentration (102.4 µg/mL) for all CNTs. However, absorbance was still well above 0 for MWCNT-P, -OH and -COOH. In terms of MWCNT-$NH_2$, a much lower absorbance was detected overall, compared to the other MWCNTs. However, absorbance above 0.1 was detected at the two highest concentrations.

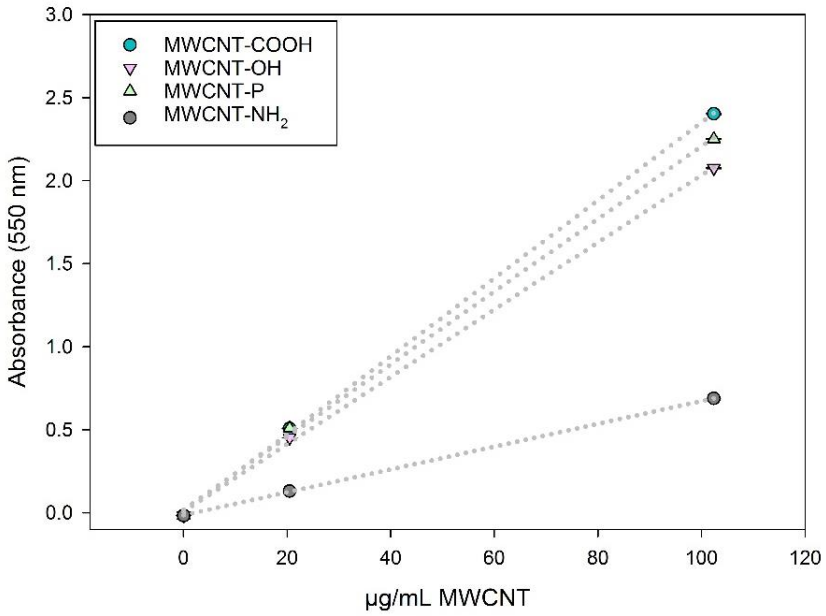


**Figure 3.3: Absorbance (550 nm) of four MWCNTs (-COOH, -OH, -$NH_2$ and pristine) at three concentrations (0.05, 20.48, 102.4 µg/mL)**. The concentrations are those estimated to remain in the wells after washing at a low (1 µg/mL) and the highest (2048 µg/mL) concentration used in the MTT-assay. Each symbol is the mean of three replicates (n=3) ± standard deviation.

## 3.3 Cytotxicity of MWCNTs to PLHC-1 cells

### 3.3.1 Cell viability of PLHC-1 exposed to MWCNTs dispersed in BSA water

Initially, MWCNTs were dispersed in BSA water (0.05%) according to the Nanogenotox protocol (Jensen et al., 2011), as a standardisation measure. The percentage cell viability relative to control for MWCNT-OH and COOH dispersed in BSA water is illustrated in Figures 3.4 and 3.5 respectively. Data was obtained by the MTT-assay, and raw data can be found in Appendix VI.

In Figure 3.4, PLHC-1 cells were exposed to MWCNT-OH dispersed in BSA water (0.05%) at concentrations of 0.5-32 µg/mL. Cell viability was reduced the most at the two lowest concentrations, followed by the two highest concentrations. The cell viability was highest at the middle concentrations (2, 4 and 8 µg/mL). Cells exposed to the BSA water control showed a reduction in cell viability to about 55%. Relatively large standard deviations were observed for all the samples, including the BSA water control.

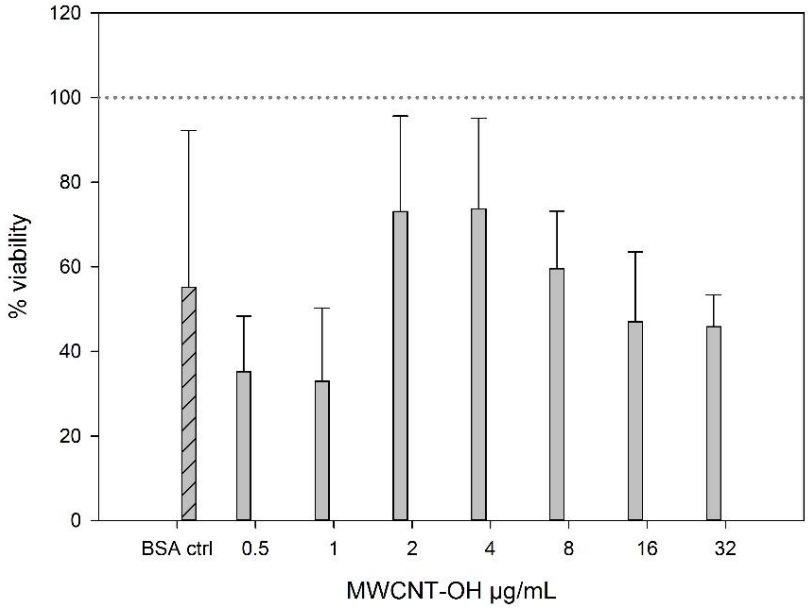


**Figure 3.4: Viability of PLHC-1 cells as percentage of control after exposure to MWCNT-OH dispersed in BSA water (0.05%)**. Each bar represents the mean percentage viability relative to control ± standard deviation, n=6. The control is indicated by the dotted line at 100%. Vehicle control for the experiment is represented by the patterned bar (n=3).

PLHC-1 cells exposed to MWCNT-COOH dispersed in BSA water (0.05%) are displayed in Figure 3.5. This experiment was repeated once, with concentrations from 0.5 – 256 µg/mL. Cell viability of cells in the first experiment (dark grey bars) demonstrated lowest viability at 8, 16, 128 and 256 µg/mL of MWCNT-COOH. The second experiment (light grey bars), show a similar pattern as seen for cells exposed to MWCNT-OH (lowest viability at low and high concentrations, and highest viability at middle concentrations). Both BSA water controls showed a reduction in cell viability of ~20 %. Standard deviations were mostly relatively low in these experiments, but the second experiment (light grey bars) demonstrated some large standard deviations.

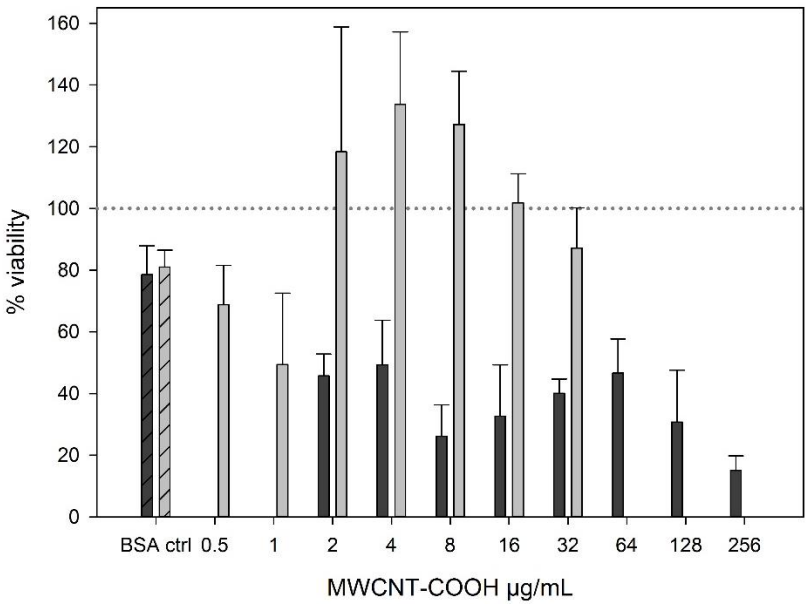


**Figure 3.5. Viability of PLHC-1 cells as percentage of control after exposure to MWCNT-COOH dispersed in BSA water (0.05%).** Independent experiments are marked with different colours, and each bar represent the mean values of viability relative to control ± standard deviation, n=6. The control is indicated by the dotted line at 100%. Vehicle control for each experiment is represented by patterned bars (n=2-3).

### 3.3.2 Cell viability of PLHC-1 exposed to MWCNTs dispersed in growth medium

The cytotoxic effects of the four MWCNTs dispersed in growth medium were assessed as percentage cell viability of control, as a function of increasing concentrations of each CNT. The MTT-assay was used to assess the cell viability and all raw data are included in Appendix VI. The cell viability upon exposure to each MWCNT is presented in Figures 3.6-3.9 below.

Figure 3.6 demonstrates a slow decrease in cell viability with increasing concentrations of pristine MWCNT, compared to control. However, between ~16-128 µg/mL MWCNT-P, cell viability seems to slightly stabilise before continuing to decrease. At the two highest concentrations of MWCNT-P, cell viability was reduced by more than 50% compared to control. Standard deviations decreased at the highest concentrations. From the regression analysis a five parameter exponential decay curve was found to give the best fit ($R^2 = 0.913$), but a linear regression was also performed (see Appendix VIII).

Figure 3.7 also demonstrates a gradual decrease in cell viability with increasing concentrations of MWCNT-COOH compared to control. Cell viability data was relatively scattered at all concentrations of MWCNT-COOH, and a clear trend was not observed. From the regression analysis a triple, seven parameter exponential decay curve was found to give the best fit ($R^2 = 0.987$), but a linear regression was also performed (see Appendix VIII). The fit of the linear regression was also quite good ($R^2 = 0.965$).

Figure 3.8 demonstrates a gradual decrease in cell viability with increasing concentrations of MWCNT-OH relative to control. Cell viability appear to stabilise slightly at around 10 µg/mL before toxicity increases again at around 100 µg/mL. At the two highest concentrations of MWCNT-OH, cell viability was reduced below 50% compared to control. Standard deviations decreased at the highest concentrations. From the regression analysis a triple, seven parameter exponential decay curve was found to give the best fit ($R^2$ = 0. 962), but a linear regression was also performed (see Appendix VIII).

Figure 3.9 indicates a negative dose-response relationship between cell viability and MWCNT-$NH_2$ concentration. Concentrations of MWCNT-$NH_2$ below 100 µg/mL appear to have low or no cytotoxic effect. At concentrations of MWCNT-$NH_2$ higher than 100 µg/mL, reductions in cell viability is observed. At around 1000 µg/mL of MWCNT-$NH_2$ cell viability is reduced below 50% relative to control. From the regression analysis a five parameter sigmoid curve was found to give the best fit ($R^2$ = 0.953).

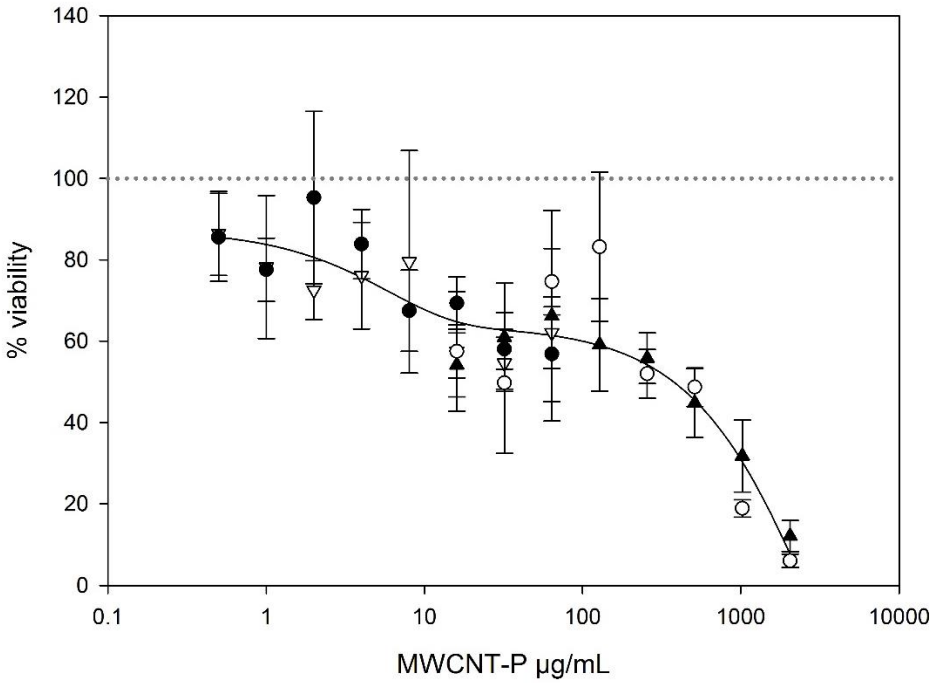


**Figure 3.6: Cell viability of PLHC-1 cells as percentage of control after 48hrs exposure to pristine MWCNT (0.5-2048 µg/mL).** Each symbol represents the mean viability ± standard deviation of an experiment, n=6. Separate experiments are marked with different symbols. The curve fit is based on average cell viability at each MWCNT-Pristine concentration, and is given by a five parameter exponential decay function $R^2$= 0.913.

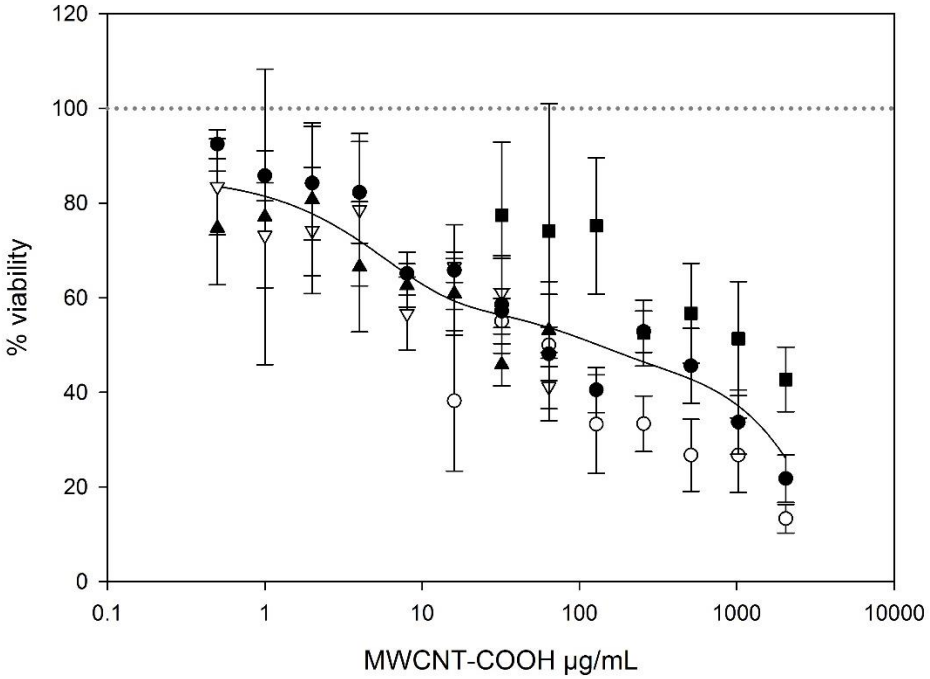


**Figure 3.7: Cell viability of PLHC-1 cells as percentage of control after 48hrs exposure to MWCNT-COOH (0.5-2048 µg/mL).** Each symbol represents the mean viability ± standard deviation of an experiment, n=6. Separate experiments are marked with different symbols. The curve fit is based on average cell viability at each MWCNT-COOH concentration, and is given by a triple, seven parameter exponential decay function $R^2$= 0.987.

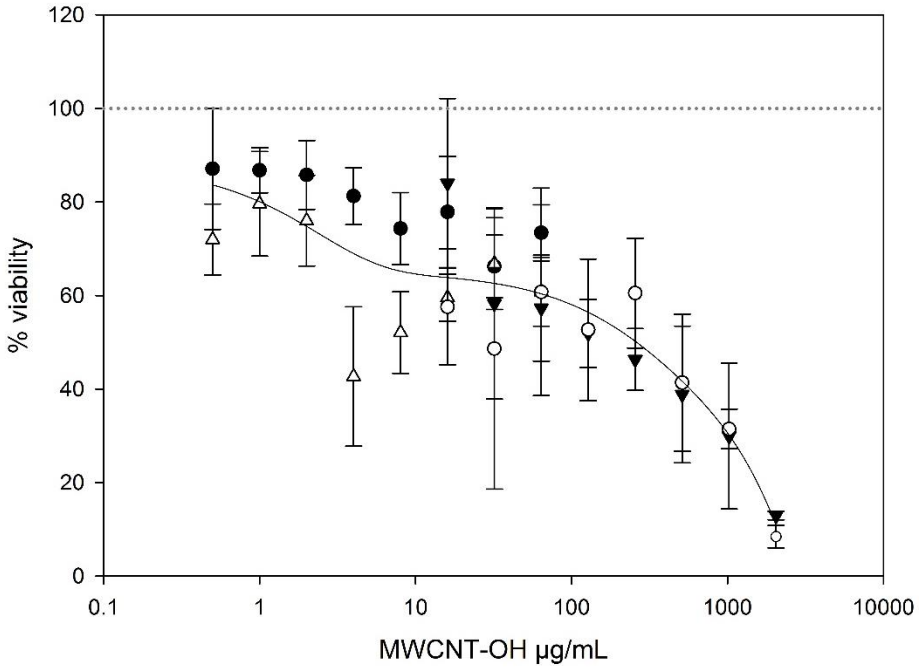


**Figure 3.8: Cell viability of PLHC-1 cells as percentage of control after 48hrs exposure to MWCNT-OH (0.5-2048 µg/mL).** Each symbol represents the mean viability ± standard deviation of an experiment, n=6. Separate experiments are marked with different symbols. The curve fit is based on average cell viability at each MWCNT-OH concentration, and is given by a triple, seven parameter exponential decay function $R^2$= 0.962.

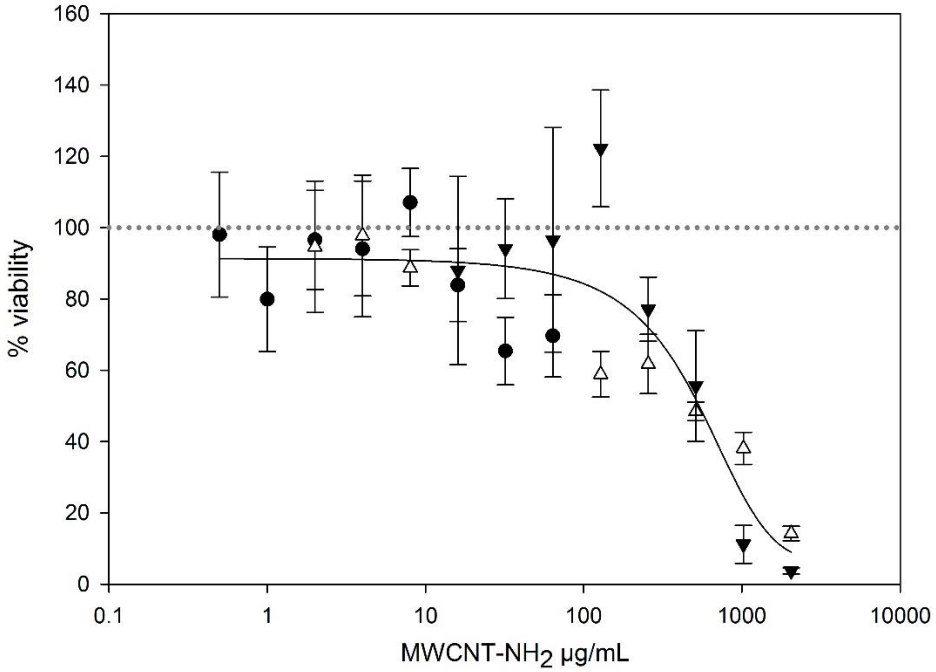


**Figure 3.9: Cell viability of PLHC-1 cells as percentage of control after 48hrs exposure to MWCNT-$NH_2$ (0.5-2048 µg/mL**). Each symbol represents the mean viability ± standard deviation of an experiment, n=6. Separate experiments are marked with different symbols. The curve fit is based on average cell viability at each MWCNT- $NH_2$ concentration, and is given by a five parameter sigmoid function $R^2$= 0.953.

## 3.4 Genotoxicity of MWCNTs in PLHC-1 cells

Genotoxicity of MWCNTs was assessed by two methods based on agarose gel electrophoresis data. The first method evaluated the fraction of total DNA that migrates into the gel (DNA-FTM), relative to the total amount that was loaded. These data are a measure of the potential increase in DSB frequency. The second method used to evaluate DNA damage was assessment of the median molecular length (MML) of the DNA that had migrated into the gel. A lower MML generally indicates more damaged DNA.

### 3.4.1 Fraction of electrophoresed DNA

Double strand break frequency as measured by DNA-FTM are reported in Figures 3.10 - 3.14 below. From Figure 3.10, it was observed that MWCNT-Pristine demonstrated varying results between the two experiments conducted. Whereas the black bars (first experiment) indicate a slow increase in DNA-FTM from control to the highest concentration; the grey series (second experiment) indicates a significantly ($p<0.05$) lower level of DNA-FTM in the low exposure group, relative to control and high exposure groups.

In Figure 3.11 DNA-FTM increased slightly for MWCNT-COOH exposed groups relative to control in the first the experiment (black series). In the second experiment (grey series), no differences in DNA-FTM were observed.

In Figure 3.12, the high exposure to MWCNT-OH demonstrated a statistically ($p<0.05$) higher level of DNA-FTM relative to the control and low exposure (4 µg/mL) groups, in the first experiment (black series). No differences were observed in the second experiment (grey series).

In Figure 3.13, the high exposure (64 µg/mL) to MWCNT-$NH_2$ demonstrated significantly lower ($p<0.05$) DNA-FTM level relative to the low exposure (first experiment, black series). In the second experiment (grey series), a slight increase in DNA-FTM was observed from low to high exposure. Comparison of DNA-FTM levels between the four MWCNTs indicated an overall lower level in MWCNT-$NH_2$ exposed cells than for the other MWCNTs.

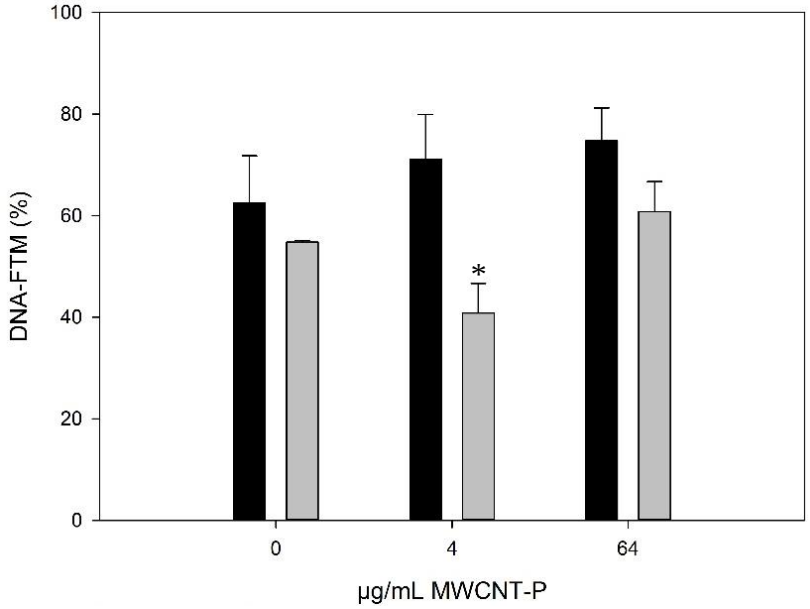


**Figure 3.10: Fraction of total DNA that migrated (DNA-FTM) into the gel relative to the total amount loaded, after 48 hours exposure to MWCNT-Pristine (4 and 64 µg/mL).** Differently coloured bars indicate different experiments, with each individual bar representing the mean DNA-FTM (%) ± standard deviation, n=2 for controls and n=6 for each exposure condition (except low exposure in experiment 2, n=4). Statistical significance (One-Way ANOVA, Tukey's) relative to the control and high exposure group is denoted with *, $p<0.05$.

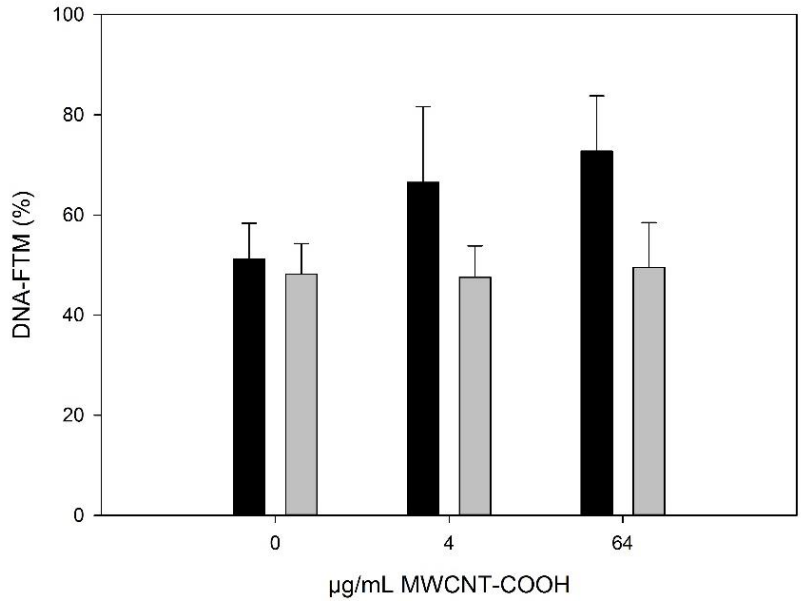


**Figure 3.11: Fraction of total DNA that migrated (DNA-FTM) into the gel relative to the total amount loaded, after 48 hours exposure to MWCNT-COOH (4 and 64 µg/mL).** Differently coloured bars indicate different experiments, with each individual bar representing the mean DNA-FTM (%) ± standard deviation, n=2 for controls and n=6 for each exposure condition.

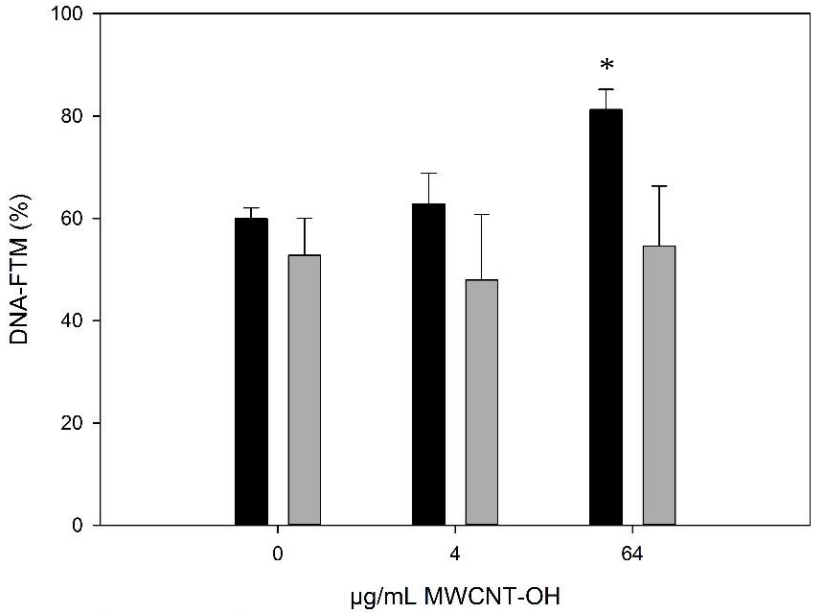


**Figure 3.12: Fraction of total DNA that migrated (DNA-FTM) into the gel relative to the total amount loaded, after 48 hours exposure to MWCNT-OH (4 and 64 µg/mL).** Differently coloured bars indicate different experiments, with each individual bar representing the mean DNA-FTM (%) ± standard deviation, n=2 for controls and n=6 for each exposure condition. Statistical significance (Kruskal-Wallis and Dunn's) relative to control and the low exposure group (4µg/mL) is denoted with *, $p<0.05$.

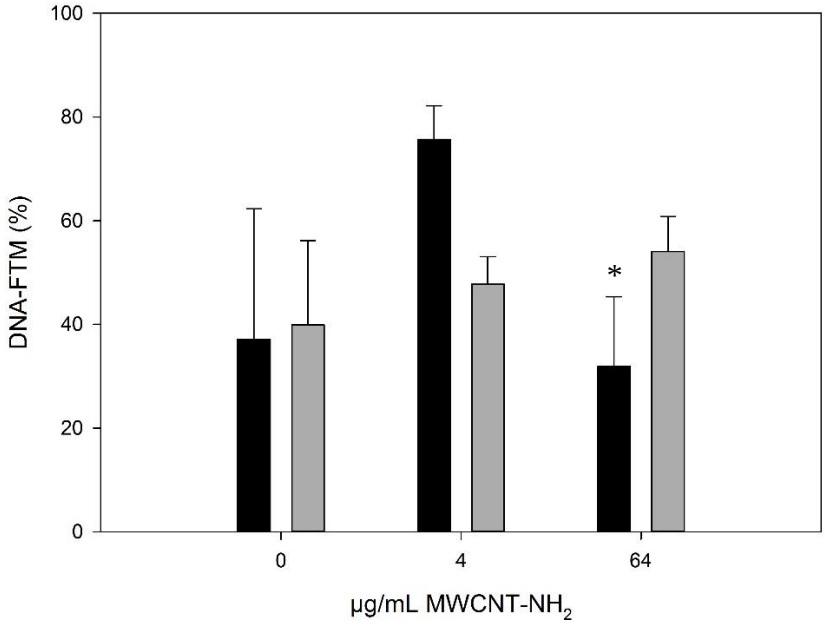


**Figure 3.13: Fraction of total DNA that migrated (DNA-FTM) into the gel relative to the total amount loaded, after 48 hours exposure to MWCNT-$NH_2$ (4 and 64 µg/mL).** Differently coloured bars indicate different experiments, with each individual bar representing the mean DNA-FTM (%) ± standard deviation, n=2 for controls, n=5 in high exposure group in experiment one, and n=6 for the remaining exposure conditions. Statistical significance (One-way ANOVA, Games-Howell) relative to the low exposure group (4µg/mL) is denoted with *, $p<0.05$.

### 3.4.2 Median molecular length of DNA fragments

Median molecular length (MML) of the DNA-FTM was determined as illustrated in Figures 3.14 to 3.17 below. In Figure 3.14, there were no observed differences in MML between any of the exposure conditions (control, low and high exposure), after exposure to MWCNT-P. The first experiment (black bars) had slightly lower MMLs than in the second experiment (grey bars).

In Figure 3.15, no differences in MML between exposure conditions were observed after exposure to MWCNT-COOH. There was a relatively small difference between experiments, however a slightly smaller MML overall was observed in the second experiment (grey series).

Figure 3.16, shows some differences in MML between exposure conditions after MWCNT-OH exposure. In both experiments, MML was significantly higher ($p<0.05$) in the high exposure group compared to the low exposure group. Median molecular lengths also appeared to be slightly lower in the first experiment (black series), than in the second experiment (grey series). Relatively large standard deviations were observed in the control group.

In Figure 3.17, exposure to MWCNT-$NH_2$ did not demonstrate obvious differences between exposure groups. However, a significant decrease in MML was observed at the high

exposure, relative to the low exposure, in the second experiment (grey bar). Relatively large standard deviations were observed in the control group.

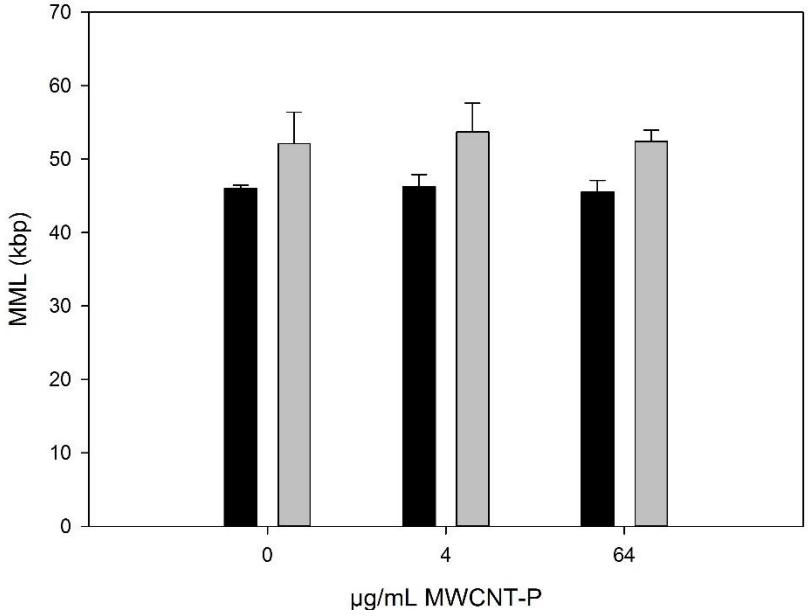


**Figure 3.14: Median molecular length (MML) in kilobase pairs of fragmented DNA, after 48 hours exposure to MWCNT-P (4 and 64 µg/mL).** Differently coloured bars indicate different experiments, with each individual bar representing the mean MML ± standard deviation, n=2 for controls and n=6 for each exposure condition.

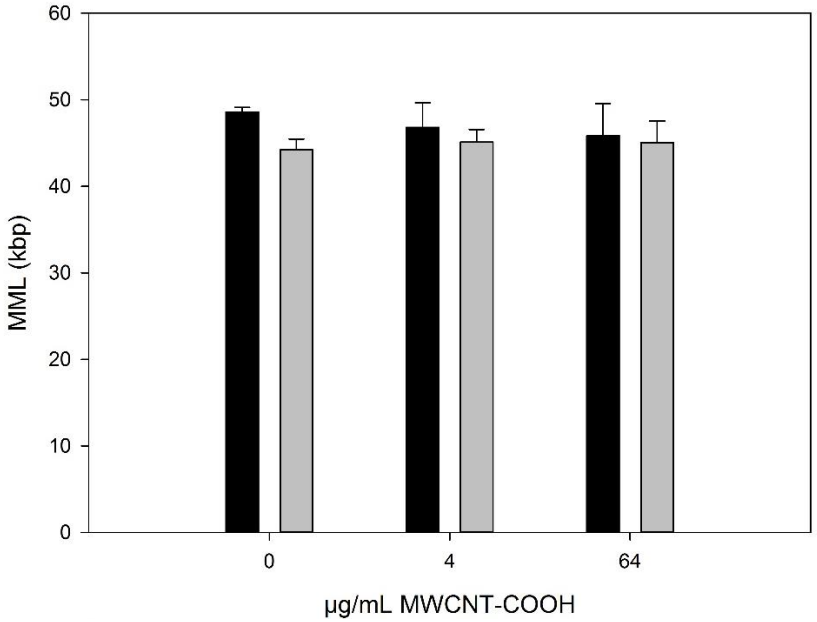


**Figure 3.15: Median molecular length (MML) in kilobase pairs of fragmented DNA, after 48 hours exposure to MWCNT-COOH (4 and 64 µg/mL).** Differently coloured bars indicate different

experiments, with each individual bar representing the mean MML ± standard deviation, n=2 for controls and n=6 for each exposure condition.

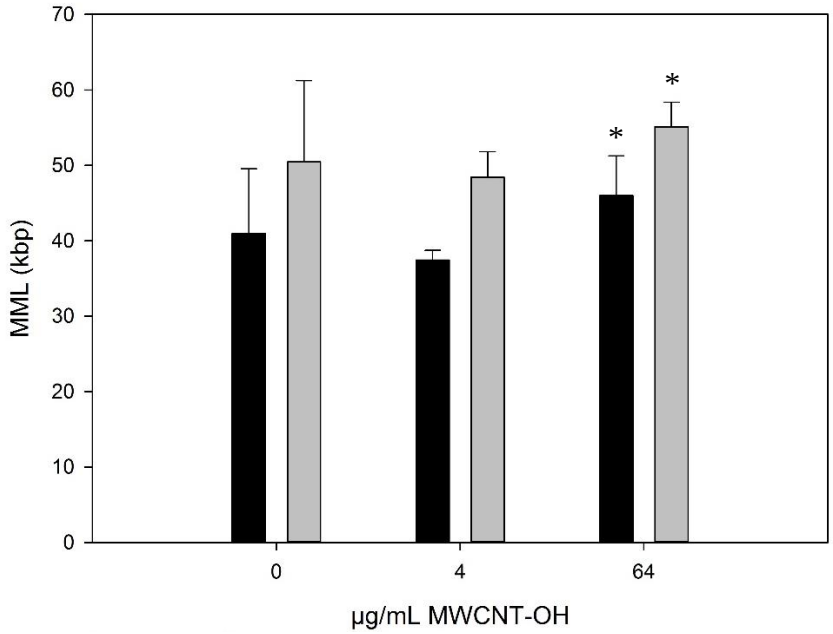


**Figure 3.16: Median molecular length (MML) in kilobase pairs of fragmented DNA, after 48 hours exposure to MWCNT-OH (4 and 64 µg/mL).** Differently coloured bars indicate different experiments, with each individual bar representing the mean MML ± standard deviation, n=2 for controls and n=6 for each exposure condition. Statistical significance (One-Way ANOVA, Games-Howell) relative to the low exposure group (4µg/mL) is denoted with *, $p<0.05$.

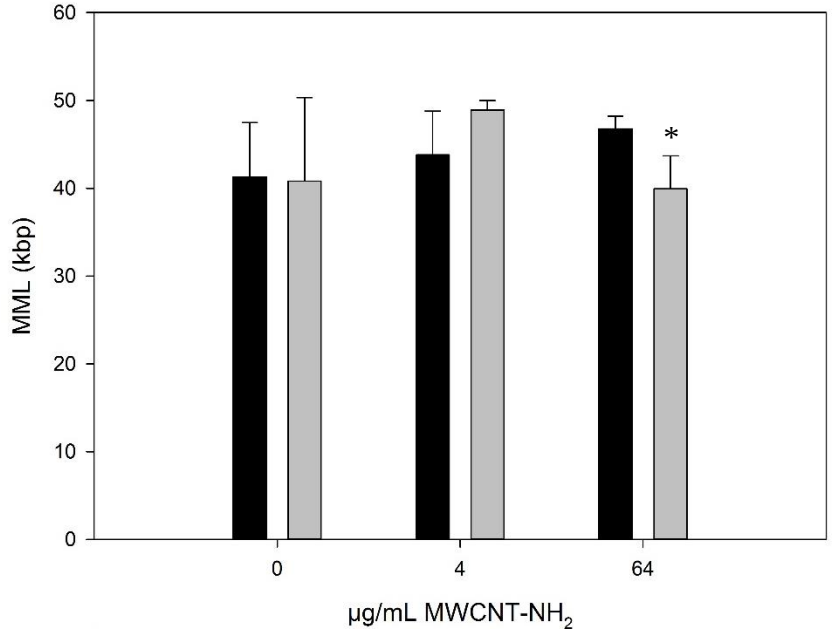


**Figure 3.17: Median molecular length (MML) in kilobase pairs of fragmented DNA, after 48 hours exposure to MWCNT-$NH_2$ (4 and 64 µg/mL).** Differently coloured bars indicate different experiments, with each individual bar representing the mean MML ± standard deviation, n=2 for controls and n=6 for each exposure condition. Statistical significance (One-Way ANOVA, Games-Howell) relative to the low exposure group (4µg/mL) is denoted with *, $p<0.05$.

### 3.4.3 Positive control

A positive control was also included in the experiment where cells were exposed to methyl methanesulfonate (MMS) dissolved in DMSO or growth medium (Figure 3.18 and 3.19). In the positive control, there was no clear relationship between exposure condition and DNA-FTM (Figure 3.18). In the first experiment (black series), MMS was dissolved in growth medium prior to exposure, and this experiment appears to have a higher overall DNA-FTM than the other series. In the second experiment (grey series) MMS was dissolved in DMSO prior to exposure, and there were no substantial differences between the vehicle control and the MMS exposure.

In Figure 3.19 MMLs of the positive control is illustrated, and observed to be quite similar across the exposure conditions. However, at the two highest exposure concentrations (20 and 40 mg/L), MMLs appear to be slightly lower (black bars) or higher (grey bars) relative to control. DMSO control samples had substantially lower MMLs than the MMS samples, also in the control group.

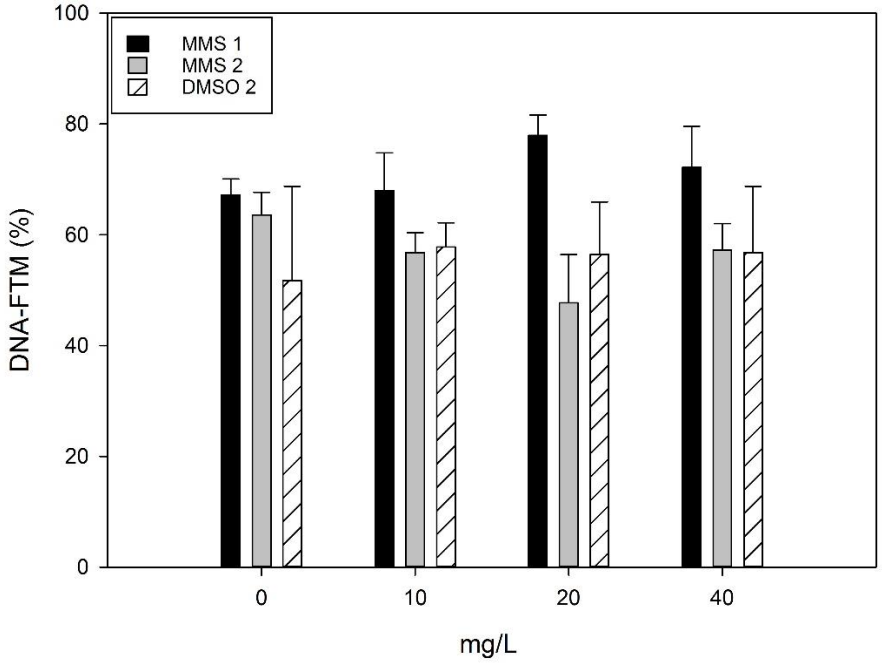


**Figure 3.18: Fraction of total DNA that migrated (DNA-FTM) into the gel relative to the total amount loaded, after 48 hours exposure to MMS or DMSO (10, 20 and 40 mg/L).** Differently coloured bars indicate different experiments, with each individual bar representing the mean DNA-FTM (%) ± standard deviation, n=3. DMSO (patterned bars) was included as a vehicle control in the second experiment, as it was used to dissolve MMS.

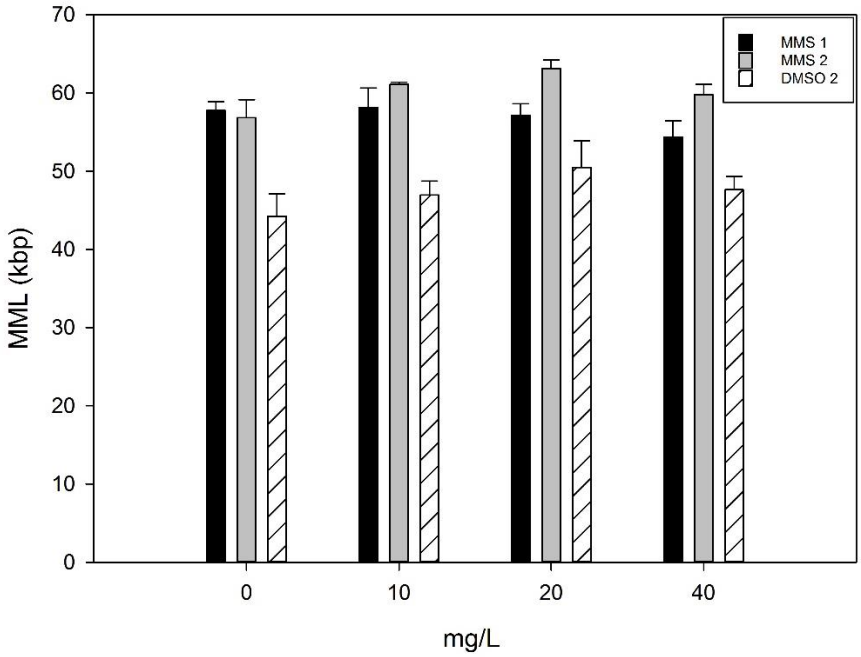


**Figure 3.19: Median molecular length (MML) in kilobase pairs of fragmented DNA, after 48 hours exposure to MWCNT-P (4 and 64 µg/mL).** Differently coloured bars indicate different experiments, with each individual bar representing the mean MML ± standard deviation, n=3. DMSO (patterned bars) was included as a vehicle control in the second experiment, as it was used to dissolve MMS.

# 4 Discussion

In this section, results are discussed in the same order as they were presented in the results section (Section 3). The impacts of MWCNTs with different functional groups were assessed by the MTT assay and the DNA DSB assay. The cell concentrations used in the MTT assay as a basis of the linear area of formazan formation is discussed, together with an evaluation of the use of this assay with MWCNTs. The cytotoxicity data is discussed in relation to its its consistency with other studies, as well as the differences between the MWCNTs. The impact of BSA water as a dispersion medium is also discussed in this section. The results from the DNA-DSB analyses, as DNA-FTM and MML, were discussed in relation to differences between the four MWCNTs and results from other studies.

## 4.1 MTT assay optimisation

### 4.1.1 The influence of cell variability – linear area of formazan formation

To enable more precise detection of formazan production by cells in the MTT assay, the linear area of formazan formation was established. In the current study, the linear area of formazan formation for PLHC-1 cells was found to be between zero and approximately 300 000 cells/mL (Figure 3.1). A similar range (0-200 000 cells/mL) was reported in the thesis of a previous master student (Størdal, 2011). A cell concentration of ~170 000 cells/mL was then used in the following cytotoxicity assays. The cells were seeded with this concentration to obtain an optimal density for formazan detection after 72 hours (the length of the assay).

The cell concentrations were obtained by counting cells in grids on a haemocytometer, which is a very subjective procedure. Counting technique is therefore assumed to vary between individuals and between each counting. Consequently, it is important to be as consistent as possible in the counting technique to avoid large variations between experiments, and to maintain the optimal seeding density in each experiment. Furthermore, cell concentrations reported by different individuals are therefore not considered to be directly comparable.

Despite measures to control cell variability, systems with cells and other living organisms are always subject to natural variability. In the current study, the PLHC-1 cells were observed to form cell aggregates upon passaging, which can often complicate the counting and mixing procedures. This can especially influence the homogeneity of a cell suspension, and it can be difficult to break up these cell clusters without greatly reducing cell viability. In the current study, gentle mixing by inverting the tube with cell suspension a few times was used to increase homogeneity, before counting/seeding.

## 4.2 Detection of MWCNT absorbance at 550 nm

### 4.2.1 MWCNT interference with the MTT assay

Absorbance at 550 nm was tested for the four MWCNTs used in the current study, to determine if this could interfere with the MTT-assay results. In a first test, MWCNT-OH and –COOH absorbance was tested after a washing step, followed by 4 hours incubation with MTT. The test was conducted with a low concentration range (1 – 32 µg/mL) in the absence of cells (Figure 3.2). The data revealed low absorbance (below 0.025) of the MWCNTs, mostly at the level of the blank control, with no MWCNTs clearly absorbing more than the

others. MWCNT absorbance did not seem to increase substantially with higher MWCNT concentrations. Thus, these MWCNT's appear to not stick substantially to the wells or cause major interferences with formazan detection by their absorbance.

However, results from the MTT assays revealed absorbances as low as ~0.07 (see Appendix VI) for cells exposed to 2048 µg/mL of MWCNT-OH. Therefore, it could be that cytotoxicity data recorded at high MWCNT concentrations could be confounded by CNT absorbance. This could be due to a higher amount of CNTs remaining in the wells at high concentrations, which would have more impact on the data, since cell viability absorbances at this CNT concentration can be quite low. In that case, cell viability may appear to be higher than it actually is. Moreover, it should be considered that MWCNTs are found to stick to cells (Geys et al., 2010) as observed also in the current study; and therefore the observed absorbances in Figure 3.2 may not be representative of the actual CNT concentration remaining after washing.

In a second test, absorbance (550 nm) of all four MWCNTs was assessed at concentrations of CNTs estimated to remain in the wells after the washing step at the highest and a low concentration (Figure 3.3). The low concentration (representing 5% of 1 µg/mL) showed no detectable absorbance for any of the MWCNTs. At the highest concentration (representing 5% of 2048 µg/mL) a very high absorbance (~2.0 – 2.5) was demonstrated for MWCNT-P, -OH and -COOH. This was higher than any absorbance detected in an exposure, and the possibility for this concentration of CNTs was therefore dismissed. A second concentration was tested which represented 1% of 2048 µg/mL. This concentration still gave a high absorbance reading (~0.5) for MWCNT-P, OH and COOH; which was (much) higher than detected at MTT assay exposures of 2048 µg/mL (0.025 – 0.3, see Appendix VI). Therefore, the concentration of MWCNT-P/OH/COOH that remain in the well after washing is probably lower than 1%. However, it is evident that MWCNT-P, -OH and –COOH absorb at 550 nm and therefore that absorbances detected, especially at high exposure concentrations, may be somewhat confounded by CNT absorbance.

It is also interesting to observe that MWCNT absorbance at the highest concentration tested (102.4 µg/mL) was higher in the order MWCNT-COOH > -P > -OH. However, at the middle concentration (20.48 µg/mL), this relationship was only apparent for MWCNT-OH whereas the other two CNTs demonstrated similar absorbance. Yet, this indicates that at high concentrations, MWCNT-COOH may have a greater confounding influence on the results, followed by MWCNT-P and then MWCNT-OH. This effect will probably be influenced by the effectiveness of the washing step. MWCNT-$NH_2$ on the other hand, demonstrated low absorbance overall ($\leq 0.69$), compared to the other MWCNTs. During the washing step of the MTT assay, this CNT was also fairly easy to remove and did not appear to attach well to the cells (as opposed to MWCNT-COOH). Thus, it can be assumed that this MWCNT would probably produce less artifactual results, due to CNT absorbance, than the other CNTs tested.

The influence of CNT dye adsorption is another aspect to consider when evaluating the toxicity of MWCNTs by the MTT assay. In the literature, the assessment of CNT toxicity has thus far been conducted mostly through traditional toxicological assays, as it was in the current study. However, these assays were developed for chemicals and may not be suitable

for CNTs (Kroll et al., 2009, Dhawan and Sharma, 2010). Typically these assays use colorimetric or fluorimetric dyes as markers to determine cell viability, membrane integrity or cell metabolism. Carbon nanotubes, having high surface areas can therefore easily interfere with assay components or products and influence the results (Forest et al., 2015). Carbonaceous NPs have for example been found to bind to alamar blue (Casey et al., 2007), coomassie blue (Casey et al., 2007), neutral red (Monteiro-Riviere and Inman, 2006, Casey et al., 2007), MTT dye (Monteiro-Riviere and Inman, 2006, Wörle-Knirsch et al., 2006, Casey et al., 2007, Holder et al., 2012) and WST-1 dye (Casey et al., 2007).

In terms of MWCNTs specifically, there was less information about their interferences with MTT assay constituents compared to other carbonaceous nanoparticles. However, Coccini et al. (2010) reported conflicting results in terms of MWCNT (pristine and functionalised) cytotoxicity observed in the MTT and calcein/PI assays, which was suggested to be due to a false positive cytotoxicity signal in the MTT assay. Support for this interference with the MTT assay has been reported by other studies. Qi et al. (2011), found that out of six different nanofiber mats, those containing MWCNTs (3 and 5%) demonstrated the highest percentage formazan adsorption, thereby causing false positive results for cytotoxicity. Similarly, Pulskamp et al. (2007) observed cytotoxicity in the MTT assay, but not in the WST-1 assay, when rat alveolar macrophages were exposed to MWCNTs. Verification by a third assay (PI/annexin V staining) confirmed that the MWCNTs were not toxic to the cells, and MWCNTs were suggested to associate with the insoluble formazan product. Simon-Deckers et al. (2008) also reported probable MWCNT interference with the MTT assay, as cytotoxicity was observed after only 1 hour of exposure in this assay, but after 48 hours in XTT and LDH assays (which have been claimed reliable in CNT assessment). In contrast to all these studies, Geys et al. (2010) reported similar viability results between the MTT and alamarblue assays in A549 cells, concluding that MWCNTs did not interfere with assay constituents. Moreover, the MWCNTs were not observed to absorb at 550 nm when bound to cells, in absence of MTT dye.

Despite some conflicting data on this topic, it appears that MWCNTs have the ability to interact with certain test system constituents. Although this interference may depend on various MWCNT parameters or cell systems it is important to be cautious about results obtained from such assays, and do further tests to validate the results. In the current study, only the MTT assay could be performed due to time restraints. However, inherent MWCNT absorbance was tested in both the test system and independently from the test system. As could be seen from the results (Figure 3.3), MWCNTs could potentially disguise some cytotoxicity by their inherent absorbance (550nm), causing false negative results. However, this would probably only be an issue at very high concentrations where much of the CNTs remain in the well; and for those MWCNTs which absorbs the most (MWCNT-COOH/P/OH). MWCNT interference with MTT/formazan dye cannot be excluded in the current study, and may have led to false positive results for cytotoxicity. For a full discussion of the impacts of these parameters on the cytotoxicity data obtained in the present study, see section 4.3.2.

## 4.3 Cytotoxicity of MWCNTs to PLHC-1 cells

### 4.3.1 Cytotoxicity of MWCNTs dispersed in BSA water

Cytotoxicity of MWCNTs was initially assessed by dispersing the CNTs in BSA water according to a standardised protocol (Jensen et al., 2011). This would more easily enable comparison to other studies using the same protocol. However, it was observed that the BSA control seemed to reduce cell viability in all of the experiments using this procedure (Figure 3.4 and 3.5). Due to the consistent reduction in cell viability of the vehicle control, it was decided to discontinue the use of BSA water (0.05%) as a dispersion medium (and replace it with growth medium). It was unclear why the vehicle control had an impact on cell viability. It could be that BSA water had been contaminated, especially since antibiotics were not added to the BSA waster (as opposed to in the growth medium), and the sterile working conditions during sonication were not optimal.

Another possibility could be that the BSA itself induced some toxicity. In carp gill cells exposed to high concentrations of metal ions (3000 µM) and 1% BSA, an increased level of lipid peroxidation was observed compared to at lower metal levels. This same exposure also caused a significant decline in antioxidant (GSH) content. Complexes of metal ions and thiol (-SH) groups of the BSA were suggested to act as potential cell toxicants (Arabi, 2004). In the current study, no metals were used in exposure or during preparation of BSA, but BSA interaction with other compounds may have occurred. It is well known that serum albumin binds to a wide range of endogenous and exogenous ligands which may have various effects on cells (Carter and Ho, 1994). Human serum albumin with a high fatty acid content was for example found to induce toxicity to human kidney cells (Erkan et al., 2005). Thus, albumin may have induced toxicity indirectly through a similar mechanism.

Although serum albumin may be toxic in some regards, studies have also reported no cytotoxic effects of this protein. Vehicle controls for BSA (0.01%) used to disperse SWCNTs for exposure in Japanese medaka, did not demonstrate any difference in ecotoxicity relative to distilled water (Sohn et al., 2015). Similarly, Farcal et al. (2015) reported no induction of cytotoxicity in Caco-2 human intestinal cells when exposed to a BSA solvent control (0.05% BSA). Evidently, there are many factors which can influence the potential toxicity of BSA. In the current study, it could not be determined why the vehicle control induced toxicity in the cells. Further evaluations would have to be conducted to determine this.

In terms of the toxicity evaluation of the CNTs dispersed in BSA water, the results were not considered reliable due to the potential bias of the BSA water. Moreover, the standard deviations for the MWCNT-OH and first exposure to MWCNT-COOH were mostly considerably large; which also caused uncertainty about the results. Furthermore, there were no clear dose-response relationship between MWCNT concentration and cytotoxicity, which made it difficult to interpret the data. This may be due to the confounding effect of the BSA water and/or due to adjustment to the method, which may have caused greater variability in the data.

### 4.3.2 Cytotoxicity of MWCNTs dispersed in growth medium

It is important to assess the MWCNT potential for toxicity in the aquatic environment due to the continued increase in MWCNT production (see section 1). In the current study, the cytotoxic effect of four different MWCNTs was investigated with the MTT-assay. Three of the MWCNTs (MWCNT-P, MWCNT-COOH and MWCNT-OH) displayed similar dose response curves, with slowly decreasing cell viability upon increasing concentrations of the nanomaterial. However, cells exposed to MWCNT-$NH_2$ displayed a different dose-response curve, with cytotoxicity occurring after a certain concentration (100 µg/mL).

Relatively large variability was observed in each experiment. Methodological variability in steps such as cell counting, washing steps etc. may have contributed to some of the variability observed. Variability in cell incubation times and MWCNT dispersion settling were also an issue in this study, as logistical measures made it difficult to comply with ideal time spans. Nevertheless, time spans were usually quite consistent between experiments. Sterile conditions were not sufficiently met during dispersion preparation, due to the location of the apparatus, and could also have impacted on toxicity results. Some variability can also be attributed to natural variations in cell growth and condition, especially at higher concentrations of cells. No apparent reduction in variability was observed between experiments in the beginning and toward the end.

MWCNT absorbance at 550 nm and/or CNT interaction with formazan is another important parameter that could have influenced both the variability and the cytotoxicity of the current experiment (refer to section 4.2). The cytoxicity data indicated that MWCNT-COOH was the most toxic of the four CNTs tested. However, this could also be an effect of adsorption of formazan by the CNT, thus falsely reducing viability. This cytotoxicity curve was also close to being linear in shape, which may be due to a proportional adsorbance of formazan with increasing CNT concentrations. Lower adsorption could be the case with MWCNT-P and MWCNT-OH. MWCNT-$NH_2$ on the other hand, demonstrated the lowest cytotoxicity of all CNTs. However, this CNT was reported to have the highest surface area (Table 2.1), and would therefore be expected to adsorb more formazan than the other CNTs. Nevertheless, this was also the CNT that was most poorly dispersed and most easily removed during the washing step (as opposed to MWCNT-COOH). Therefore, it was less likely that MWCNT-$NH_2$ was present in amounts large enough for substantial formazan adsorption. CNT absorption of light at 550 nm may have had some impacts at high CNT concentrations, particularly for MWCNT-COOH. Despite possible impacts of confounding factors, cytotoxicity appears to be relatively low for all of the CNTs tested.

Since nanotoxicology research in fish is a relatively new area of science, few studies investigating the effect of MWCNTs in fish are available (Handy et al., 2011). In the literature very few studies were found that have been conducted using fish cells. One study exposed epithelioma *Papulosum cyprini* (EPC) carp cells for $10^{-10}$ g – $10^{-2}$ g (exposure concentration not specified) MWCNT (10-30 nm diameter, 5-20 µm length) for various lengths of time. The study reported a slight toxic effect on the cells at the highest concentration tested, using the alamarblue assay (Taylor et al., 2014). The results from another study also indicated relatively low toxicity of MWCNTs in fish. Lee et al. (2015)

investigated the *in vivo* effect of MWCNTs (10-15 nm diameter, 20 µm length) on apoptotic and antioxidant gene expression in gill and liver in japanese medaka. After 14 days exposure to 100 mg/L MWCNTs, apoptotic genes were induced in the liver, but no apoptosis was observed histologically. The gills were found to be more sensitive to MWCNT toxicity than the other organs, and there was also observed higher apoptosis gene induction in males than females. Campos-Garcia et al. (2015) also reported low toxicity of MWCNTs to the freshwater fish *Nile tilapia*. The fish was exposed *in vivo* to MWCNT-$HNO_3$ (containing a mixture of -COOH, -OH and =O functional groups, diameter 10-40 nm, length <0.5 µm) at exposure concentrations ranging from 0.1 – 3 mg/L. No toxicity was observed at exposure times up to 96 hours. The results from these studies support the data from the current study, which indicates that MWCNTs exhibit relatively low toxicity even at high concentrations (100 mg/L).

However, in zebrafish embryos injected with MWCNTs, Cheng et al. (2009) reported detection of immune responses and lowered survival rate of second generation larvae. BSA functionalised MWCNTs on the other hand, showed good biocompatibility. A later study by Cheng and Cheng (2012) also detected severe developmental toxicity in zebrafish embryos injected with shorter length MWCNT-BSA (~0.2 µm), but no obvious toxicity for longer length MWCNT-BSA (~0.8 µm). This indicates that toxic effects in fish is related to both length of MWCNTs and life stage of the organism. Early life stages of fish have long been known to be more susceptible to toxic effects of pollutants and poor water quality (Eddy and Talbot, 1985). However, the effect of various MWCNT parameters is still under investigation in fish cells, and was the target of investigation in the current study. To find data on this, human and rodent cell line studies were examined.

### 4.3.3 Differences in cytotoxicity of functionalised MWCNTs

Human and rodent cell lines have been much more applied in studies of MWCNT toxicity than fish cells. In the present study, the aim was to determine if different functionalisation of MWCNTs with the same length exhibited different toxicities. The results indicate that MWCNT-$NH_2$ demonstrate a lower toxic effect than the other three CNTs, and that MWCNT-COOH may be slightly more toxic than pristine and MWCNT-OH. In a recent study on macrophages (Fraczek-Szczypta et al., 2012), similar results in terms of cell proliferation were observed. Lowest cell proliferation was observed for MWCNT-F (oxidised) followed by MWCNT-NH and then pristine MWCNT, and was suggested to be due to better dispersability and lower aggregate size of MWCNT-F. However, in terms of toxicity, the effect of all the MWCNTs were quite similar. Another study found similar results, where cytotoxicity of functionalised MWCNTs to human lung cells were in the order COOH> $O^+$ >$NH_2$ > pristine (Chatterjee et al., 2014). This study also reported cytotoxicity curves similar to those demonstrated in the present study. Conversely, Ursini et al. (2012a) found pristine MWCNTs to be more cytotoxic to cell membranes of human lung cells than MWCNT-OH. Yet, MWCNT-OH exposed cells showed higher apoptosis induction than pristine MWCNTs. Size differences between these CNTs could have influenced the result.

As opposed to the above mentioned studies, the present study did not demonstrate obvious differences in cytotoxicity between pristine and oxidised MWCNTs. This may be due to presence of oxygen groups also in the pristine MWCNTs (see Table 2.1), which could suggest that this CNT was not as pristine as expected. In terms of MWCNT-COOH, this CNT seemed to be the most toxic of the four, which is consistent with the above mentioned studies. This may be due to the higher dispersability, and consequently bioavailability, of this MWCNT, due to its more hydrophilic -COOH group relative to the other CNTs tested. In contrast, MWCNT-$NH_2$ was not found to contain oxygen groups (see Table 2.1) and was poorly dispersed in medium, which seem to have reduced its toxicity in agreement with the mentioned studies. In addition, aggregate size as a function of dispersability, and differences in surface area, may have influenced the observed differences. Moreover, as demonstrated by Fraczek-Szczypta et al. (2012), the effect of MWCNTs on cell proliferation may be equally responsible for observed cytotoxicity in this study as that of the CNTs themselves. However, differences between MWCNTs from different manufacturers, dispersion techniques, exposure conditions and different species and cell lines makes comparison difficult.

Another explanation for the different toxicity observed for the CNTs could be due to varying protein adsorption abilities. Sohaebuddin et al., (2010) reported a significant depletion ($p<0.05$) of proteins from cell culture medium by pristine MWCNTs with diameter 20-30 nm and length 0.5-2 µm. Cell medium protein depletion was also observed for shorter and longer diameter MWCNTs. Hence, reduced cell viability of PLHC-1 cells may be a function of protein scavenging effect of each MWCNT. In this case, oxidised and pristine MWCNTs may have been able to adsorb more growth medium proteins than MWCNT-$NH_2$ in the current study; which could have limited nutrient uptake and caused a gradual reduction in cell proliferation with increasing CNT concentrations. However, the $NH_2$ functionalised CNT has the largest surface area of the four CNTs tested (Table 2.1). Hence, it is less likely that the results observed in this study is due to scavenging of serum constituents. Nonetheless, it is important to note that formation of protein coronas have been found to facilitate cellular association, which may increase the potential for cellular uptake of the nanomaterial and in turn cause toxicity (Ehrenberg et al., 2009).

Some studies have also reported a lack of differences in cytotoxicity between different functionalised MWCNTs. Jackson et al. (2015) reported no significant cytotoxic effects of either COOH, OH or $NH_2$ functionalised MWCNTS in mouse lung epithelial cells after 24 hours exposure. However, various MWCNTs were found to induce ROS production, and reduce cell proliferation at concentrations of 200 µg/mL. Similarly, Cheng et al. (2011) assessed the toxicity of MWCNTs with various degree of oxidation in a vascular endothelial cell line (EA.hy926). By use of the MTS assay a slight reduction in cell viability was seen after 48 hours. Although differences were observed between the different oxidation degrees, no obvious trends were observed between them. Thus, there are still conflicting results in terms of how functionalization affects cytotoxicity, and standardisation is crucial to enable comparisons.

The mechanisms underlying observed cytotoxicity of MWCNTs are still being elucidated. However, suggestions for these mechanisms include production of ROS (Kermanizadeh et

al., 2012, Jiang et al., 2013), reduction of antioxidant levels (Kermanizadeh et al., 2012), induction of apoptosis (Ursini et al., 2012a, Ursini et al., 2012b, Jiang et al., 2013) loss of membrane integrity (Cavallo et al., 2012), decrease in mitochondrial membrane potential (Liu et al., 2014), pro-inflammatory (Tabet et al., 2011, Bussy et al., 2012) and pro-oxidative effects (Bussy et al., 2012).

## 4.4 Genotoxic effect of functionalised MWCNTs in PLHC-1 cells

Genotoxic effects of MWCNTs was investigated by agarose gel electrophoresis to determine the frequency of DNA DSBs. The fraction of DNA that migrated into the gel (DNA-FTM) relative to the amount loaded was used as a measure, together with the median molecular length (MML) of the migrated fragments. Two exposure conditions were tested, one low (4 µg/mL) and one high (64 µg/mL), for each MWCNT, due to the ambiguous cytotoxicity curves obtained for three of the MWCNTs.

### 4.4.1 Genotoxicity assessed by DNA-FTM

The DNA-FTM data indicated overall inconsistencies between the first and second experiments (section 3.4.1) for all MWCNTs. In the first experiment, there was a slight increase in DNA-FTM levels across the exposure range for all MWCNTs except MWCNT-$NH_2$. A significantly higher level of DNA-FTM was observed at the high exposure (relative to control and low exposure) to MWCNT-OH. This may indicate more frequent DNA damage at higher concentrations for this MWCNT, although it could also be the result of lysis (which was a problem in all of the first experiments). Substantial lysis was noted in samples exposed to MWCNT-$NH_2$ which most likely explains the significant difference observed. Therefore, the second experiment was considered more representative for most of the MWCNTs (excluded MWCNT-P).

In the second experiment, no apparent differences in DNA-FTM levels between exposure conditions were observed for either MWCNT-COOH or –OH. This indicates that these MWCNTs may not be particularly genotoxic at the concentrations tested. However, a significantly lower level of DNA-FTM was observed at the low exposure of MWCNT-P, relative to the control and high exposure groups. Substantial lysis was observed in all these MWCNT-P samples, which probably explains this difference. Therefore, DNA-FTM data for this MWCNT was not very reliable. In the case of MWCNT-$NH_2$, a slight increase in DNA-FTM was observed at the highest exposure condition, which could indicate some genotoxicity at this concentration. However, the DNA-FTM data obtained in the current study was not reliable enough to draw any conclusions for any of the MWCNTs.

Moreover, DNA-FTM levels were generally lower in the second experiment for all the MWCNTs. This indicates that cells in the first experiment may have been subject to more lysis during the experimental procedure, rather than being damaged by MWCNTs. Nonetheless, DNA damage induced by cell lysis may have masked potential genotoxic effects exerted by MWCNTs. Due to time restraints, it was not possible to conduct further experiments to investigate this.

In terms of differences in DNA-FTM levels between the MWCNTs, there were no obvious differences between MWCNT-OH, -COOH and –P. However, MWCNT-$NH_2$ appeared to have an overall lower level of DNA-FTM than the other MWCNTs. This is consistent with the results observed in the MTT assay, where MWCNT-$NH_2$ also appeared to be the least cytotoxic MWCNT. However, further testing would have to be conducted to confirm this. Moreover, due to time restraints and the number of samples that had to be run on each gel, only two control samples were included per gel in the MWCNT experiments. This made it difficult to obtain reliable control means and consequently reliable evaluation of differences between exposed samples and controls. Hence, it could not be determined from these experiments whether or not the tested MWCNTs induced a genotoxic effect in PLHC-1 cells.

### 4.4.2 Genotoxicity assessed by MML

The median molecular length of the fragments of DNA that had migrated into the gel demonstrated different trends with different MWCNT exposure. MWCNT-P and -COOH did not demonstrate any differences in MML between exposure groups. Moreover, the MML between the two experiments were relatively similar, especially in MWCNT-COOH samples. Thus, it appears that these two MWCNTs did not the increase frequency of DNA DSBs in PLHC-1 cells when measured by MML. This is mostly consistent with the DNA-FTM data where no obvious differences could be found which was not attributed to lysis.

In terms of MWCNT-OH and -$NH_2$, significant differences in MML between the high exposure group and the low exposure group was detected. For MWCNT-OH treated cells, a significant decrease in MML was detected at the low exposure concentration in both experiments (relative to the high exposure). Hence, it seems that MWCNT-OH may be more genotoxic at the low exposure concentration (4 µg/mL), than at the high exposure. This was the opposite of the expected result, where a higher concentration of CNT was expected to cause more damage to the DNA. However, it could be that more DNA damage was observed in the low exposure group due to a higher degree of CNT aggregation and agglomeration at higher concentrations, which may reduce CNT uptake/bioavailability to the cells.

In the exposure with MWCNT-OH it was difficult to obtain a base line MML value due to the low number of controls (n=2) with large standard deviations. Yet, there seemed to be a consistent trend in MML data between the two experiments, with lower MML levels at the low exposure condition than at the high exposure. However, this does not correspond with DNA-FTM data for MWCNT-OH, where either no differences were observed, or higher DNA damage was detected at high exposure. However, due to the problems with cell lysis, the damage detected with the MML method may have been masked when using the DNA-FTM method.

In regards to MML data obtained for MWCNT-$NH_2$, no significant differences were observed in the first experiment. In the second experiment, however, a significant decrease in MML was observed from the low to the high exposure group. This could indicate a higher genotoxic effect of this CNT at the highest exposure tested, which corresponds with the expected result. This result also corresponded well with the DNA-FTM of the second experiment (the first experiment was subject to substantial lysis and was not considered

representative), where an apparent higher level of DNA damage was observed at the highest concentration of CNT.

When comparing the MMLs of the four MWCNTs, it seemed that MWNCT-OH and $NH_2$ had slightly lower MMLs than –P and –COOH; and that MWNCT-OH and $NH_2$ induced significant damage at low and high exposures respectively. Thus, from these data –OH and –$NH_2$ functionalised MWCNTs appeared to be the most genotoxic of the four CNTs tested. However, these data require validation by further experiments. Furthermore, the overall MML data for MWCNT-$NH_2$ was inconsistent with the overall DNA-FTM data, where MWCNT-$NH_2$ seemed to be the least genotoxic of the CNTs tested, although this difference was not very obvious. MWCNT-OH similarly, was not found to induce a significant increase in DNA-FTM levels (at low exposure) in the second experiment (only at high exposure in the first experiment, which was subject to more lysis). Consequently, the lack of reliability in the current genotoxicity data (due to lysis, few control samples and few repetitions of each experiment) prevents any conclusions to be made without further validations.

### 4.4.3 Genotoxic effects reported in the literature

According to Filho et al. (2014) only a few studies in the field of aquatic toxicology have looked at genotoxic effects of CNTs in aquatic organisms. Of these, genotoxic effects were assessed *in vivo* in freshwater snail (Ali et al., 2014) and amphibian larvae (Mouchet et al., 2011). Results of the former study demonstrated that SWCNTs induced significant DNA damage in hepatopancreas cells as observed by the comet assay. However, the latter study reported no genotoxic effect in the form of micronuclei (MN) formation in erythrocytes exposed to double walled CNTs without surfactant. Consistent with this, Filho et al. (2014) reported that no genotoxic effects (comet assay and MN test) were observed in zebrafish exposed to a network of MWCNTs *in vivo*. Results from the current study were too ambivalent to be able to conclude in either of these directions

In human and rodent cell lines, MWCNT genotoxicity has been studied much more extensively than in aquatic organisms. Induction of DNA strand breaks (comet assay) have been reported by several studies (Di Giorgio et al., 2011, Ghosh et al., 2011, Cavallo et al., 2012, Lindberg et al., 2012) at concentrations as low as 2 µg/mL. However, it has also been reported that direct DNA damage was minimal after exposure to MWCNTs (comet assay) (McShan and Yu, 2012). Consequently, there is still controversy related to MWCNT genotoxicity, especially since methods, CNTs and cell lines differ considerably between experiments. Other studies, which have investigated the induction of chromosome breaks (MN test) by MWCNTs are also contradictory and reported to give both negative (Szendi and Varga, 2008, Ponti et al., 2013) and positive results (Migliore et al., 2010, Kato et al., 2012) for genotoxicity. Consequently, there is a need for additional and standardised studies on genotoxic effects of nanomaterials (Doak et al., 2012).

In the current study, the aim was to also investigate if there were potential differences in genotoxicity of differently functionalised MWCNTs. As mentioned earlier, it was difficult to determine any differences in genotoxicity between the four MWCNTs, and it was difficult to

draw conclusions from the reported data. In the literature, Ponti et al. (2013) reported no genotoxicity (MN test) in mouse fibroblast cells at concentrations up to 100 µg/mL, exposed to pristine, -OH, -COOH and $–NH_2$ functionalised MWCNTs. Conversely, genotoxic effects were detected in human lung epithelial cells after exposure to both pristine and OH-functionalised MWCNTs (FPG-comet assay) (Ursini et al., 2012a). The MWCNT-OH was genotoxic at a lower concentration (5µg/mL) than the nude CNT. Jackson et al. (2015) similarly reported a significantly higher level of DNA strand breaks induced by MWCNT-COOH than pristine and –OH functionalised MWCNTs in mouse lung epithelial cells. Consistent with this, it was reported that functionalised MWCNTs were most genotoxic in the order COOH> $O^+$, $NH_2$ > pristine in human bronchial epithelial cells, assessed by the comet assay (Chatterjee et al., 2014). In contrast, it was found that a higher number of micronuclei were detected in human lung epithelium cells exposed to MWCNT-P than –COOH (Visalli et al., 2015).

The genotoxic effect of MWCNT functionalization varies between different studies. Again, it is necessary to do more research on this topic with standardised procedures to enable study comparison. However, there are indications of differences in genotoxic effects between various functionalisations from the above mentioned studies. Hence, future studies may eventually reveal underlying mechanisms for these potential differences. For an overview of potential mechanisms involved in genotoxicity refer to section 1.3.2.

### 4.4.4 Positive control

In the current study it was attempted to run a positive control for DNA damage by using MMS. This compound has in previous studies been found to induce adenine and guanine alkylation which may lead to mispairing of bases and blocked DNA replication (Beranek, 1990). MMS in itself was not found to be responsible for DNA DSBs, but alkylated bases resulting from MMS exposure could induce DSBs upon heating (such as during incubation with proteinase K) (Lundin et al., 2005). In the current study DNA DSB induction by MMS was assessed by both DNA-FTM (Figure 3.18) and MML (Figure 3.19) of migrated fragments. MMS was dissolved in DMSO in the second experiment in order to ensure proper dissolution of the compound (which could have an impact on the results). Results showed that there was no significant increase in DNA-FTM of MMS exposed samples relative to control. A clear relationship between MMS exposure and DNA-FTM was not observed. The DMSO control, did not seem to have had an impact on the data. No clear relationship between MMS concentration and MML could be determined. Median molecular lengths were relatively similar overall in both experiments. Although the DMSO samples demonstrated lower MMLs than the MMS samples, the control group for this experiment also demonstrated a low MML. Therefore, it did not appear that DMSO had any impact on DNA damage measured by MML. Conclusively, the results obtained in the current study support the findings of Lundin et al. (2005), in that MMS does not directly induce DNA DSBs. This is also consistent with Wyatt and Pittman (2006), who reported that MMS carries a misleading reputation of being a radiomimetic (capable of inducing strand breaks directly).

## 4.5 Impacts of MWCNTs to the aquatic environment

Overall, data from this study and other studies conducted in fish indicate that various MWCNTs appear to exhibit relatively low toxicity to adult stage fish; even at relatively high concentrations (mg/L). Thus the toxic effects observed in this study are unlikely to be seen in the aquatic environment, where predicted environmental concentrations of CNTs are in the ng/L (Gottschalk et al., 2009) and µg/L range (Mueller and Nowack, 2008, Gottschalk et al., 2013). Furthermore, the prospect of MWCNT uptake into the fish liver appears to be rather low, as discussed in section 1.2.1. Although MWCNTs may not be particularly toxic to fish in themselves thus far, environmental concentrations will slowly increase as production and use increases (Mueller and Nowack, 2008, Gottschalk et al., 2009). Moreover, MWCNTs have been found to increase the toxic effect of other pollutants such as pesticides and lead (Martinez et al., 2013, Campos-Garcia et al., 2015) and their bioaccumulation (Sun et al., 2013). Thus, it is necessary to continue to be cautious in the production and use of MWCNTs and carry out further research on this topic.

# 5 Summary and conclusion

The aim of this study was to assess if differently functionalised MWCNTs of constant size had the potential to induce cytotoxic and genotoxic damage in fish liver cells (PLHC-1); and if this potential damage differed with type of functionalisation.

The results showed that each of the four MWCNTs tested, induced some cytotoxicity (MTT-assay), but at relatively high concentrations. MWCNT-COOH appeared to be slightly more cytotoxic than the other CNTs, whereas MWCNT-$NH_2$ appeared to be the least cytotoxic. MWCNT-$NH_2$ was not particularly cytotoxic until a concentration of ~100 µg/mL was reached. The difference in cytotoxicity was hypothesised to be due to degree of dispersability and therefore bioavailability of the CNT, which was related to surface functionalisation of the CNT. However, CNT adsorption of formazan could have influence the results, causing false positive results for cytotoxicity. CNT absorption of light at the same wavelength as formazan was found to be mostly negligible, except at very high CNT concentrations. Moreover, the results of this study indicated that BSA water as a CNT dispersant was not suitable for this cell line, due to cytotoxic effects.

Results obtained in the genotoxicity assay were inconsistent, mostly due to problems with cell lysis. Hence it was difficult to determine DNA damage from DNA-FTM levels, and no apparent differences were observed between MWCNT groups or within each group. However, investigation of median molecular lengths (MMLs) of the damaged DNA indicated that MWCNT-P and –COOH did not seem to induce any genotoxic effects. In contrast, MWCNT-OH seemed to be genotoxic at the low exposure concentration (4 µg/mL), whereas MWCNT-$NH_2$ seemed to be genoxotocity at the high exposure concentration (64 µg/mL). Due to inconsistencies in the genotoxic data it was difficult to draw any conclusions on the genotoxic potential of any of the MWCNTs. However, there were some indications of DNA damage, especially for MWCNT-OH and MWCNT-$NH_2$.

The results from this study indicates that the risk of cytotoxic effects to fish liver cells is relatively small even at high concentrations (mg/L). Since current environmental concentrations are much lower (ng-µg/L), cytotoxic effects in liver of adult fish in the environment is relatively unlikely. However, the current study was conducted *in vitro*, therefore it was not possible to study toxicokinetics in relation to CNTs. Moreover, it could not be determined with accuracy at what concentrations genotoxic effects may occur. It is also important to consider that CNTs may interact with other toxic substances (such as pesticides) and enhance their toxic effects. Future evaluations of CNT toxicity would benefit from keeping a higher level of standardisation, as well as determining CNT interactions with assay/serum components and cells.

# 6 References


AJAYAN, P. M. & LIJIMA, S. 1993. Capillarity-induced filling of carbon nanotubes. *Nature,* 361**,** 333-334.

ALI, D., AHMED, M., ALARIFI, S. & ALI, H. 2014. Ecotoxicity of single-wall carbon nanotubes to freshwater snail *Lymnaea luteola L.*: Impacts on oxidative stress and genotoxicity. *Environmental Toxicology,* 30**,** 674-82.

ARABI, M. 2004. Analyses of impact of metal ion contamination on carp (*Cyprinus carpio L.*) gill cell suspensions. *Biol Trace Elem Res,* 100**,** 229-45.

BACHTOLD, A., STRUNK, C., SALVETAT, J.-P., BONARD, J.-M., FORRÓ, L., NUSSBAUMER, T. & SCHÖNENBERGER, C. 1999. Aharonov–Bohm oscillations in carbon nanotubes. *Nature,* 397**,** 673-675.

BANDARU, P. R. 2007. Electrical Properties and Applications of Carbon Nanotube Structures. *Journal of Nanoscience and Nanotechnology,* 4-5**,** 1239-1267.

BERANEK, D. T. 1990. Distribution of methyl and ethyl adducts following alkylation with monofunctional alkylating agents. *Mutation Research/Fundamental and Molecular Mechanisms of Mutagenesis,* 231**,** 11-30.

BERRIDGE, M. V. & TAN, A. S. 1993. Characterization of the cellular reduction of 3-(4,5-dimethylthiazol-2-yl)-2,5-diphenyltetrazolium bromide (MTT): subcellular localization, substrate dependence, and involvement of mitochondrial electron transport in MTT reduction. *Archives of Biochemistry and Biophysics,* 303**,** 474-82.

BIANCO, A., KOSTARELOS, K. & PRATO, M. 2005. Applications of carbon nanotubes in drug delivery. *Current Opinion in Chemical Biology,* 9**,** 674-679.

BLUNK, T., HOCHSTRASSER, D. F., SANCHEZ, J. C., MULLER, B. W. & MULLER, R. H. 1993. Colloidal carriers for intravenous drug targeting: plasma protein adsorption patterns on surface-modified latex particles evaluated by two-dimensional polyacrylamide gel electrophoresis. *Electrophoresis,* 14**,** 1382-7.

BOOTH, A. & SØRENSEN, L. 2013. Preparation of aqueous dispersions of carbon nanotubes (CNTs). Trondheim, Norway: SINTEF.

BUSSY, C., PINAULT, M., CAMBEDOUZOU, J., LANDRY, M. J., JEGOU, P., MAYNE-L'HERMITE, M., LAUNOIS, P., BOCZKOWSKI, J. & LANONE, S. 2012. Critical role of surface chemical modifications induced by length shortening on multi-walled carbon nanotubes-induced toxicity. *Particle and Fibre Toxicology,* 9**,** 46.

CAMPOS-DELGADO, J., MACIEL, I. O., CULLEN, D. A., SMITH, D. J., JORIO, A., PIMENTA, M. A., TERRONES, H. & TERRONES, M. 2010. Chemical vapor deposition synthesis of N-, P-, and Si-doped single-walled carbon nanotubes. *ACS Nano,* 4**,** 1696-1702.

CAMPOS-GARCIA, J., MARTINEZ, D. S. T., ALVES, O. L., LEONARDO, A. F. G. & BARBIERI, E. 2015. Ecotoxicological effects of carbofuran and oxidised multiwalled carbon nanotubes on the freshwater fish *Nile tilapia*: Nanotubes enhance pesticide ecotoxicity. *Ecotoxicology and Environmental Safety,* 111**,** 131-137.

CARTER, D. C. & HO, J. X. 1994. Structure of serum albumin. *Advances in Protein Chemistry,* 45**,** 153-203.

CASEY, A., HERZOG, E., DAVOREN, M., LYNG, F. M., BYRNE, H. J. & CHAMBERS, G. 2007. Spectroscopic analysis confirms the interactions between single walled carbon nanotubes and various dyes commonly used to assess cytotoxicity. *Carbon,* 45**,** 1425-1432.

CAVALLO, D., FANIZZA, C., URSINI, C. L., CASCIARDI, S., PABA, E., CIERVO, A., FRESEGNA, A. M., MAIELLO, R., MARCELLONI, A. M., BURESTI, G., TOMBOLINI, F., BELLUCCI, S. & IAVICOLI, S. 2012. Multi-walled carbon nanotubes induce cytotoxicity and genotoxicity in human lung epithelial cells. *Journal of Applied Toxicology,* 32**,** 454-64.

CELLOT, G., CILIA, E., CIPOLLONE, S., RANCIC, V., SUCAPANE, A., GIORDANI, S., GAMBAZZI, L., MARKRAM, H., GRANDOLFO, M., SCAINI, D., GELAIN, F., CASALIS, L., PRATO, M., GIUGLIANO,

M. & BALLERINI, L. 2009. Carbon nanotubes might improve neuronal performance by favouring electrical shortcuts. *Nature Nanotechnology,* 4**,** 126-133.
CELLOT, G., TOMA, F. M., VARLEY, Z. K., LAISHRAM, J., VILLARI, A., QUINTANA, M., CIPOLLONE, S., PRATO, M. & BALLERINI, L. 2011. Carbon nanotube scaffolds tune synaptic strength in cultured neural circuits: novel frontiers in nanomaterial-tissue interactions. *Journal of Neuroscience,* 31**,** 12945-53.
CHATTERJEE, N., YANG, J., KIM, H.-M., JO, E., KIM, P.-J., CHOI, K. & CHOI, J. 2014. Potential Toxicity of Differential Functionalized Multiwalled Carbon Nanotubes (MWCNT) in Human Cell Line (BEAS2B) and *Caenorhabditis elegans*. *Journal of Toxicology and Environmental Health, Part A,* 77**,** 1399-1408.
CHEN, J., HAMON, M. A., HU, H., CHEN, Y., RAO, A. M., EKLUND, P. C. & HADDON, R. C. 1998. Solution Properties of Single-Walled Carbon Nanotubes. *Science,* 282**,** 95-98.
CHEN, K. L. & ELIMELECH, M. 2007. Influence of humic acid on the aggregation kinetics of fullerene (C60) nanoparticles in monovalent and divalent electrolyte solutions. *Journal of Colloid and Interface Science,* 309**,** 126-134.
CHENG, J., CHAN, C. M., VECA, L. M., POON, W. L., CHAN, P. K., QU, L., SUN, Y.-P. & CHENG, S. H. 2009. Acute and long-term effects after single loading of functionalized multi-walle carbon nanotubes into zebrafish (*Danio rerio*). *Toxicology and Applied Pharmacology,* 235**,** 216-225.
CHENG, J. & CHENG, S. H. 2012. Influence of carbon nanotube length on toxicity to zebrafish embryos. *International Journal of Nanomedicine,* 7**,** 3731-3739.
CHENG, X., ZHONG, J., MENG, J., YANG, M., JIA, F., XU, Z., KONG, H. & XU, H. 2011. Characterization of Multiwalled Carbon Nanotubes Dispersing in Water and Association with Biological Effects. *Journal of Nanomaterials,* 2011**,** e938491.
CHERUKURI, P., BACHILO, S. M., LITOVSKY, S. H. & WEISMAN, R. B. 2004. Near-Infrared Fluorescence Microscopy of Single-Walled Carbon Nanotubes in Phagocytic Cells. *Journal of the American Chemical Soicety,* 126**,** 15638-15639.
CHO, Y. & BORGENS, R. B. 2010. The effect of an electrically conductive carbon nanotube/collagen composite on neurite outgrowth of PC12 cells. *Journal of Biomedical Materials Research Part A,* 95A**,** 510-517.
CLIFT, M. J., BHATTACHARJEE, S., BROWN, D. M. & STONE, V. 2010. The effects of serum on the toxicity of manufactured nanoparticles. *Toxicology Letters,* 198**,** 358-65.
COCCINI, T., RODA, E., SARIGIANNIS, D. A., MUSTARELLI, P., QUARTARONE, E., PROFUMO, A. & MANZO, L. 2010. Effects of water-soluble functionalized multi-walled carbon nanotubes examined by different cytotoxicity methods in human astrocyte D384 and lung A549 cells. *Toxicology,* 269**,** 41-53.
COLLINS, P. G., ARNOLD, M. S. & AVOURIS, P. 2001. Engineering carbon nanotubes and nanotube circuits using electrical breakdown. *Science,* 292**,** 706-709.
DE JONGE, N., LAMY, Y., SCHOOTS, K. & OOSTERKAMP, T. H. 2002. High brightness electron beam from a multi-walled carbon nanotube. *Nature,* 420**,** 393-395.
DHAWAN, A. & SHARMA, V. 2010. Toxicity assessment of nanomaterials: methods and challenges. *Analytical and Bioanalytical Chemistry,* 398**,** 589-605.
DI GIORGIO, M. L., BUCCHIANICO, S. D., RAGNELLI, A. M., AIMOLA, P., SANTUCCI, S. & POMA, A. 2011. Effects of single and multi walled carbon nanotubes on macrophages: Cyto and genotoxicity and electron microscopy. *Mutation Research/Genetic Toxicology and Environmental Mutagenesis,* 722**,** 20-31.
DOAK, S. H., MANSHIAN, B., JENKINS, G. J. S. & SINGH, N. 2012. In vitro genotoxicity testing strategy for nanomaterials and the adaptation of current OECD guidelines. *Mutation Research/Genetic Toxicology and Environmental Mutagenesis,* 745**,** 104-111.
DUJARDIN, E., EBBESEN, T. W., KRISHNAN, A. & TREACY, M. M. J. 1998. Purification of Single-Shell Nanotubes. *Advanced Materials,* 10**,** 611-613.
DURÁN, N., GUTERRES, S. S. & ALVES, O. L. 2014. *Nanotoxicology,* New York, Springer Science & Business Media.

EDDY, F. B. & TALBOT, C. 1985. Sodium balance in eggs and dechorionated embryos of the atlantic salmon *Salmo salar L*. exposed to zinc, aluminium and acid waters. *Comparative Biochemistry and Physiology Part C: Comparative Pharmacology,* 81**,** 259-266.

EHRENBERG, M. S., FRIEDMAN, A. E., FINKELSTEIN, J. N., OBERDÖRSTER, G. & MCGRATH, J. L. 2009. The influence of protein adsorption on nanoparticle association with cultured endothelial cells. *Biomaterials,* 30**,** 603-610.

ELLIOTT, W. H. & ELLIOTT, D. C. 1997. *Biochemistry and Molecular Biology,* New York, Oxford University Press.

ERKAN, E., DEVARAJAN, P. & SCHWARTZ, G. J. 2005. Apoptotic response to albumin overload: proximal vs. distal/collecting tubule cells. *American Journal of Nephrology,* 25**,** 121-31.

ESCHER, B. I., BEHRA, R., EGGEN, R. I. L. & FENT, K. 1997. Molecular Mechanisms in Ecotoxicology: An Interplay between Environmental Chemistry and Biology. *CHIMIA International Journal for Chemistry,* 51**,** 915-921.

FABBRO, A., PRATO, M. & BALLERINI, L. 2013. Carbon nanotubes in neuroregeneration and repair. *Advanced Drug Delivery Reviews,* 65**,** 2034-2044.

FABBRO, A., VILLARI, A., LAISHRAM, J., SCAINI, D., TOMA, F. M., TURCO, A., PRATO, M. & BALLERINI, L. 2012. Spinal Cord Explants Use Carbon Nanotube Interfaces To Enhance Neurite Outgrowth and To Fortify Synaptic Inputs. *ACS Nano,* 6**,** 2041-2055.

FARCAL, L., TORRES ANDON, F., DI CRISTO, L., ROTOLI, B. M., BUSSOLATI, O., BERGAMASCHI, E., MECH, A., HARTMANN, N. B., RASMUSSEN, K., RIEGO-SINTES, J., PONTI, J., KINSNER-OVASKAINEN, A., ROSSI, F., OOMEN, A., BOS, P., CHEN, R., BAI, R., CHEN, C., ROCKS, L., FULTON, N., ROSS, B., HUTCHISON, G., TRAN, L., MUES, S., OSSIG, R., SCHNEKENBURGER, J., CAMPAGNOLO, L., VECCHIONE, L., PIETROIUSTI, A. & FADEEL, B. 2015. Comprehensive In Vitro Toxicity Testing of a Panel of Representative Oxide Nanomaterials: First Steps towards an Intelligent Testing Strategy. *PLoS One,* 10**,** e0127174.

FENSTAD, A. A., JENSSEN, B. M., MOE, B., HANSSEN, S. A., BINGHAM, C., HERZKE, D., BUSTNES, J. O. & KROKJE, A. 2014. DNA double-strand breaks in relation to persistent organic pollutants in a fasting seabird. *Ecotoxicology and Environmental Safety,* 106**,** 68-75.

FERNÁNDEZ-CRUZ, M. L., LAMMEL, T., CONNOLLY, M., CONDE, E., BARRADO, A. I., DERICK, S., PEREZ, Y., FERNANDEZ, M., FURGER, C. & NAVAS, J. M. 2013. Comparative cytotoxicity induced by bulk and nanoparticulated ZnO in the fish and human hepatoma cell lines PLHC-1 and Hep G2. *Nanotoxicology,* 7**,** 935-952.

FILHO, J. D. S., MATSUBARA, E. Y., FRANCHI, L. P., MARTINS, I. P., RIVERA, L. M. R., ROSOLEN, J. M. & GRISOLIA, C. K. 2014. Evaluation of carbon nanotubes network toxicity in zebrafish (*Danio rerio*) model. *Environmental Research,* 134**,** 9-16.

FOREST, V., FIGAROL, A., BOUDARD, D., COTTIER, M., GROSSEAU, P. & POURCHEZ, J. 2015. Adsorption of Lactate Dehydrogenase Enzyme on Carbon Nanotubes: How to Get Accurate Results for the Cytotoxicity of These Nanomaterials. *Langmuir,* 31**,** 3635-3643.

FRACZEK-SZCZYPTA, A., MENASZEK, E., SYEDA, T. B., MISRA, A., ALAVIJEH, M., ADU, J. & BLAZEWICZ, S. 2012. Effect of MWCNT surface and chemical modification on in vitro cellular response. *Journal of Nanoparticle Research,* 14**,** 1181.

GAO, J., LLANEZA, V., YOUN, S., SILVERA-BATISTA, C. A., ZIEGLER, K. J. & BONZONGO, J.-C. J. 2012. Aqueous suspension methods of carbon-based nanomaterials and biological effects on model aquatic organisms. *Environmental Toxicology and Chemistry,* 31**,** 210-214.

GEYS, J., NEMERY, B. & HOET, P. H. M. 2010. Assay conditions can influence the outcome of cytotoxicity tests of nanomaterials: Better assay characterization is needed to compare studies. *Toxicology in Vitro,* 24**,** 620-629.

GHOSH, M., CHAKRABORTY, A., BANDYOPADHYAY, M. & MUKHERJEE, A. 2011. Multi-walled carbon nanotubes (MWCNT): induction of DNA damage in plant and mammalian cells. *Journal of Hazardous Materials,* 197**,** 327-36.

GOTTSCHALK, F., SONDERER, T., SCHOLZ, R. W. & NOWACK, B. 2009. Modeled Environmental Concentrations of Engineered Nanomaterials (TiO2, ZnO, Ag, CNT, Fullerenes) for Different Regions. *Environmental Science & Technology,* 43**,** 9216-9222.

GOTTSCHALK, F., SONDERER, T., SCHOLZ, R. W. & NOWACK, B. 2010. Possibilities and limitations of modeling environmental exposure to engineered nanomaterials by probabilistic material flow analysis. *Environmental Toxicology and Chemistry,* 29**,** 1036-1048.

GOTTSCHALK, F., SUN, T. & NOWACK, B. 2013. Environmental concentrations of engineered nanomaterials: review of modeling and analytical studies. *Environmental Pollution,* 181**,** 287-300.

GREEN, A. A. & HERSAM, M. C. 2011. Properties and Application of Double-Walled Carbon Nanotubes Sorted by Outer-Wall Electronic Type. *ACS Nano,* 5**,** 1459-1467.

HANDY, R., VON DER KAMMER, F., LEAD, J., HASSELLÖV, M., OWEN, R. & CRANE, M. 2008a. The ecotoxicology and chemistry of manufactured nanoparticles. *Ecotoxicology,* 17**,** 287-314.

HANDY, R. D., AL-BAIRUTY, G., AL-JUBORY, A., RAMSDEN, C. S., BOYLE, D., SHAW, B. J. & HENRY, T. B. 2011. Effects of manufactured nanomaterials on fishes: a target organ and body systems physiology approach. *Journal of Fish Biology,* 79**,** 821-853.

HANDY, R. D., HENRY, T. B., SCOWN, T. M., JOHNSTON, B. D. & TYLER, C. R. 2008b. Manufactured nanoparticles: their uptake and effects on fish—a mechanistic analysis. *Ecotoxicology,* 17**,** 396-409.

HELLEDAY, T., LO, J., VAN GENT, D. C. & ENGELWARD, B. P. 2007. DNA double-strand break repair: from mechanistic understanding to cancer treatment. *DNA Repair (Amst.),* 6**,** 923-35.

HIGHTOWER, L. E. & RENFRO, J. L. 1988. Recent applications of fish cell culture to biomedical research. *Journal of Experimental Zoology,* 248**,** 290-302.

HIRSCH, A. & VOSTROWSKY, O. 2005. Functionalization of Carbon Nanotubes. *In:* SCHLÜTER, A. D. (ed.) *Functional Molecular Nanostructures.* Germany: Springer Berlin Heidelberg.

HOLBROOK, R. D., KLINE, C. N. & FILLIBEN, J. J. 2010. Impact of Source Water Quality on Multiwall Carbon Nanotube Coagulation. *Environmental Science and Technology,* 44**,** 1386-1391.

HOLCOMBE, B. 2001. Textiles as a Communication Platform. *CSIRO TFT.* Australia.

HOLDER, A. L., GOTH-GOLDSTEIN, R., LUCAS, D. & KOSHLAND, C. P. 2012. Particle-Induced Artifacts in the MTT and LDH Viability Assays. *Chemical Research in Toxicology,* 25**,** 1885-1892.

HOLZINGER, M., HIRSCH, A., BERNIER, P., DUESBERG, G. S. & BURGHARD, M. 2000. A new purification method for single-wall carbon nanotubes (SWNTs). *Applied Physics A,* 70**,** 599-602.

HOU, W.-C., WESTERHOFF, P. & POSNER, J. D. 2013. Biological accumulation of engineered nanomaterials: a review of current knowledge. *Environmental Science: Processes & Impacts,* 15**,** 103-122.

HU, H., NI, Y., MONTANA, V., HADDON, R. C. & PARPURA, V. 2004. Chemically Functionalized Carbon Nanotubes as Substrates for Neuronal Growth. *Nano Letters,* 4**,** 507-511.

IIJIMA, S. 1991. Helical microtubules of graphitic carbon. *Nature,* 354**,** 56-58.

JACKSON, P., JACOBSEN, N. R., BAUN, A., BIRKEDAL, R., KÜHNEL, D., JENSEN, K. A., VOGEL, U. & WALLIN, H. 2013. Bioaccumulation and ecotoxicity of carbon nanotubes. *Chemistry Central Journal,* 7**,** 154.

JACKSON, P., KLING, K., JENSEN, K. A., CLAUSEN, P. A., MADSEN, A. M., WALLIN, H. & VOGEL, U. 2015. Characterization of genotoxic response to 15 multiwalled carbon nanotubes with variable physicochemical properties including surface functionalizations in the FE1-Muta(TM) mouse lung epithelial cell line. *Environmental and Molecular Mutagenesis,* 56**,** 183-203.

JACKSON, S. P. 1999. Detection, repair and signalling of DNA double-strand breaks. *Biochemical Society Transactions.,* 27**,** 1-13.

JANG, M. J., NAMGUNG, S., HONG, S. & NAM, Y. 2010. Directional neurite growth using carbon nanotube patterned substrates as a biomimetic cue. *Nanotechnology,* 21**,** 235102.

JEGGO, P. A. 1998. Identification of genes involved in repair of DNA double-strand breaks in mammalian cells. *Radiation Research,* 150**,** S80-91.
JENSEN, K. A., KEMBOUCHE, Y., CHRISTIANSEN, E., JACOBSEN, N. R. & WALLIN, H. 2011. The generic NANOGENOTOX dispersion protocol. Copenhagen,Denmark: NRCWE.
JIANG, Y., ZHANG, H., WANG, Y., CHEN, M., YE, S., HOU, Z. & REN, L. 2013. Modulation of Apoptotic Pathways of Macrophages by Surface-Functionalized Multi-Walled Carbon Nanotubes. *PLoS One,* 8**,** e65756.
JIN, G.-Z., KIM, M., SHIN, U. S. & KIM, H.-W. 2011a. Neurite outgrowth of dorsal root ganglia neurons is enhanced on aligned nanofibrous biopolymer scaffold with carbon nanotube coating. *Neuroscience Letters,* 501**,** 10-14.
JIN, G. Z., KIM, M., SHIN, U. S. & KIM, H. W. 2011b. Effect of carbon nanotube coating of aligned nanofibrous polymer scaffolds on the neurite outgrowth of PC-12 cells. *Cell Biology International,* 35**,** 741-745.
KANAAR, R., HOEIJMAKERS, J. H. J. & VAN GENT, D. C. 1998. Molecular mechanisms of DNA double-strand break repair. *Trends in Cell Biology,* 8**,** 483-489.
KANG, S., MAUTER, M. S. & ELIMELECH, M. 2009. Microbial Cytotoxicity of Carbon-Based Nanomaterials: Implications for River Water and Wastewater Effluent. *Environmental Science and Technology,* 43**,** 2648-2653.
KARAJANAGI, S. S., VERTEGEL, A. A., KANE, R. S. & DORDICK, J. S. 2004. Structure and function of enzymes adsorbed onto single-walled carbon nanotubes. *Langmuir,* 20**,** 11594-9.
KARLSSON, H. L., CRONHOLM, P., GUSTAFSSON, J. & MOLLER, L. 2008. Copper oxide nanoparticles are highly toxic: a comparison between metal oxide nanoparticles and carbon nanotubes. *Chemical Research in Toxicology,* 21**,** 1726-32.
KASHIWADA, S. 2006. Distribution of Nanoparticles in the See-through Medaka (*Oryzias latipes*). *Environmental Health Perspectives,* 114**,** 1697-1702.
KATO, T., TOTSUKA, Y., ISHINO, K., MATSUMOTO, Y., TADA, Y., NAKAE, D., GOTO, S., MASUDA, S., OGO, S., KAWANISHI, M., YAGI, T., MATSUDA, T., WATANABE, M. & WAKABAYASHI, K. 2012. Genotoxicity of multi-walled carbon nanotubes in both in vitro and in vivo assay systems. *Nanotoxicology,* 7**,** 452-461.
KERMANIZADEH, A., GAISER, B. K., HUTCHISON, G. R. & STONE, V. 2012. An in vitro liver model - assessing oxidative stress and genotoxicity following exposure of hepatocytes to a panel of engineered nanomaterials. *Particle and Fibre Toxicology,* 9**,** 28.
KHIM CHNG, E. L., CHUA, C. K. & PUMERA, M. 2014. Graphene oxide nanoribbons exhibit significantly greater toxicity than graphene oxide nanoplatelets. *Nanoscale,* 6**,** 10792-7.
KISIN, E. R., MURRAY, A. R., SARGENT, L., LOWRY, D., CHIRILA, M., SIEGRIST, K. J., SCHWEGLER-BERRY, D., LEONARD, S., CASTRANOVA, V., FADEEL, B., KAGAN, V. E. & SHVEDOVA, A. A. 2011. Genotoxicity of carbon nanofibers: are they potentially more or less dangerous than carbon nanotubes or asbestos? *Toxicology and Applied Pharmacology,* 252**,** 1-10.
KLAINE, S. J., ALVAREZ, P. J. J., BATLEY, G. E., FERNANDES, T. F., HANDY, R. D., LYON, D. Y., MAHENDRA, S., MCLAUGHLIN, M. J. & LEAD, J. R. 2008. Nanomaterials in the environment: behaviour, fate, bioavailability, and effects. *Environmental Toxicology and Chemistry,* 27**,** 1825-1851.
KRØKJE, Å., BINGHAM, C., HUSMO TUVEN, R. & WING GABRIELSEN, G. 2006. Chromosome Aberrations and DNA Strand Breaks in Glaucous Gull (*Larus Hyperboreus*) Chicks Fed Environmentally Contaminated Gull Eggs. *Journal of Toxicology and Environmental Health, Part A,* 69**,** 159-174.
KROLL, A., PILLUKAT, M. H., HAHN, D. & SCHNEKENBURGER, J. 2009. Current in vitro methods in nanoparticle risk assessment: Limitations and challenges. *European Journal of Pharmaceutics and Biopharmaceutics,* 72**,** 370-377.
KUNHIKRISHNAN, A., SHON, H. K., BOLAN, N. S., EL SALIBY, I. & VIGNESWARAN, S. 2014. Sources, Distribution, Environmental Fate, and Ecological Effects of Nanomaterials in Wastewater Streams. *Critical Reviews in Environmental Science and Technology,* 45**,** 277-318.

LAMMEL, T. & NAVAS, J. M. 2014. Graphene nanoplatelets spontaneously translocate into the cytosol and physically interact with cellular organelles in the fish cell line PLHC-1. *Aquatic Toxicology,* 150**,** 55-65.

LEAD, J. R. & WILKINSON, K. J. 2006. Environmental colloids: Current knowledge and future developments. *In:* WILKINSON, K. J. & LEAD, J. R. (eds.) *Environmental Colloids: Behaviour, Structure and Characterization.* Chichester, UK: John Wiley.

LEE, J., FORTNER, J. D., HUGHES, J. B. & KIM, J.-H. 2007. Photochemical Production of Reactive Oxygen Species by C60 in the Aqueous Phase During UV Irradiation. *Environmental Science & Technology,* 41**,** 2529-2535.

LEE, J. W., CHOI, Y. C., KIM, R. & LEE, S. K. 2015. Multiwall Carbon Nanotube-Induced Apoptosis and Antioxidant Gene Expression in the Gills, Liver, and Intestine of *Oryzias latipes*. *BioMed Research International,* 2015**,** e485343.

LINDBERG, H. K., FALCK, G. C.-M., SINGH, R., SUHONEN, S., JÄRVENTAUS, H., VANHALA, E., CATALÁN, J., FARMER, P. B., SAVOLAINEN, K. M. & NORPPA, H. 2012. Genotoxicity of short single-wall and multi-wall carbon nanotubes in human bronchial epithelial and mesothelial cells in vitro. *Toxicology,* 313**,** 24-37.

LIU, J., RINZLER, A. G., DAI, H., HAFNER, J. H., BRADLEY, R. K., BOUL, P. J., LU, A., IVERSON, T., SHELIMOV, K., HUFFMAN, C. B., RODRIGUEZ-MACIAS, F., SHON, Y.-S., LEE, T. R., COLBERT, D. T. & SMALLEY, R. E. 1998. Fullerene Pipes. *Science,* 280**,** 1253-1256.

LIU, Y., PETERSON, D. A., KIMURA, H. & SCHUBERT, D. 1997. Mechanism of cellular 3-(4,5-dimethylthiazol-2-yl)-2,5-diphenyltetrazolium bromide (MTT) reduction. *Journal of Neurochemistry,* 69**,** 581-93.

LIU, Z., DONG, X., SONG, L., ZHANG, H., LIU, L., ZHU, D., SONG, C. & LENG, X. 2014. Carboxylation of multiwalled carbon nanotube enhanced its biocompatibility with L02 cells through decreased activation of mitochondrial apoptotic pathway. *Journal of Biomedical Materials Research Part A,* 102**,** 665-673.

LIU, Z., FAN, A. C., RAKHRA, K., SHERLOCK, S., GOODWIN, A., CHEN, X., YANG, Q., FELSHER, D. W. & DAI, H. 2009. Supramolecular stacking of doxorubicin on carbon nanotubes for in vivo cancer therapy. *Angewandte Chemie International Edition in English,* 48**,** 7668-72.

LIU, Z., WINTERS, M., HOLODNIY, M. & DAI, H. 2007. siRNA delivery into human T cells and primary cells with carbon-nanotube transporters. *Angewandte Chemie International Edition in English,* 46**,** 2023-7.

LUNDIN, C., NORTH, M., ERIXON, K., WALTERS, K., JENSSEN, D., GOLDMAN, A. S. & HELLEDAY, T. 2005. Methyl methanesulfonate (MMS) produces heat-labile DNA damage but no detectable in vivo DNA double-strand breaks. *Nucleic Acids Research,* 33**,** 3799-811.

LYNCH, I., CEDERVALL, T., LUNDQVIST, M., CABALEIRO-LAGO, C., LINSE, S. & DAWSON, K. A. 2007. The nanoparticle-protein complex as a biological entity; a complex fluids and surface science challenge for the 21st century. *Advances in Colloid and Interface Science,* 134-135**,** 167-74.

MARCHES, R., MIKORYAK, C., WANG, R. H., PANTANO, P., DRAPER, R. K. & VITETTA, E. S. 2011. The importance of cellular internalization of antibody-targeted carbon nanotubes in the photothermal ablation of breast cancer cells. *Nanotechnology,* 22**,** 095101.

MARTINEZ, D. S. T., ALVES, O. L. & BARBIERI, E. 2013. Carbon nanotubes enhanced the lead toxicity on the freshwater fish. *Journal of Physics: Conference Series,* 429**,** 012043.

MARULANDA, J. M. 2011. *Carbon Nanotubes Applications on Electron Devices,* New York, InTech.

MAUTER, M. S. & ELIMELECH, M. 2008. Environmental Applications of Carbon-Based Nanomaterials. *Environmental Science and Technology,* 42**,** 5843-5859.

MAWHINNEY, D. B., NAUMENKO, V., KUZNETSOVA, A., YATES, J. T., LIU, J. & SMALLEY, R. E. 2000. Infrared Spectral Evidence for the Etching of Carbon Nanotubes: Ozone Oxidation at 298 K. *Journal of American Chemical Soicety,* 122**,** 2383-2384.

MAYNARD, A. D. 2006. Nanotechnology: A Research Strategy for Addressing Risk *In:* MAYNARD, A.D. (ed.). Washington DC, USA.

MCSHAN, D. & YU, H. 2012. DNA damage in human skin keratinocytes caused by multi-walled carbon nanotubes with carboxylate functionalization. *Toxicology and industrial health,* 30**,** 489-498.
MIGLIORE, L., SARACINO, D., BONELLI, A., COLOGNATO, R., D'ERRICO, M. R., MAGRINI, A., BERGAMASCHI, A. & BERGAMASCHI, E. 2010. Carbon nanotubes induce oxidative DNA damage in RAW 264.7 cells. *Environmental and Molecular Mutagenisis,* 51**,** 294-303.
MILNE, W. I., TEO, K. B. K., AMARATUNGA, G. A. J., LEGAGNEUX, P., GANGLOFF, L., SCHNELL, J. P., SEMET, V., THIEN BINH, V. & GROENING, O. 2004. Carbon nanotubes as field emission sources. *Journal of Materials Chemistry,* 14**,** 933-943.
MONTEIRO-RIVIERE, N. A. & INMAN, A. O. 2006. Challenges for assessing carbon nanomaterial toxicity to the skin. *Carbon,* 44**,** 1070-1078.
MOSMANN, T. 1983. Rapid colorimetric assay for cellular growth and survival - Application to proliferation and cyto-toxicity assays. *Journal of Immunological Methods,* 65**,** 55-63.
MOUCHET, F., LANDOIS, P., DATSYUK, V., PUECH, P., PINELLI, E., FLAHAUT, E. & GAUTHIER, L. 2011. International amphibian micronucleus standardized procedure (ISO 21427-1) for in vivo evaluation of double-walled carbon nanotubes toxicity and genotoxicity in water. *Environmental Toxicology,* 26**,** 136-45.
MUELLER, N. C. & NOWACK, B. 2008. Exposure modeling of engineered nanoparticles in the environment. *Environmental Science and Technology,* 42**,** 4447-53.
NAHA, P. C. & BYRNE, H. J. 2013. Generation of intracellular reactive oxygen species and genotoxicity effect to exposure of nanosized polyamidoamine (PAMAM) dendrimers in PLHC-1 cells in vitro. *Aquatic Toxicology,* 132–133**,** 61-72.
NEL, A. E., MADLER, L., VELEGOL, D., XIA, T., HOEK, E. M., SOMASUNDARAN, P., KLAESSIG, F., CASTRANOVA, V. & THOMPSON, M. 2009. Understanding biophysicochemical interactions at the nano-bio interface. *Nature Materials,* 8**,** 543-57.
OBERDÖRSTER, G., KANE, A. B., KLAPER, R. D. & HURT, R. H. 2013. Nanotoxicology. *In:* KLAASSEN, C. D. (ed.) *Casarett & Doull's Toxicology: The Basic Science of Poisons.* New York, USA: McGraw-Hill Professional. p.1189-1229.
OBERDÖRSTER, G., STONE, V. & DONDALDSON, K. 2007. Toxicology of nanoparticles: A historical perspective. *Nanotoxicology,* 1**,** 2-25.
PANHUIS, M. I. H., WU, J., ASHRAF, S. A. & WALLACE, G. G. 2007. Conducting textiles from single-walled carbon nanotubes. *Synthetic Metals,* 157**,** 358-362.
PARK, S., VOSGUERICHIAN, M. & BAO, Z. 2013. A review of fabrication and applications of carbon nanotube film-based flexible electronics. *Nanoscale,* 5**,** 1727-1752.
PATEL, V. 2011. *Global carbon nanotubes market - industry beckons* [Online]. Nanotech Insights. Available: http://www.nanowerk.com/spotlight/spotid=23118.php [Accessed 10.05.2015].
PATLOLLA, A., PATLOLLA, B. & TCHOUNWOU, P. 2010. Evaluation of cell viability, DNA damage, and cell death in normal human dermal fibroblast cells induced by functionalized multiwalled carbon nanotube. *Molecular and Cellular Biochemistry,* 338**,** 225-232.
PELKA, J., GEHRKE, H., RECHEL, A., KAPPES, M., HENNRICH, F., HARTINGER, C. G. & MARKO, D. 2013. DNA damaging properties of single walled carbon nanotubes in human colon carcinoma cells. *Nanotoxicology,* 7**,** 2-20.
PETERSEN, E. J. & HENRY, T. B. 2012. Methodological considerations for testing the ecotoxicity of carbon nanotubes and fullerenes: review. *Environmental Toxicology and Chemistry,* 31**,** 60-72.
PETERSEN, E. J., PINTO, R. A., MAI, D. J., LANDRUM, P. F. & WEBER, W. J. J. 2011. Influence of polyethyleneimine graftings of multi-walled carbon nanotubes on their accumulation and elimination by and toxicity to *Daphnia magna*. *Environmental Science and Technology,* 45**,** 1133-1138.
PFEIFFER, P. 1998. The mutagenic potential of DNA double-strand break repair. *Toxicology Letters,* 96-97**,** 119-29.
PONTI, J., BROGGI, F., MARIANI, V., DE MARZI, L., COLOGNATO, R., MARMORATO, P., GIORIA, S., GILLILAND, D., PASCUAL GARCÌA, C., MESCHINI, S., STRINGARO, A., MOLINARI, A.,

RAUSCHER, H. & ROSSI, F. 2013. Morphological transformation induced by multiwall carbon nanotubes on Balb/3T3 cell model as an in vitro end point of carcinogenic potential. *Nanotoxicology,* 7**,** 221-233.

POP, E., MANN, D., WANG, Q., GOODSON, K. & DAI, H. 2006. Thermal Conductance of an Individual Single-Wall Carbon Nanotube above Room Temperature. *Nano Letters,* 6**,** 96-100.

PULSKAMP, K., DIABATÉ, S. & KRUG, H. F. 2007. Carbon nanotubes show no sign of acute toxicity but induce intracellular reactive oxygen species in dependence on contaminants. *Toxicology Letters,* 168**,** 58-74.

QI, R., SHEN, M., CAO, X., GUO, R., TIAN, X., YU, J. & SHI, X. 2011. Exploring the dark side of MTT viability assay of cells cultured onto electrospun PLGA-based composite nanofibrous scaffolding materials. *Analyst,* 136**,** 2897-2903.

RINZLER, A. G., LIU, J., DAI, H., NIKOLAEV, P., HUFFMAN, C. B., RODRÍGUEZ-MACÍAS, F. J., BOUL, P. J., LU, A. H., HEYMANN, D., COLBERT, D. T., LEE, R. S., FISCHER, J. E., RAO, A. M., EKLUND, P. C. & SMALLEY, R. E. 1998. Large-scale purification of single-wall carbon nanotubes: process, product, and characterization. *Applied Physics A,* 67**,** 29-37.

ROBERTSON, J. 2004. Realistic applications of CNTs. *Materials Today,* 7**,** 46-52.

ROCHA, A. M. D., FERREIRA, J. R., BARROS, D. M., PEREIRA, T. C. B., BOGO, M. R., OLIVEIRA, S., GERALDO, V., LACERDA, R. G., FERLAUTO, A. S., LADEIRA, L. O., PINHEIRO, M. V. B. & MONSERRAT, J. M. 2013. Gene expression and biochemical responses in brain of zebrafish *Danio rerio* exposed to organic nanomaterials: Carbon nanotubes (SWCNT) and fullerenol (C60(OH)18–22(OK4)). *Comparative Biochemistry and Physiology, Part A,* 165**,** 460-467.

RYAN, J. A. & HIGHTOWER, L. E. 1994. Evaluation of heavy-metal ion toxicity in fish cells using a combined stress protein and cytotoxicity assay. *Environmental Toxicology and Chemistry,* 13**,** 1231-1240.

SAITO, R., DRESSELHAUS, G. & DRESSELHAUS, M. 1993. Electronic structure of double-layer graphene tubules. *Journal of Applied Physics,* 73**,** 494-500.

SARGENT, L. M., HUBBS, A. F., YOUNG, S. H., KASHON, M. L., DINU, C. Z., SALISBURY, J. L., BENKOVIC, S. A., LOWRY, D. T., MURRAY, A. R., KISIN, E. R., SIEGRIST, K. J., BATTELLI, L., MASTOVICH, J., STURGEON, J. L., BUNKER, K. L., SHVEDOVA, A. A. & REYNOLDS, S. H. 2012. Single-walled carbon nanotube-induced mitotic disruption. *Mutation Research/Genetic Toxicology and Environmental Mutagenesis,* 745**,** 28-37.

SAYES, C. M., GOBIN, A. M., AUSMAN, K. D., MENDEZ, J., WEST, J. L. & COLVINA, V. L. 2005. Nano-C60 cytotoxicity is due to lipid peroxidation. *Biomaterials,* 26**,** 7587-7595.

SCHULTZ, M. E. & SCHULTZ, J. R. 1985. Transplantable chemically-induced liver tumors in the viviparous fish *Poeciliopsis*. *Experimental and Molecular Pathology,* 42**,** 320-330.

SCIENCES, C. A. O. 2014. *Products, MWCNTs* [Online]. Chinese Academy of Sciences. Available: http://www.timesnano.com/en/view.php?prt=3,29,50,81&id=244 [Accessed 10.05.2015].

SERVICE, R. F. 2003. Electronic textiles charge ahead. *Science,* 301**,** 909-911.

SGOBBA, V. & GULDIA, D. M. 2009. Carbon nanotubes—electronic/electrochemical properties and application for nanoelectronics and photonics. *Chemical Society Reviews,* 38**,** 165-184.

SHUGART, L. 2000. DNA Damage as a Biomarker of Exposure. *Ecotoxicology,* 9**,** 329-340.

SHVEDOVA, A. A., KISIN, E., MURRAY, A. R., JOHNSON, V. J., GORELIK, O., AREPALLI, S., HUBBS, A. F., MERCER, R. R., KEOHAVONG, P., SUSSMAN, N., JIN, J., YIN, J., STONE, S., CHEN, B. T., DEYE, G., MAYNARD, A., CASTRANOVA, V., BARON, P. A. & KAGAN, V. E. 2008. Inhalation vs. aspiration of single-walled carbon nanotubes in C57BL/6 mice: inflammation, fibrosis, oxidative stress, and mutagenesis. *American Journal of Physiology, Lung Cellular and Molecular Physiology,* 295**,** L552-65.

SILVA, G., MUSUMECI, A., GOMES, A., LIU, J.-W., WACLAWIK, E., GEORGE, G., FROST, R. & PIMENTA, M. 2009. Characterization of commercial double-walled carbon nanotube material: composition, structure, and heat capacity. *Journal of Materials Science,* 44**,** 3498-3503.

SIMON-DECKERS, A., GOUGET, B., MAYNE-L'HERMITE, M., HERLIN-BOIME, N., REYNAUD, C. & CARRIÈRE, M. 2008. In vitro investigation of oxide nanoparticle and carbon nanotube toxicity and intracellular accumulation in A549 human pneumocytes. *Toxicology,* 253**,** 137-146.

SINGH, A., MISRA, R., MOHANTY, C. & SAHOO, S. K. 2010. Applications of Nanotechnology in Vaccine Delivery. *International Journal of Green Nanotechnology: Biomedicine,* 2**,** B25-B45.

SINGH, N., MANSHIAN, B., JENKINS, G. J., GRIFFITHS, S. M., WILLIAMS, P. M., MAFFEIS, T. G., WRIGHT, C. J. & DOAK, S. H. 2009. NanoGenotoxicology: the DNA damaging potential of engineered nanomaterials. *Biomaterials,* 30**,** 3891-914.

SMITH, C. J., SHAW, B. J. & HANDY, R. D. 2007. Toxicity of single walled carbon nanotubes to rainbow trout, (*Oncorhynchus mykiss*): Respiratory toxicity, organ pathologies, and other physiological effects. *Aquatic Toxicology,* 82**,** 94-109.

SOHAEBUDDIN, S. K., THEVENOT, P. T., BAKER, D., EATON, J. W. & TANG, L. 2010. Nanomaterial cytotoxicity is composition, size, and cell type dependent. *Particle and Fibre Toxicology,* 7**,** 22.

SOHN, E. K., CHUNG, Y. S., JOHARI, S. A., KIM, T. G., KIM, J. K., LEE, J. H., LEE, Y. H., KANG, S. W. & YU, I. J. 2015. Acute Toxicity Comparison of Single-Walled Carbon Nanotubes in Various Freshwater Organisms. *BioMed Research International,* 2015**,** 7.

SONG, L., CONNOLLY, M., FERNÁNDEZ-CRUZ, M. L., VIJVER, M. G., FERNÁNDEZ, M., CONDE, E., DE SNOO, G. R., PEIJNENBURG, W. J. G. M. & NAVAS, J. M. 2014. Species-specific toxicity of copper nanoparticles among mammalian and piscine cell lines. *Nanotoxicology,* 8**,** 383-393.

STØRDAL, I. F. 2011. *Induction of CYP 1A enzyme activity and genotoxicity from ternary mixtures of produced water relevant compounds, evaluated by in vitro methods.* Master, NTNU.

SUMANASEKERA, G. U., ALLEN, J. L., FANG, S. L., LOPER, A. L., RAO, A. M. & EKLUND, P. C. 1999. Electrochemical Oxidation of Single Wall Carbon Nanotube Bundles in Sulfuric Acid. *The Journal of Physical Chemistry B,* 103**,** 4292-4297.

SUN, H., RUAN, Y., ZHU, H., ZHANG, Z., ZHANG, Y. & YU, L. 2013. Enhanced bioaccumulation of pentachlorophenol in carp in the presence of multi-walled carbon nanotubes. *Environmental Science and Pollution Research,* 21**,** 2865-2875.

SZENDI, K. & VARGA, C. 2008. Lack of genotoxicity of carbon nanotubes in a pilot study. *Anticancer Research,* 28**,** 349-52.

TABET, L., BUSSY, C., SETYAN, A., SIMON-DECKERS, A., ROSSI, M., BOCZKOWSKI, J. & LANONE, S. 2011. Coating carbon nanotubes with a polystyrene-based polymer protects against pulmonary toxicity. *Particle and Fibre Toxicology,* 8**,** 1-13.

TANS, S. J., DEVORET, M. H., DAI, H., THESS, A., SMALLEY, R. E., GEERLIGS, L. J. & DEKKER, C. 1997. Individual single-wall carbon nanotubes as quantum wires. *Nature,* 386**,** 474-477.

TAYLOR, A. A., ARON, G. M., BEALL, G. W., DHARMASIRI, N., ZHANG, Y. & MCLEAN, R. J. C. 2014. Carbon and clay nanoparticles induce minimal stress responses in gram negative bacteria and eukaryotic fish cells. *Environmental Toxicology,* 29**,** 961-968.

TEDJA, R., LIM, M., AMAL, R. & MARQUIS, C. 2012. Effects of serum adsorption on cellular uptake profile and consequent impact of titanium dioxide nanoparticles on human lung cell lines. *ACS Nano,* 6**,** 4083-93.

THACKER, J. 1986. The nature of mutants induced by ionising radiation in cultured hamster cells III. Molecular characterization of HPRT-deficient mutants induced by γ-rays or α-particles showing that the majority have deletions of all or part of the *hprt* gene. *Mutation Research/Fundamental and Molecular Mechanisms of Mutagenesis,* 160**,** 267-275.

THEODORAKIS, C. W., D'SURNEY, S. J. & SHUGART, L. R. 1994. Detection of Genotoxic Insult as DNA strand breaks in fish blood cells by agarose gel electrophoresis. *Environmental Toxicology and Chemistry,* 13**,** 1023-1031.

TOHJI, K., GOTO, T., TAKAHASHI, H., SHINODA, Y., SHIMIZU, N., JEYADEVAN, B., MATSUOKA, I., SAITO, Y., KASUYA, A., OHSUNA, T., HIRAGA, K. & NISHINA, Y. 1996. Purifying single-walled nanotubes. *Nature,* 383**,** 679-679.

URSINI, C. L., CAVALLO, D., FRESEGNA, A. M., CIERVO, A., MAIELLO, R., BURESTI, G., CASCIARDI, S., TOMBOLINI, F., BELLUCCI, S. & IAVICOLI, S. 2012a. Comparative cyto-genotoxicity assessment of functionalized and pristine multiwalled carbon nanotubes on human lung epithelial cells. *Toxicology In Vitro,* 26**,** 831-40.

URSINI, C. L., CAVALLO, D., FRESEGNA, A. M., CIERVO, A., MAIELLO, R., CASCIARDI, S., TOMBOLINI, F., BURESTI, G. & IAVICOLI, S. 2012b. Study of Cytotoxic and Genotoxic Effects of Hydroxyl-Functionalized Multiwalled Carbon Nanotubes on Human Pulmonary Cells. *Journal of Nanomaterials,* 2012**,** e815979.

VAN BERLO, D., CLIFT, M. J., ALBRECHT, C. & SCHINS, R. P. 2012. Carbon nanotubes: an insight into the mechanisms of their potential genotoxicity. *Swiss Medical Weekly,* 142**,** w13698.

VISALLI, G., BERTUCCIO, M. P., IANNAZZO, D., PIPERNO, A., PISTONE, A. & DI PIETRO, A. 2015. Toxicological assessment of multi-walled carbon nanotubes on A549 human lung epithelial cells. *Toxicology in Vitro,* 29**,** 352-362.

WALKEY, C. D. & CHAN, W. C. 2012. Understanding and controlling the interaction of nanomaterials with proteins in a physiological environment. *Chemical Society Reviews,* 41**,** 2780-99.

WANG, X., GUO, J., CHEN, T., NIE, H., WANG, H., ZANG, J., CUI, X. & JIA, G. 2012. Multi-walled carbon nanotubes induce apoptosis via mitochondrial pathway and scavenger receptor. *Toxicology in Vitro,* 26**,** 799-806.

WILSON, M., KANNANGARA, K., SMITH, G., SIMMONS, M. & RAGUSE, B. 2002. The carbon age. *In:* WILSON, M. (ed.) *Nanotechnology: Basic Science and Emerging Technologies.* Sydney, Australia: Chapman and Hall/CRC press. p. 87-100.

WLODEK, D., BANATH, J. & OLIVE, P. L. 1991. Comparison between pulsed-field and constant-field gel electrophoresis for measurement of DNA double-strand breaks in irradiated Chinese hamster ovary cells. *International Journal of Radiation Biology,* 60**,** 779-90.

WÖRLE-KNIRSCH, J. M., PULSKAMP, K. & KRUG, H. F. 2006. Oops they did it again! Carbon nanotubes hoax scientists in viability assays. *Nano Letters,* 6**,** 1261-8.

WU, H., LIU, G., ZHUANG, Y., WU, D., ZHANG, H., YANG, H., HUA, H. & YANG, S. 2011. The behavior after intravenous injection in mice of multiwalled carbon nanotube / Fe3O4 hybrid MRI contrast agents. *Biomaterials,* 32**,** 4867-4876.

WU, N., WANG, Q. & ARASH, B. 2012. Ejection of DNA molecules from carbon nanotubes. *Carbon,* 50**,** 4945-4952.

WU, Y., PHILLIPS, J. A., LIU, H., YANG, R. & TAN, W. 2008. Carbon nanotubes protect DNA strands during cellular delivery. *ACS Nano,* 2**,** 2023-8.

WURGLER, F. E. & KRAMERS, P. G. 1992. Environmental effects of genotoxins (eco-genotoxicology). *Mutagenesis,* 7**,** 321-7.

WYATT, M. D. & PITTMAN, D. L. 2006. Methylating agents and DNA repair responses: Methylated bases and sources of strand breaks. *Chemical Research in Toxicology,* 19**,** 1580-94.

ZHU, L., CHANG, D. W., DAI, L. & HONG, Y. 2007. DNA damage induced by multiwalled carbon nanotubes in mouse embryonic stem cells. *Nano Letters,* 7**,** 3592-7.

ZUCKER, D., ANDRIYANOV, A. V., STEINER, A., RAVIV, U. & BARENHOLZ, Y. 2012. Characterization of PEGylated nanoliposomes co-remotely loaded with topotecan and vincristine: relating structure and pharmacokinetics to therapeutic efficacy. *Journal of Controlled Release,* 160**,** 281-9.

# APPENDIX I. Solutions

## 1. Cultivating cells

**Phosphate Buffered Saline, 500 mL, pH 7.4, autoclaved**
1 PBS tablet
500 mL MQ water

**2.5% Trypsin with 1% EDTA, 10 mL**
0.537 mL 0.5M EDTA
9.463 mL 2.5% Trypsin

**Growth medium, 500 mL**
500 mL Mimimal Essential Medium, Eagle's
50 mL FBS
5 mL Penicillin-streptomycin (5000 Units/mL- 5000 µg/mL)

**70 % Ethanol, 1L**
730 mL 96% ethanol
270 mL distilled water

**EDTA 0.5 M, 500 mL, pH 8.0**
93.5 g EDTA

## 2. MWCNT dispersions

**BSA-water stock (1% w/v)**
1g BSA
100 mL MQ-water

## 3. MTT-assay

**MTT-solution, 1 mL**
0.005 g MTT salt
1 mL PBS

**MTT/Medium-solution, per well (200 uL)**
20 µL MTT-solution
180 µL growth medium

## 4. Gel Electrophoresis

**10% SDS, 100 mL**
10 g SDS
Distilled water

**Digestion buffer, 200 mL, pH 8**

1.1688 g NaCl
0.2423 g TRIS
10 mL 0.5 M EDTA
10 mL 10% SDS

**Lambda-marker solution, 200 µL**
100 µL λ/HIND III (50 µg)
37 µL λ-DNA (11 µg)
63 µL TE-buffer

**5×TBE-buffer, 1 L, pH 8**
54 g Tris base
27.5 g Boric acid, $H_3BO_3$
20 mL 0.5 M EDTA

**TE- buffer, 500 mL, pH 8**
0.6057 g Tris
1 mL 0.5 M EDTA

**EDTA 0.5 M, 500 mL, pH 8**
93.5 g EDTA

## APPENDIX II. Calibration curves

Calibration curves for all four MWCNTs are displayed in the figure below. Construction of the calibration curve for MWCNT-Pristine was repeated once.

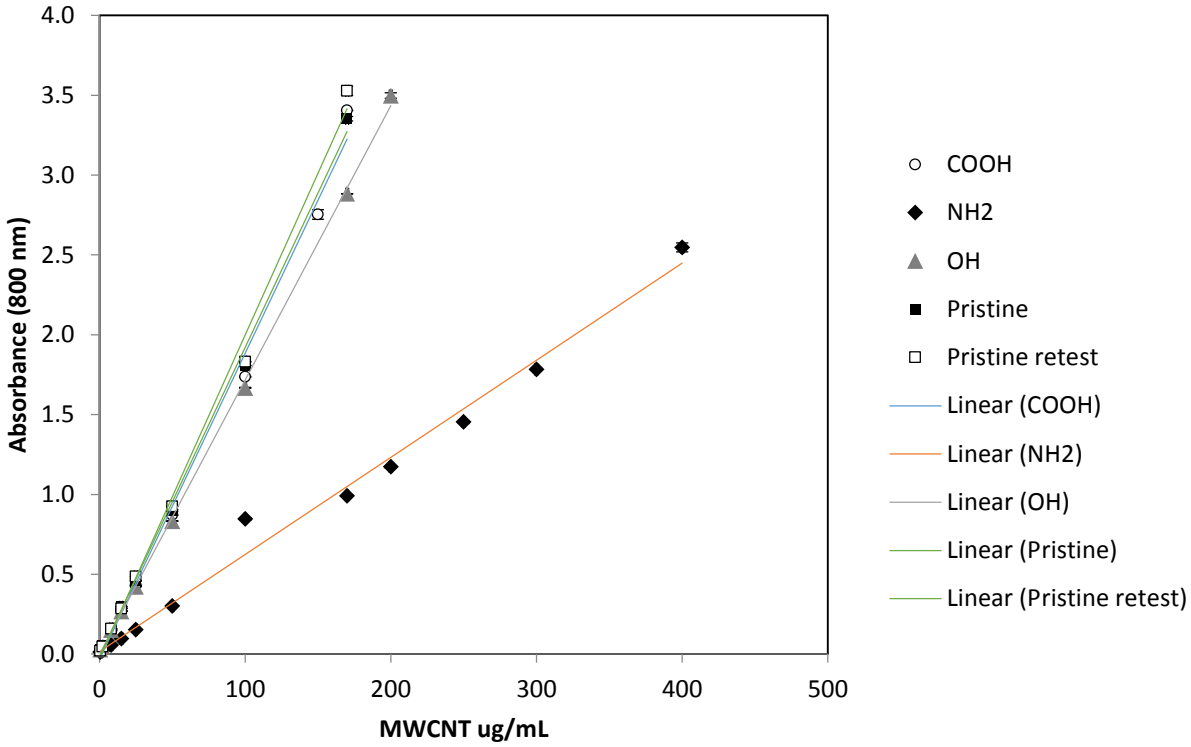


**Figure 1**: Calibration curves for four MWCNTs. Different symbols represent different MWCNT and absorbance at 800 nm ± standard deviation, n=3.

## APPENDIX III. Ethanol absorbance and volume testing

Absorbances for BSA water 0.05% (3 mL) with 15 µL ethanol is reported below in Table 1. The influence of reducing volume of test sample in the cuvette was also tested (see Table 1). Approximately 3 mL is the standard testing volume, but 2 mL sample also proved to be reliable.

**Table 1:** Results from testing for impacts of ethanol and/or cuvette volume on absorbance values.

| **Bsa water testing in UV-vis spectrometer** | | |
|---|---|---|
| **Sample** | **Absorbance (800 nm)** | **Comments** |
| Autozero | 0.001 | |
| BSA/MQ | 0.000 | Testing if BSA water 0.05% (3mL) absorbs at 800 nm |
| BSA/MQ | 0.000 | |
| BSA/MQ | 0.000 | |
| Autozero control | 0.000 | |
| BSA/MQ + EtOH | 0.000 | Testing importance of volume **(3mL)** and EtOH |
| BSA/MQ + EtOH | 0.000 | Testing importance of volume **(2mL)** and EtOH |
| BSA/MQ + EtOH | 0.000 | Testing importance of volume **(2mL)** and EtOH |
| BSA/MQ + EtOH | 0.002 | Testing importance of volume **(1.5 mL)** and EtOH |
| Autozero control | 0.000 | |
| BSA/MQ + EtOH | 0.001 | Testing importance of volume **(2 mL)** and EtOH |
| BSA/MQ + EtOH | 0.000 | Testing importance of volume **(1.5 mL)** and EtOH |

## APPENDIX IV. Calculations to determine cell concentration

**A.** Finding cell concentration in a cell suspension:

$$Cells\ per\ \mu L = \frac{mean\ cells\ per\ grid * dilution\ factor}{counted\ surface\ (mm^2) * chamber\ depth\ (mm)}$$

**Example: PLHC-1**

1. Counted cells: 176
2. Counted surface: 3 large squares (1 $mm^2$ each)
3. Chamber depth: 0.1 mm
4. Dilution: 1:10

$$\frac{cells}{uL} = \frac{176 * 10}{3 * 0.1} = 17666$$

**B.** Volume of known cell concentration to be seeded in wells for the MTT assay was calculated from the following equation:

$$Volume\ cell\ suspension\ (mL) = \frac{target\ cell\ concentration\ (mL) * final\ volume\ (mL)}{counted\ cells/mL}$$

## APPENDIX V. Calculations for DNA DSB assay

Sample calculation for determining the amount of harvested cells to add to a 24 well plate to be used in DSB analysis. The data in Table 1 is an example of how the amount of cell suspension to be seeded in 24 well plates was determined.

**Table 1**: Data used to calculate amount of cell suspension to be seeded in 24 well plates.

| | |
|---|---|
| **Total growth area culture flask** | 75 $cm^2$ |
| **Total growth area 24 well plate** | 45.6 $cm^2$ |
| **Cell harvest volume** | 2 mL |
| **Initial cell density required*** | 30% |
| **Total required volume for 24 wells** | 27 mL |

*Initial cell density was calculated from cell doubling time (39.4 hours), by backcalculating from assumed 100% cell density after 72 hours incubation. See Figure1.

The above information was used in the following calculation (example calculation):

$$Cell\ suspension\ (mL) = \left(2\ mL * \frac{45.6\ cm^2}{75\ cm^2}\right) * 0.3$$

The calculated amount of cell suspension was then added to growth medium to a final concentration of 27 mL. This cell suspension was then mixed well and seeded into wells.

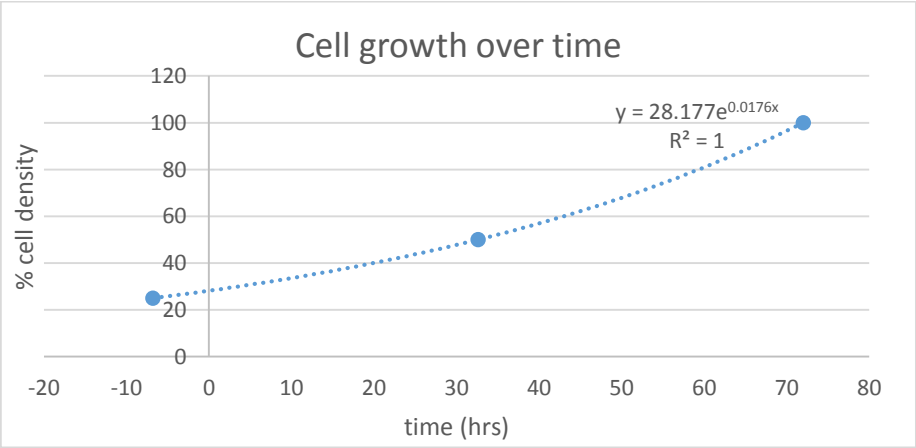


**Figure 1**: Cell density as a function of time, showing calculated cell densities at 0 and 72 hours incubation when cell doubling time is 39.4 hours.

# APPENDIX VI. MTT assay raw data

## Standard curve

**Table 1:** Absorbance at 550 nm for PLHC-1 cells at different cell concentrations.

| Cells/mL | $1.7*10^6$ | $8.7*10^5$ | $4.4*10^5$ | $2.9*10^5$ | $2.2*10^5$ | $1.7*10^5$ | $8.7*10^4$ | $5.8*10^4$ | $4.4*10^4$ | $3.5*10^4$ |
|---|---|---|---|---|---|---|---|---|---|---|
| **1** | 3.005 | 2.610 | 2.028 | 1.410 | 1.645 | 1.235 | 0.566 | 0.428 | 0.312 | 0.280 |
| **2** | 3.459 | 2.861 | 2.130 | 1.575 | 1.010 | 1.162 | 0.534 | 0.570 | 0.326 | 0.299 |
| **3** | 3.460 | 3.188 | 1.951 | 1.575 | 1.367 | 1.017 | 0.819 | 0.523 | 0.364 | 0.317 |
| **4** | 3.460 | 2.884 | 1.993 | 1.613 | 1.317 | 0.568 | 0.538 | 0.555 | 0.403 | 0.383 |
| **5** | 3.460 | 2.355 | 1.935 | 1.805 | 1.321 | 1.287 | 0.568 | 0.446 | 0.342 | 0.358 |
| **6** | 3.460 | 3.192 | 1.627 | 1.816 | 1.384 | 1.535 | 0.832 | 0.526 | 0.447 | 0.280 |
| **Mean absorbance (550nm)** | 3.384 | 2.848 | 1.944 | 1.632 | 1.340 | 1.134 | 0.643 | 0.509 | 0.366 | 0.319 |
| **SD** | 0.186 | 0.327 | 0.170 | 0.155 | 0.202 | 0.325 | 0.142 | 0.058 | 0.051 | 0.043 |

**Dispersion medium: BSA water (0.05%)**

**Table 2**: Absorbance at 550 nm for PLHC-1 cells exposed to four MWCNTs. BSA control is the top three values of the coloumn marked BSA/DMSO, and DMSO control the bottom three values. The same system is used in the last coloumn.

| MWCNT-COOH µg /mL (20.02.15) | 256 | 128 | 64 | 32 | 16 | 8 | 4 | 2 | BSA/ DMSO | No cell/No exposure |
|---|---|---|---|---|---|---|---|---|---|---|
| **1** | 0.2427 | 0.1817 | 0.4977 | 0.4867 | 0.5657 | 0.4007 | 0.7877 | 0.5877 | 0.6247* | 0.004778 |
| **2** | 0.1267 | 0.6797 | 0.5437 | 0.3507 | 0.4287 | 0.2907 | 0.4397 | 0.3627 | 0.694778 | 0.008778 |
| **3** | 0.1247 | 0.2637 | 0.3677 | 0.4187 | 0.4077 | 0.1787 | 0.4337 | 0.4567 | 0.893778 | 0.012778 |
| **4** | 0.1497 | 0.2987 | 0.4617 | 0.4437 | 0.4187 | 0.1407 | 0.4847 | 0.4777 | 0.236778 | 1.176778 |
| **5** | 0.1207 | 0.3027 | 0.4067 | 0.3917 | 0.1257 | 0.2587 | 0.6227 | 0.5127 | 0.264778 | 0.961778 |
| **6** | 0.1997 | 0.2357 | 0.6977 | 0.4637 | 0.1397 | 0.3967 | 0.3777 | 0.5177 | 0.079778 | 1.049778 |
| **Mean absorbance (550 nm)** | 3.384 | 2.848 | 1.944 | 1.632 | 1.340 | 1.134 | 0.643 | 0.509 | | |
| **SD** | 0.186 | 0.327 | 0.170 | 0.155 | 0.202 | 0.325 | 0.142 | 0.058 | | |

* This sample was contaminated with CNTs and was excluded.

| MWCNT-COOH µg/mL (28.02.15) | 32 | 16 | 8 | 4 | 2 | 1 | 0.5 | CNT only | BSA/ DMSO | No cell/No exposure |
|---|---|---|---|---|---|---|---|---|---|---|
| **1** | 0.224 | 0.267 | 0.283 | 0.387 | 0.254 | 0.128 | 0.195 | 0.018 | 0.198 | 0.012 |
| **2** | 0.251 | 0.237 | 0.316 | 0.465 | 0.226 | 0.056 | 0.226 | 0.011 | 0.223 | 0.008 |
| **3** | 0.218 | 0.311 | 0.336 | 0.299 | 0.499 | 0.074 | 0.188 | 0.008 | 0.223 | 0.007 |
| **4** | 0.28 | 0.281 | 0.321 | 0.34 | 0.319 | 0.148 | 0.195 | 0.008 | 0.085 | 0.207 |
| **5** | 0.177 | 0.257 | 0.348 | 0.325 | 0.366 | 0.227 | 0.163 | 0.011 | 0.052 | 0.269 |
| **6** | 0.236 | 0.267 | 0.419 | 0.31 | 0.218 | 0.152 | 0.127 | 0.02 | 0.098 | 0.317 |
| **Mean absorbance** | 0.231 | 0.27 | 0.3371 | 0.3543 | 0.3136 | 0.1308 | 0.1823 | 0.0126 | | |

| | | | | | | | | | | |
|---|---|---|---|---|---|---|---|---|---|---|
| **(550 nm) SD** | 0.0345 | 0.0248 | 0.0457 | 0.0623 | 0.1072 | 0.0613 | 0.0337 | 0.0345 | | |

| **MWCNT-OH µg /mL (28.02.15)** | **32** | **16** | **8** | **4** | **2** | **1** | **0.5** | **CNT only** | **BSA/ DMSO** | **No cell/No exposure** |
|---|---|---|---|---|---|---|---|---|---|---|
| **1** | 0.313 | 0.21 | 0.36 | 0.429 | 0.31 | 0.106 | 0.134 | 0.009 | 0.716 | 0.013 |
| **2** | 0.441 | 0.236 | 0.322 | 0.698 | 0.619 | 0.105 | 0.308 | 0.014 | 0.358 | 0.01 |
| **3** | 0.332 | 0.444 | 0.488 | 0.486 | 0.499 | 0.21 | 0.312 | 0.012 | 0.168 | 0.011 |
| **4** | 0.288 | 0.497 | 0.406 | 0.328 | 0.778 | 0.36 | 0.355 | 0.011 | 0.182 | 0.493 |
| **5** | 0.378 | 0.447 | 0.59 | 0.711 | 0.428 | 0.29 | 0.333 | 0.013 | 0.195 | 0.714 |
| **6** | 0.312 | 0.284 | 0.517 | 0.667 | 0.657 | 0.414 | 0.144 | 0.011 | 0.123 | 1.045 |
| **Mean absorbance (550 nm)** | 0.344 | 0.353 | 0.4471 | 0.5531 | 0.5485 | 0.2475 | 0.2643 | | | |
| **SD** | 0.0562 | 0.1238 | 0.1018 | 0.1609 | 0.1692 | 0.1295 | 0.0985 | | | |

**Dispersion medium: Growth medium**

**Table 3**: Absorbance at 550 nm for PLHC-1 cells exposed to four MWCNTs. No cell control is the top three values of the coloumn marked No cell/DMSO, and DMSO control the bottom three values.

| **MWCNT-OH µg /mL (07.03.15)** | **64** | **32** | **16** | **8** | **4** | **2** | **1** | **0.5** | **No treatment** | **No cell/ DMSO** |
|---|---|---|---|---|---|---|---|---|---|---|
| **1** | 0.531 | 0.433 | 0.494 | 0.635 | 0.597 | 0.635 | 0.604 | 0.756 | 0.785 | 0.028 |
| **2** | 0.508 | 0.511 | 0.582 | 0.611 | 0.599 | 0.569 | 0.623 | 0.599 | 0.752 | 0.04 |
| **3** | 0.602 | 0.481 | 0.565 | 0.503 | 0.587 | 0.636 | 0.696 | 0.676 | 0.767 | 0.035 |
| **4** | 0.505 | 0.464 | 0.549 | 0.551 | 0.706 | 0.742 | 0.66 | 0.725 | 0.706 | 0.094 |
| **5** | 0.577 | 0.544 | 0.578 | 0.489 | 0.587 | 0.65 | 0.691 | 0.49 | 0.569 | 0.098 |
| **6** | 0.602 | 0.567 | 0.759 | 0.577 | 0.604 | 0.653 | 0.657 | 0.699 | 0.95 | 0.102 |
| **Mean absorbance (550 nm)** | 0.5541 | 0.500 | 0.5878 | 0.561 | 0.6133 | 0.6475 | 0.6551 | 0.6575 | 0.754833 | |
| **SD** | 0.0451 | 0.0503 | 0.0897 | 0.0581 | 0.0458 | 0.0555 | 0.0364 | 0.0977 | 0.123349 | |

| **MWCNT-P µg /mL (07.03.15)** | **64** | **32** | **16** | **8** | **4** | **2** | **1** | **0.5** | **No treatment** | **No cell/ DMSO** |
|---|---|---|---|---|---|---|---|---|---|---|
| **1** | 0.57 | 0.465 | 0.511 | 0.949 | 0.699 | 0.54 | 0.412 | 0.615 | 0.834 | 0.011 |
| **2** | 0.544 | 0.451 | 0.469 | 0.588 | 0.656 | 0.608 | 0.791 | 0.599 | 0.76 | 0.013 |
| **3** | 0.45 | 0.364 | 0.415 | 0.678 | 0.468 | 0.57 | 0.689 | 0.701 | 0.789 | 0.01 |
| **4** | 0.409 | 0.36 | 0.374 | 0.616 | 0.652 | 0.581 | 0.62 | 0.799 | 0.747 | 0.015 |
| **5** | 0.435 | 0.459 | 0.403 | 0.47 | 0.492 | 0.45 | 0.521 | 0.599 | 0.747 | 0.038 |
| **6** | 0.429 | 0.396 | 0.453 | 0.331 | 0.515 | 0.568 | 0.54 | 0.639 | 0.695 | 0.04 |
| **Mean absorbance (550 nm)** | 0.4728 | 0.4158 | 0.4375 | 0.6053 | 0.5803 | 0.5528 | 0.5955 | 0.6586 | 0.762 | |
| **SD** | 0.067 | 0.0484 | 0.0497 | 0.2085 | 0.0996 | 0.0549 | 0.1340 | 0.0786 | 0.04656 | |

| MWCNT-OH µg /mL (15.03.15) | 2048 | 1024 | 512 | 256 | 128 | 64 | 32 | 16 | No treatment | No cell/ DMSO |
|---|---|---|---|---|---|---|---|---|---|---|
| **1** | 0.081 | 0.176 | 0.133 | 0.3 | 0.32 | 0.385 | 0.254 | 0.426 | 0.871 | 0.013 |
| **2** | 0.091 | 0.091 | 0.226 | 0.321 | 0.429 | 0.315 | 0.359 | 0.497 | 0.631 | 0.022 |
| **3** | 0.076 | 0.392 | 0.236 | 0.257 | 0.297 | 0.329 | 0.335 | 0.58 | 0.14 | 0.014 |
| **4** | 0.087 | 0.182 | 0.209 | 0.339 | 0.316 | 0.507 | 0.313 | 0.458 | 0.379 | 0.019 |
| **5** | 0.09 | 0.167 | 0.304 | 0.246 | 0.319 | 0.395 | 0.385 | 0.755 | 1.086 | 0.017 |
| **6** | 0.082 | 0.165 | 0.413 | 0.351 | 0.351 | 0.314 | 0.637 | 0.574 | 0.81 | 0.031 |
| **Mean absorbance (550 nm)** | 0.0845 | 0.1955 | 0.2535 | 0.3023 | 0.3386 | 0.3741 | 0.3805 | 0.5483 | 0.652833 | |
| **SD** | 0.0058 | 0.1018 | 0.0954 | 0.0431 | 0.0475 | 0.0739 | 0.1333 | 0.1184 | 0.345945 | |

| MWCNT-P µg /mL (15.03.15) | 2048 | 1024 | 512 | 256 | 128 | 64 | 32 | 16 | No treatment | No cell/ DMSO |
|---|---|---|---|---|---|---|---|---|---|---|
| **1** | 0.048 | 0.258 | 0.301 | 0.302 | 0.267 | 0.236 | 0.376 | 0.388 | 0.5 | 0.012 |
| **2** | 0.108 | 0.175 | 0.326 | 0.412 | 0.332 | 0.249 | 0.473 | 0.391 | 0.83 | 0.012 |
| **3** | 0.062 | 0.275 | 0.368 | 0.387 | 0.458 | 0.593 | 0.261 | 0.371 | 0.343 | 0.011 |
| **4** | 0.063 | 0.117 | 0.239 | 0.34 | 0.445 | 0.587 | 0.384 | 0.268 | 0.7 | 0.037 |
| **5** | 0.105 | 0.201 | 0.321 | 0.372 | 0.424 | 0.384 | 0.411 | 0.404 | 0.777 | 0.064 |
| **6** | 0.093 | 0.234 | 0.22 | 0.4 | 0.424 | 0.582 | 0.515 | 0.324 | 0.818 | 0.095 |
| **Mean absorbance (550 nm)** | 0.0798 | 0.21 | 0.2958 | 0.3688 | 0.3916 | 0.4385 | 0.4033 | 0.3576 | 0.6613 | |
| **SD** | 0.0253 | 0.0584 | 0.056 | 0.0411 | 0.0754 | 0.1711 | 0.088 | 0.0520 | 0.1976 | |

| MWCNT-$NH_2$ µg /mL (21.03.15) | 64 | 32 | 16 | 8 | 4 | 2 | 1 | 0.5 | No treatment | No cell/ DMSO |
|---|---|---|---|---|---|---|---|---|---|---|
| **1** | 0.529 | 0.471 | 0.644 | 0.886 | 0.865 | 0.704 | 0.545 | 0.665 | 1.32 | 0.011 |
| **2** | 0.695 | 0.467 | 0.594 | 0.878 | 0.576 | 0.9 | 0.575 | 0.858 | 0.526 | 0.012 |
| **3** | 0.576 | 0.59 | 0.677 | 0.754 | 0.837 | 0.822 | 0.624 | 0.97 | 0.843 | 0.007 |
| **4** | 0.477 | 0.407 | 0.809 | 0.733 | 0.91 | 0.821 | 0.752 | 0.73 | 0.719 | 0.045 |
| **5** | 0.562 | 0.557 | 0.61 | 0.907 | 0.598 | 0.688 | 0.487 | 0.589 | 0.649 | 0.044 |
| **6** | 0.434 | 0.581 | 0.611 | 0.875 | 0.636 | 0.605 | 0.774 | 0.798 | 0.645 | 0.044 |
| **Mean absorbance (550 nm)** | 0.5455 | 0.5121 | 0.6575 | 0.8388 | 0.737 | 0.7566 | 0.6261 | 0.7683 | 0.783667 | |
| **SD** | 0.0904 | 0.0742 | 0.0799 | 0.0749 | 0.1495 | 0.1090 | 0.1151 | 0.1370 | 0.282528 | |

| MWCNT-COOH µg /mL (21.03.15) | 64 | 32 | 16 | 8 | 4 | 2 | 1 | 0.5 | No treatment | No cell/ DMSO |
|---|---|---|---|---|---|---|---|---|---|---|
| **1** | 0.532 | 0.423 | 0.429 | 0.594 | 0.576 | 0.675 | 0.69 | 0.771 | 0.804 | 0.011 |
| **2** | 0.475 | 0.436 | 0.672 | 0.608 | 0.523 | 0.558 | 0.635 | 0.52 | 0.848 | 0.019 |
| **3** | 0.48 | 0.5 | 0.631 | 0.655 | 0.669 | 0.945 | 1.32 | 0.772 | 0.641 | 0.015 |

| | | | | | | | | | | |
|---|---|---|---|---|---|---|---|---|---|---|
| **4** | 0.487 | 0.413 | 0.588 | 0.535 | 0.474 | 0.72 | 0.534 | 0.697 | 1.266 | 0.081 |
| **5** | 0.625 | 0.373 | 0.55 | 0.604 | 0.829 | 0.939 | 0.621 | 0.835 | 1.205 | 0.125 |
| **6** | 0.409 | 0.452 | 0.579 | 0.551 | 0.698 | 0.741 | 0.567 | 0.64 | 0.901 | 0.15 |
| **Mean absorbance (550 nm)** | 0.5013 | 0.4328 | 0.5748 | 0.5911 | 0.6281 | 0.763 | 0.7278 | 0.7058 | 0.944167 | |
| **SD** | 0.0722 | 0.0423 | 0.0832 | 0.0431 | 0.1299 | 0.1524 | 0.2951 | 0.1133 | 0.242602 | |

| **MWCNT-COOH µg /mL (21.03.15)** | **2048** | **1024** | **512** | **256** | **128** | **64** | **32** | **16** | **No treatment** | **No cell/ DMSO** |
|---|---|---|---|---|---|---|---|---|---|---|
| **1** | 0.119 | 0.35 | 0.21 | 0.326 | 0.196 | 0.42 | 0.703 | 0.429 | 1.142 | 0.01 |
| **2** | 0.187 | 0.428 | 0.264 | 0.294 | 0.299 | 0.569 | 0.605 | 0.418 | 0.898 | 0.013 |
| **3** | 0.138 | 0.297 | 0.433 | 0.378 | 0.347 | 0.371 | 0.545 | 0.134 | 0.991 | 0.011 |
| **4** | 0.108 | 0.175 | 0.348 | 0.41 | 0.522 | 0.794 | 0.627 | 0.619 | 1.133 | 0.03 |
| **5** | 0.145 | 0.24 | 0.221 | 0.335 | 0.392 | 0.59 | 0.58 | 0.402 | 1.056 | 0.035 |
| **6** | 0.187 | 0.285 | 0.299 | 0.473 | 0.455 | 0.579 | 0.6 | 0.538 | 1.429 | 0.074 |
| **Mean absorbance (550 nm)** | 0.1473 | 0.2958 | 0.2958 | 0.3693 | 0.3685 | 0.5538 | 0.61 | 0.4233 | 1.108167 | |
| **SD** | 0.0334 | 0.0874 | 0.0842 | 0.0651 | 0.1154 | 0.1491 | 0.0532 | 0.1647 | 0.181832 | |

| **MWCNT-$NH_2$ µg /mL (27.03.15)** | **2048** | **1024** | **512** | **256** | **128** | **64** | **32** | **16** | **No treatment** | **No cell/ DMSO** |
|---|---|---|---|---|---|---|---|---|---|---|
| **1** | 0.017 | 0.052 | 0.451 | 0.572 | 0.844 | 0.424 | 0.508 | 0.331 | 0.761 | 0.006 |
| **2** | 0.02 | 0.061 | 0.344 | 0.602 | 0.876 | 0.417 | 0.638 | 0.607 | 0.342 | 0.008 |
| **3** | 0.026 | 0.047 | 0.441 | 0.471 | 0.894 | 0.932 | 0.794 | 0.738 | 0.469 | 0.007 |
| **4** | 0.026 | 0.082 | 0.485 | 0.446 | 0.887 | 0.777 | 0.676 | 0.842 | 0.899 | 0.081 |
| **5** | 0.028 | 0.067 | 0.345 | 0.497 | 0.867 | 0.799 | 0.624 | 0.546 | 0.797 | 0.108 |
| **6** | 0.034 | 0.145 | 0.197 | 0.55 | 0.605 | 0.579 | 0.591 | 0.516 | 0.801 | 0.333 |
| **Mean absorbance (550 nm)** | 0.0251 | 0.0756 | 0.3771 | 0.523 | 0.8288 | 0.6546 | 0.6385 | 0.5967 | 0.678167 | |
| **SD** | 0.0060 | 0.0361 | 0.1055 | 0.0611 | 0.1110 | 0.2136 | 0.0949 | 0.1788 | 0.219817 | |

| **MWCNT-OH µg /mL (27.03.15)** | **2048** | **1024** | **512** | **256** | **128** | **64** | **32** | **16** | **No treatment** | **No cell/ DMSO** |
|---|---|---|---|---|---|---|---|---|---|---|
| **1** | 0.057 | 0.28 | 0.17 | 0.572 | 0.295 | 0.213 | 0.48 | 0.406 | 0.963 | 0.01 |
| **2** | 0.059 | 0.258 | 0.344 | 0.549 | 0.416 | 0.598 | 0.164 | 0.496 | 0.43 | 0.009 |
| **3** | 0.059 | 0.235 | 0.495 | 0.596 | 0.377 | 0.344 | 0.185 | 0.372 | 0.874 | 0.009 |
| **4** | 0.057 | 0.22 | 0.315 | 0.321 | 0.403 | 0.659 | 0.275 | 0.467 | 0.895 | 0.082 |
| **5** | 0.102 | 0.271 | 0.281 | 0.517 | 0.665 | 0.655 | 0.823 | 0.671 | 1.134 | 0.061 |
| **6** | 0.091 | 0.321 | 0.479 | 0.496 | 0.499 | 0.594 | 0.523 | 0.49 | 0.745 | 0.095 |
| **Mean absorbance (550 nm)** | 0.0708 | 0.264 | 0.3473 | 0.5085 | 0.4425 | 0.5105 | 0.4083 | 0.4836 | 0.840167 | |
| **SD** | 0.0202 | 0.0356 | 0.1233 | 0.0987 | 0.1272 | 0.1864 | 0.2520 | 0.1039 | 0.237853 | |

| MWCNT-OH µg /mL (27.03.15) | 64 | 32 | 16 | 8 | 4 | 2 | 1 | 0.5 | No treatment | No cell/ DMSO |
|---|---|---|---|---|---|---|---|---|---|---|
| 1 | 0.692 | 0.925 | 0.665 | 0.678 | 0.398 | 0.963 | 1.072 | 0.961 | 1.604 | 0.026 |
| 2 | 0.614 | 0.599 | 0.831 | 0.554 | 0.493 | 0.874 | 0.954 | 0.712 | 1.015 | 0.025 |
| 3 | 0.864 | 0.819 | 0.684 | 0.665 | 0.343 | 0.748 | 1.035 | 0.927 | 1.397 | 0.026 |
| 4 | 0.81 | 0.862 | 0.778 | 0.526 | 0.496 | 1.094 | 0.732 | 0.904 | 0.74 | 0.228 |
| 5 | 0.753 | 0.93 | 0.723 | 0.639 | 0.594 | 1.006 | 1.035 | 0.912 | 1.499 | 0.369 |
| 6 | 0.815 | 0.863 | 0.773 | 0.833 | 0.867 | 1 | 1.126 | 0.968 | 1.224 | 0.241 |
| Mean absorbance (550 nm) | 0.758 | 0.833 | 0.742 | 0.649 | 0.532 | 0.948 | 0.992 | 0.897 | 1.247 | |
| SD | 0.092 | 0.122 | 0.063 | 0.109 | 0.186 | 0.121 | 0.139 | 0.094 | 0.324 | |

| MWCNT-P µg /mL (01.04.15) | 64 | 32 | 16 | 8 | 4 | 2 | 1 | 0.5 | No treatment | No cell/ DMSO |
|---|---|---|---|---|---|---|---|---|---|---|
| 1 | 0.662 | 0.702 | 0.707 | 0.604 | 0.97 | 0.697 | 0.731 | 0.943 | 1.495 | 0.01 |
| 2 | 0.823 | 0.58 | 0.797 | 0.718 | 0.922 | 0.975 | 0.952 | 0.953 | 1.178 | 0.009 |
| 3 | 0.574 | 0.566 | 0.634 | 0.757 | 0.829 | 0.924 | 0.894 | 0.975 | 1.014 | 0.01 |
| 4 | 0.528 | 0.674 | 0.792 | 0.671 | 0.766 | 1.327 | 0.775 | 1.061 | 1.058 | 0.314 |
| 5 | 0.461 | 0.611 | 0.765 | 0.926 | 0.973 | 1.253 | 0.891 | 0.921 | 0.716 | 0.331 |
| 6 | 0.647 | 0.64 | 0.82 | 0.719 | 0.998 | 1.023 | 0.801 | 0.71 | 1.045 | 0.222 |
| Mean absorbance (550 nm) | 0.6158 | 0.6288 | 0.7525 | 0.7325 | 0.9096 | 1.0331 | 0.8406 | 0.9271 | 1.084333 | |
| SD | 0.1260 | 0.0532 | 0.0698 | 0.1083 | 0.0924 | 0.2293 | 0.0844 | 0.1168 | 0.253092 | |

| MWCNT-P µg /mL (01.04.15) | 2048 | 1024 | 512 | 256 | 128 | 64 | 32 | 16 | No treatment | No cell/ DMSO |
|---|---|---|---|---|---|---|---|---|---|---|
| 1 | 0.039 | 0.17 | 0.379 | 0.347 | 0.674 | 0.554 | 0.564 | 0.603 | 0.784 | 0.011 |
| 2 | 0.035 | 0.152 | 0.439 | 0.347 | 0.495 | 0.511 | 0.296 | 0.294 | 0.732 | 0.009 |
| 3 | 0.05 | 0.13 | 0.338 | 0.377 | 0.546 | 0.559 | 0.233 | 0.364 | 0.532 | 0.012 |
| 4 | 0.035 | 0.128 | 0.36 | 0.421 | 0.556 | 0.623 | 0.271 | 0.401 | 0.649 | 0.204 |
| 5 | 0.053 | 0.148 | 0.349 | 0.435 | 0.652 | 0.506 | 0.425 | 0.441 | 0.816 | 0.252 |
| 6 | 0.066 | 0.135 | 0.361 | 0.452 | 0.884 | 0.662 | 0.483 | 0.527 | 1.056 | 0.24 |
| Mean absorbance (550 nm) | 0.0463 | 0.1438 | 0.371 | 0.3965 | 0.6345 | 0.5691 | 0.3786 | 0.4383 | 0.7615 | |
| SD | 0.0122 | 0.0160 | 0.0360 | 0.0457 | 0.1396 | 0.0620 | 0.1319 | 0.1120 | 0.176864 | |

| MWCNT-COOH µg /mL (18.04.15) | 64 | 32 | 16 | 8 | 4 | 2 | 1 | 0.5 | No treatment | No cell/ DMSO |
|---|---|---|---|---|---|---|---|---|---|---|
| 1 | 0.65 | 0.772 | 0.725 | 0.669 | 0.792 | 0.752 | 1.038 | 1.076 | 1.134 | 0.01 |
| 2 | 0.556 | 0.744 | 0.845 | 0.849 | 0.864 | 1.155 | 1.021 | 1.129 | 1.402 | 0.007 |
| 3 | 0.55 | 0.607 | 1.019 | 0.801 | 1.307 | 1.058 | 0.754 | 1.062 | 1.373 | 0.006 |

| | | | | | | | | | | |
|---|---|---|---|---|---|---|---|---|---|---|
| **4** | 0.472 | 0.773 | 0.794 | 0.702 | 0.942 | 0.976 | 0.727 | 1.156 | 1.153 | 0.145 |
| **5** | 0.387 | 0.801 | 0.725 | 0.635 | 1.152 | 0.735 | 0.998 | 0.799 | 1.138 | 0.537 |
| **6** | 0.479 | 0.888 | 0.889 | 0.6 | 0.85 | 0.901 | 0.962 | 1.048 | 1.315 | 0.222 |
| **Mean absorbance (550 nm)** | 0.5156 | 0.7641 | 0.8328 | 0.7093 | 0.9845 | 0.9295 | 0.916 | 1.045 | 1.2525 | |
| **SD** | 0.0901 | 0.0915 | 0.1120 | 0.0970 | 0.2017 | 0.1671 | 0.139 | 0.1273 | 0.124763 | |

| **MWCNT-COOH µg /mL (18.04.15)** | **2048** | **1024** | **512** | **256** | **128** | **64** | **32** | **No treatment** | **No treatment** | **No cell/ DMSO** |
|---|---|---|---|---|---|---|---|---|---|---|
| **1** | 0.273 | 0.324 | 0.313 | 0.319 | 0.35 | 0.322 | 0.434 | 0.498 | 0.449 | 0.135 |
| **2** | 0.361 | 0.26 | 0.404 | 0.384 | 0.495 | 0.45 | 0.504 | 0.695 | 0.63 | 0.197 |
| **3** | 0.268 | 0.306 | 0.439 | 0.394 | 0.545 | 0.51 | 0.441 | 0.644 | 0.445 | 0.219 |
| **4** | 0.304 | 0.385 | 0.444 | 0.366 | 0.584 | 0.44 | 0.597 | 0.847 | 0.535 | 0.013 |
| **5** | 0.246 | 0.398 | 0.309 | 0.446 | 0.565 | 0.537 | 0.72 | 0.805 | 0.925 | 0.013 |
| **6** | 0.357 | 0.502 | 0.493 | 0.316 | 0.647 | 0.88 | 0.584 | 1.016 | 0.983 | 0.019 |
| **Mean absorbance (550 nm)** | 0.3015 | 0.3625 | 0.4003 | 0.3708 | 0.531 | 0.5231 | 0.546 | 0.750833 | 0.661167 | |
| **SD** | 0.0482 | 0.0853 | 0.0747 | 0.0491 | 0.1016 | 0.1899 | 0.109 | 0.20602 | 0.340491 | |

| **MWCNT-$NH_2$ µg /mL (18.04.15)** | **2048** | **1024** | **512** | **256** | **128** | **8** | **4** | **2** | **No treatment** | **No cell/ DMSO** |
|---|---|---|---|---|---|---|---|---|---|---|
| **1** | 0.154 | 0.373 | 0.531 | 0.566 | 0.683 | 1.033 | 1.134 | 1.133 | 1.062 | 0.016 |
| **2** | 0.147 | 0.399 | 0.572 | 0.731 | 0.612 | 0.984 | 1.18 | 1.231 | 1.078 | 0.02 |
| **3** | 0.212 | 0.501 | 0.533 | 0.72 | 0.672 | 1.007 | 0.997 | 0.749 | 1.088 | 0.024 |
| **4** | 0.157 | 0.423 | 0.582 | 0.87 | 0.696 | 0.987 | 0.954 | 0.974 | 0.891 | 0.283 |
| **5** | 0.157 | 0.491 | 0.61 | 0.696 | 0.628 | 1.143 | 1.067 | 1.166 | 1.372 | 0.265 |
| **6** | 0.166 | 0.474 | 0.556 | 0.73 | 0.822 | 1.049 | 1.505 | 1.363 | 1.498 | 0.226 |
| **Mean absorbance (550 nm)** | 0.1655 | 0.4435 | 0.564 | 0.7188 | 0.6855 | 1.0338 | 1.1395 | 1.1026 | 1.164833 | |
| **SD** | 0.0235 | 0.0526 | 0.0303 | 0.0969 | 0.0743 | 0.0592 | 0.1976 | 0.2148 | 0.224909 | |

| **MWCNT-COOH µg /mL (26.04.15)** | **32** | **16** | **8** | **4** | **2** | **1** | **0.5** | **No treatment** | **No treatment** | **No cell/ DMSO** |
|---|---|---|---|---|---|---|---|---|---|---|
| **1** | 0.556 | 0.684 | 0.677 | 0.721 | 0.735 | 0.895 | 0.934 | 0.864 | 0.952 | 0.012 |
| **2** | 0.582 | 0.642 | 0.568 | 0.777 | 0.764 | 0.827 | 0.958 | 1.024 | 0.961 | 0.018 |
| **3** | 0.485 | 0.664 | 0.675 | 0.95 | 0.892 | 0.952 | 0.942 | 1.005 | 1.114 | 0.01 |
| **4** | 0.608 | 0.636 | 0.661 | 0.715 | 0.82 | 0.807 | 0.951 | 1.15 | 0.856 | 0.117 |
| **5** | 0.786 | 0.656 | 0.662 | 0.867 | 0.818 | 0.836 | 0.873 | 1.183 | 0.847 | 0.53 |
| **6** | 0.531 | 0.703 | 0.701 | 0.953 | 1.072 | 0.878 | 0.942 | 0.998 | 1.161 | 0.276 |
| **Mean absorbance (550 nm)** | 0.5913 | 0.6641 | 0.6573 | 0.8305 | 0.8501 | 0.8658 | 0.933 | | 1.009583 | |
| **SD** | 0.1043 | 0.0255 | 0.0460 | 0.1084 | 0.1213 | 0.0534 | 0.030 | | 0.120934 | |

| MWCNT-COOH µg /mL (26.04.15) | 2048 | 1024 | 512 | 256 | 128 | 64 | 32 | No treatment | No treatment | No cell/ DMSO |
|---|---|---|---|---|---|---|---|---|---|---|
| **1** | 0.169 | 0.358 | 0.438 | 0.51 | 0.363 | 0.54 | 0.589 | 1.074 | 0.967 | 0.013 |
| **2** | 0.247 | 0.273 | 0.369 | 0.48 | 0.381 | 0.557 | 0.61 | 1.147 | 0.927 | 0.016 |
| **3** | 0.178 | 0.3 | 0.557 | 0.51 | 0.413 | 0.517 | 0.652 | 0.857 | 1.101 | 0.013 |
| **4** | 0.188 | 0.322 | 0.546 | 0.573 | 0.497 | 0.42 | 0.574 | 0.879 | 0.915 | 0.286 |
| **5** | 0.296 | 0.341 | 0.384 | 0.584 | 0.388 | 0.425 | 0.503 | 0.902 | 1.057 | 0.364 |
| **6** | 0.256 | 0.472 | 0.5 | 0.581 | 0.44 | 0.491 | 0.576 | 1 | 1.436 | 0.336 |
| **Mean absorbance (550 nm)** | 0.2223 | 0.3443 | 0.4656 | 0.5396 | 0.4136 | 0.4916 | 0.584 | | 1.021833 | |
| **SD** | 0.0512 | 0.0693 | 0.0809 | 0.0449 | 0.0488 | 0.0580 | 0.049 | | 0.160467 | |

# APPENDIX VII. DNA DSB

The relationship between DNA staining intensity and relative front (Rf) is displayed in Figure 1 below.

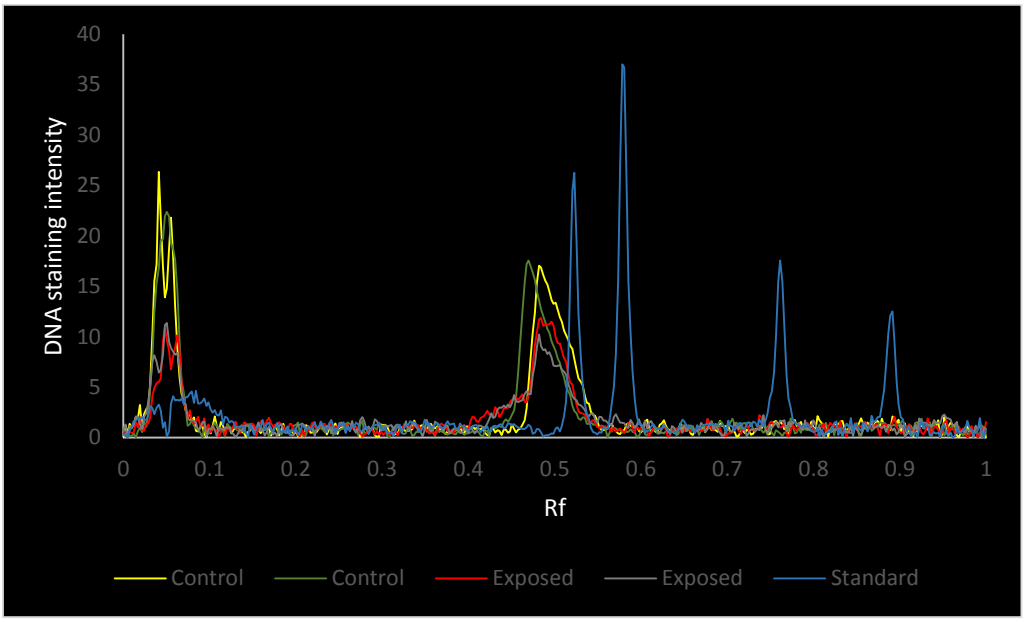


**Figure 1: DNA staining intensity (fluorescence) as a function of migratory distance (Rf).** Yellow and orange are controls, red and green represent samples exposed to 64 µg/mL MWCNT-P. Blue is the Lambda molecular marker.

### Lambda marker

The marker used to make standard curves is depicted in Figure 2. LamdaDNA/HindIII markers were used together with whole lambda DNA (48502 bp). The lambda/HindIII marker contains 8 DNA fragments with different sizes. Fragments with * can stick to each other and create new fragments. These fragments can be separated by heating the marker mix at 65°C for 5 minutes, followed by 3 minutes cooling on ice.

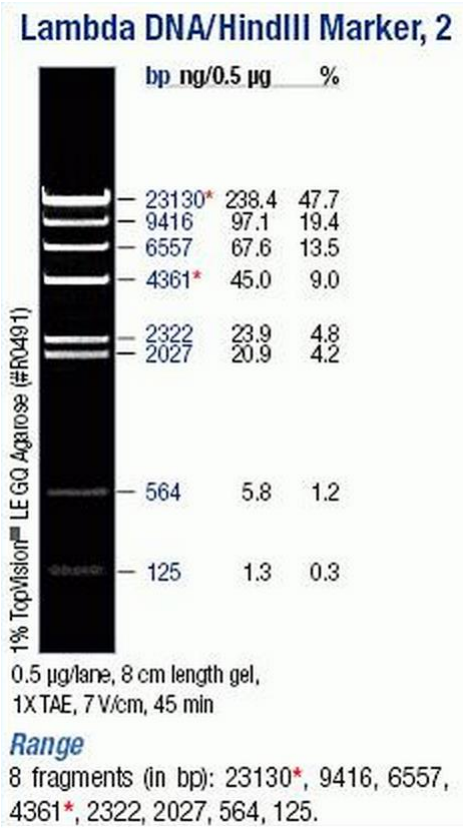


**Figure 2**: Lambda/HindII marker with known fragment size. Adapted from www.lifetechnologies.com.

**CNT interference with DNA stain**

MWCNT interference with the DNA stain detection was tested by making agarose plugs with CNTs dissolved in BSA water, and following the normal procedure for gel electrophoresis (Figure 3). However, gel was not electrophoresed. No significant CNT absorbance was detected relative to the background (Lane 2-5 and 11-14). Some fluorescence was emitted by plug controls (plugs only, Lane 1, 8 and15). Plugs with DNA fluoresced as expected (lane 6-7 and 9-10). It was unexpected that the plug controls fluoresced, however this was tested in a second run and was not detected when the gel had been electrophoresed (as digestion buffer components were removed during electrophoresis). The CNT plugs had already been stored for one day, and the digestion buffer components were therefore relatively degraded compared to the freshly produced plug controls.

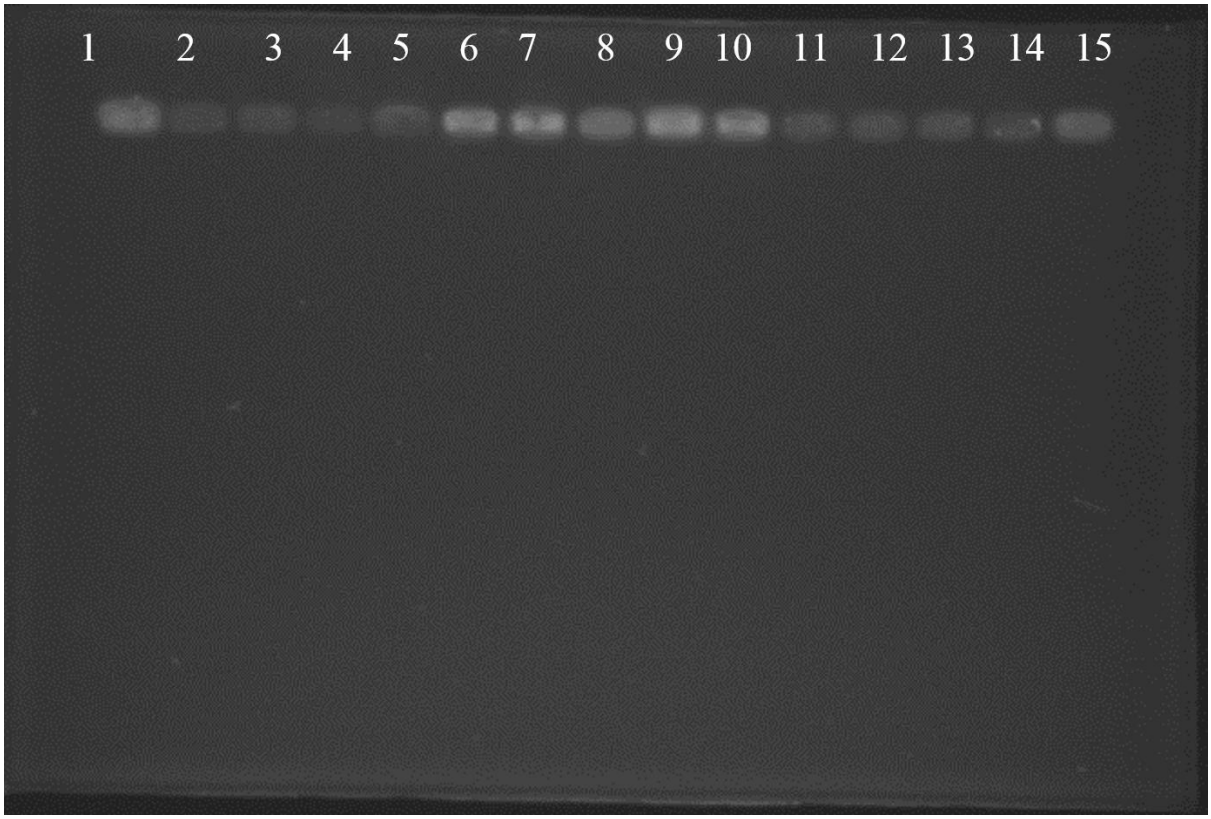


**Figure 3:** CNT fluorescence measurement.

## APPENDIX VIII. Linear regression analysis – cytotoxicity data

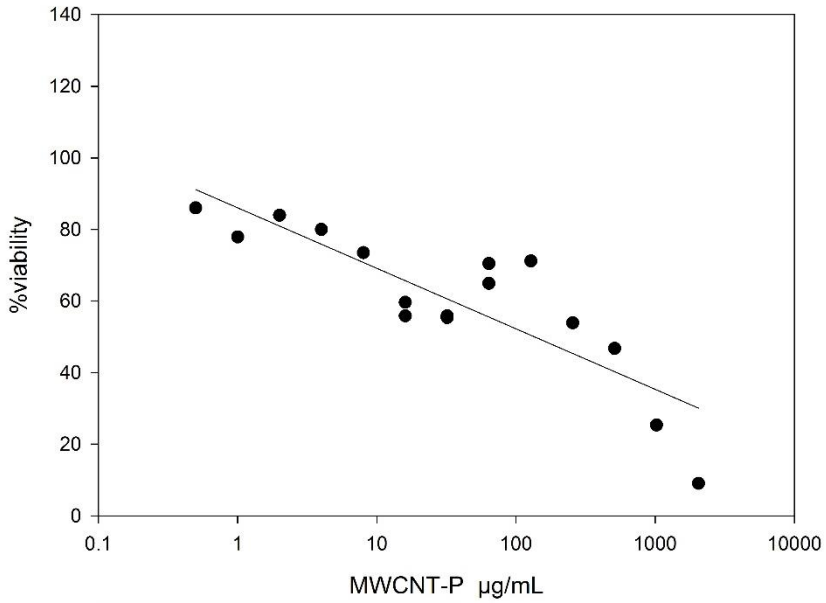


**Figure 1:** Linear regression of mean cell viability at each concentration of MWCNT-P, where the linear function is based on the logarithm of MWCNT concentration. $R^2 = 0.7362$.

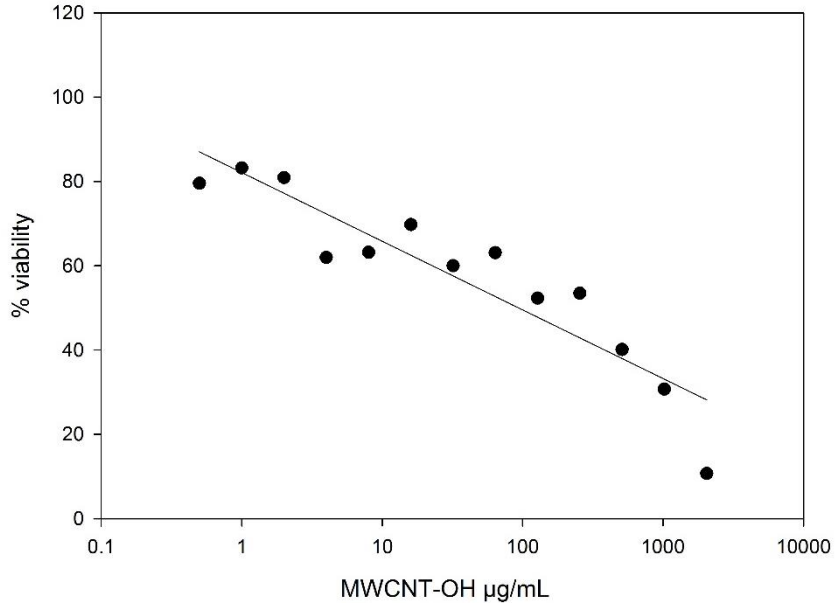


**Figure 2:** Linear regression of mean cell viability at each concentration of MWCNT-OH, where the linear function is based on the logarithm of MWCNT concentration. $R^2 = 0.8443$.

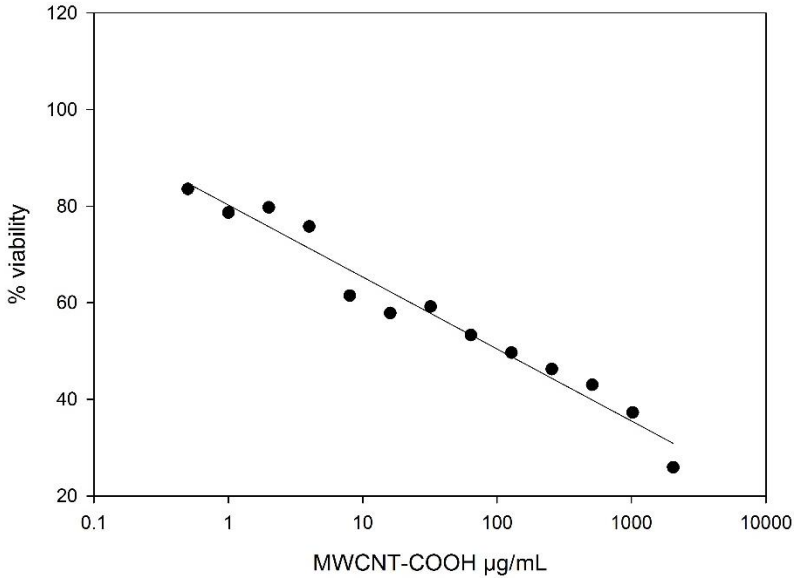


**Figure 3:** Linear regression of mean cell viability at each concentration of MWCNT-COOH, where the linear function is based on the logarithm of MWCNT concentration. $R^2 = 0.9651$.

## APPENDIX VIIII. MML and DNA-FTM raw data

**Table 1**: DNA-FTM raw data

| **Experiment 1:** | **MWCNT-P** | | |
|---|---|---|---|
| **µg/mL** | **0** | **4** | **64** |
| DNA-FTM (%) | 55.98 | 56.52 | 73.01 |
| | 69.08 | 74.45 | 71.25 |
| | | 77.30 | 69.22 |
| | | 65.78 | 71.37 |
| | | 71.40 | 86.87 |
| | | 81.08 | 76.87 |
| **Experiment 2** | | | |
| **µg/mL** | **0** | **4** | **64** |
| DNA-FTM (%) | 55.05 | 17.98* | 56.70 |
| | 54.56 | 24.84* | 65.58 |
| | | 45.78 | 51.29 |
| | | 45.98 | 67.31 |
| | | 35.80 | 62.54 |
| | | 35.75 | 61.46 |
| *Removed from average due to substantial lysis | | | |
| **Experiment 1:** | **MWCNT-OH** | | |
| **µg/mL** | **0** | **4** | **64** |
| DNA-FTM (%) | 58.45 | 69.73 | 77.89 |
| | 61.43 | 60.17 | 82.27 |
| | | 62.11 | 77.26 |
| | | 69.99 | 78.50 |
| | | 62.37 | 86.78 |
| | | 62.20 | 84.75 |
| **Experiment 2** | | | |
| **µg/mL** | **0** | **4** | **64** |
| DNA-FTM (%) | 57.92 | 48.06 | 35.36 |
| | 47.67 | 32.52 | 46.37 |
| | | 46.18 | 66.56 |
| | | 62.40 | 57.02 |
| | | 54.85 | 63.88 |
| | | 43.99 | 58.44 |
| **Experiment 1:** | **MWCNT-COOH** | | |

| µg/mL | 0 | 4 | 64 |
|---|---|---|---|
| DNA-FTM (%) | 46.23 | 48.39 | 76.62 |
| | 56.25 | 46.56 | 86.10 |
| | | 73.76 | 77.69 |
| | | 81.66 | 53.45 |
| | | 72.22 | 74.15 |
| | | 76.36 | 68.28 |

**Experiment 2**

| µg/mL | 0 | 4 | 64 |
|---|---|---|---|
| DNA-FTM (%) | 43.90 | 44.38 | 38.65 |
| | 52.50 | 40.96 | 48.51 |
| | | 44.48 | 46.28 |
| | | 51.30 | 44.65 |
| | | 58.41 | 54.34 |
| | | 45.76 | 64.55 |

**Experiment 1: MWCNT-$NH_2$**

| µg/mL | 0 | 4 | 64 |
|---|---|---|---|
| DNA-FTM (%) | 54.91 | 64.15 | 50.14 |
| | 19.27 | 81.15 | 26.31 |
| | | 76.64 | 41.76 |
| | | 72.48 | 18.66 |
| | | 78.71 | 12.02* |
| | | 80.84 | 22.51 |

**Experiment 2**

| µg/mL | 0 | 4 | 64 |
|---|---|---|---|
| DNA-FTM (%) | 51.39 | 53.04 | 47.14 |
| | 28.40 | 54.25 | 59.63 |
| | | 45.37 | 58.00 |
| | | 39.85 | 43.74 |
| | | 47.04 | 58.16 |
| | | 46.98 | 57.48 |

*Removed from results due to substantial lysis

**Experiment 1: MMS**

| mg/L | 0 | 10 | 20 | 40 |
|---|---|---|---|---|
| DNA-FTM (%) | 68.58 | 66.25 | 73.78 | 80.64 |
| | 63.90 | 75.49 | 79.24 | 66.72 |
| | 69.12 | 62.25 | 80.77 | 69.09 |

**Experiment 2**

| mg/L | 0 | 10 | 20 | 40 |
|---|---|---|---|---|
| DNA-FTM (%) | 64.61 | 53.07 | 56.65 | 54.23 |
| | 59.15 | 57.30 | 39.24 | 62.73 |
| | 67.10 | 60.14 | 47.28 | 54.88 |
| **Experiment 2 DMSO** | | | | |
| **mg/L** | **0** | **10** | **20** | **40** |
| DNA-FTM (%) | 69.18 | 52.93 | 46.42 | 43.14 |
| | 50.88 | 61.46 | 65.35 | 65.04 |
| | 35.07 | 58.95 | 57.55 | 62.29 |

**Table 2**: MML raw data

| **Experiment 1: MWCNT-P** | | | |
|---|---|---|---|
| **µg/mL** | **0** | **4** | **64** |
| MML (kbp) | 46.31 | 45.02 | 45.34 |
| | 45.66 | 44.07 | 48.35 |
| | | 45.66 | 45.66 |
| | | 48.71 | 45.66 |
| | | 47.31 | 44.38 |
| | | 46.63 | 43.76 |
| **Experiment 2** | | | |
| **µg/mL** | **0** | **4** | **64** |
| MML (kbp) | 49.07 | 46.57 | 51.76 |
| | 55.14 | 51.76 | 53.19 |
| | | 54.64 | 55.14 |
| | | 56.67 | 51.76 |
| | | 57.19 | 50.83 |
| | | 55.14 | 51.76 |

| **Experiment 1: MWCNT-OH** | | | |
|---|---|---|---|
| **µg/mL** | **0** | **4** | **64** |
| MML (kbp) | 38.77 | 38.20 | 39.91 |
| | 50.90 | 39.34 | 39.91 |
| | | 37.66 | 44.97 |
| | | 37.39 | 50.90 |
| | | 36.32 | 48.56 |
| | | 35.82 | 51.70 |
| **Experiment 2** | | | |
| **µg/mL** | **0** | **4** | **64** |

| | | | |
|---|---|---|---|
| MML (kbp) | 42.82 | 43.15 | 55.63 |
| | 58.08 | 46.74 | 57.57 |
| | | 47.89 | 51.57 |
| | | 51.57 | 50.72 |
| | | 52.44 | 56.61 |
| | | 48.69 | 58.60 |

**Experiment 1: MWCNT-COOH**

| **µg/mL** | **0** | **4** | **64** |
|---|---|---|---|
| MML (kbp) | 48.20 | 48.20 | 41.97 |
| | 48.96 | 50.55 | 41.34 |
| | | 47.44 | 45.66 |
| | | 41.97 | 46.72 |
| | | 46.02 | 50.55 |
| | | 46.72 | 48.96 |

**Experiment 2**

| **µg/mL** | **0** | **4** | **64** |
|---|---|---|---|
| MML (kbp) | 45.09 | 45.82 | 46.56 |
| | 43.34 | 43.68 | 45.82 |
| | | 44.38 | 48.10 |
| | | 45.82 | 45.82 |
| | | 47.33 | 42.33 |
| | | 43.68 | 41.69 |

**Experiment 1: MWCNT-$NH_2$**

| **µg/mL** | **0** | **4** | **64** |
|---|---|---|---|
| MML (kbp) | 36.89 | 39.15 | 44.59 |
| | 45.66 | 39.75 | 47.89 |
| | | 41.59 | 48.66 |
| | | 42.24 | 46.40 |
| | | 50.27 | 47.15 |
| | | 49.86 | 46.03 |

**Experiment 2**

| **µg/mL** | **0** | **4** | **64** |
|---|---|---|---|
| MML (kbp) | 47.55 | 50.13 | 46.71 |
| | 34.08 | 49.25 | 39.12 |
| | | 49.69 | 39.77 |
| | | 49.25 | 40.74 |
| | | 47.55 | 37.52 |
| | | 47.55 | 35.74 |

| **Experiment 1: MMS** | | | | |
|---|---|---|---|---|
| **mg/L** | **0** | **10** | **20** | **40** |
| MML (kbp) | 58.41 | 58.41 | 58.41 | 55.55 |
| | 56.49 | 55.55 | 57.44 | 55.55 |
| | 58.41 | 60.45 | 55.55 | 51.97 |
| **Experiment 2** | | | | |
| **mg/L** | **0** | **10** | **20** | **40** |
| MML (kbp) | 56.51 | 61.24 | 64.33 | 61.24 |
| | 59.29 | 61.24 | 62.76 | 59.29 |
| | 54.71 | 60.75 | 62.25 | 58.82 |
| **Experiment 2 DMSO** | | | | |
| **mg/L** | **0** | **10** | **20** | **40** |
| MML (kbp) | 46.10 | 44.92 | 53.66 | 48.17 |
| | 45.69 | 47.76 | 50.81 | 45.69 |
| | 40.91 | 48.17 | 46.92 | 49.02 |